CHALMERS

Effect of spray characteristics on the evaporation and decomposition of a urea-water-solution

Master of Science Thesis

JORUN WEDLUND

Department of Chemical and Biological Engineering

Division of Chemical Reaction Engineering

CHALMERS UNIVERSITY OF TECHNOLOGY

Gothenburg, Sweden, 2012

Influence of spray characteristics on the evaporation and decomposition of a urea-water-solution
JORUN WEDLUND

Department of Chemical and Biological Engineering
Chalmers University of Technology
SE-412 96 Göteborg
Sweden
Telephone + 46 (0)31-772 1000

Influence of spray characteristics on the evaporation and decomposition of a urea-water-solution
JORUN WEDLUND
Department of Chemical and Biological Engineering
Chalmers University of Technology

Abstract

Even though urea-SCR is a well-established technique to reduce emissions of nitrogen oxides from diesel engines it is not without problems. The residence time in the silencer is limited and it is therefore necessary to have a well designed system where the urea solution can evaporate quickly. Moreover, deposit formation may occur if the system is not properly designed. The characteristics of the spray has been identified as one the parameters that may affect the evaporation of urea as well as the formation of deposits. In this thesis the influence of certain spray characteristics on the evaporation of AdBlue as well as wall film formation has been investigated.

An experimental investigation has been done in a test rig that was designed to obtain a plug flow. Investigated spray characteristics includes the dosing unit pressure, the spray angle and the dosing frequency that could all influence the droplet size of the spray. The evaporation rate has been estimated from FTIR measurements as well as temperature measurements on a wheel inserted in the pipe. The estimated depletion times based on earlier experimental data indicate that the difference for the investigated droplet sizes should be large. The FTIR measurements did not indicate significant effects for any of the tested parameters. For high temperatures the differences are small and could be due to differences in the radial distribution. For low temperatures liquid AdBlue still remains that disturbs the FTIR signal and could be converted to ammonia in the filter of the FTIR instrument.

The evaporation rate was better captured with the temperature measurements where significant effects could be observed for lower temperatures and flow rates. Also it was possible to capture the radial distribution of the spray. It was however observed that a plug flow was not obtained and that droplets were entrained towards the upper part of the pipe.

The temperature measurements indicate that the larger droplets that are produced with a lower dosing unit pressure leads to a significant decrease in the evaporation rate for low temperatures and gas flow rates. The droplets are also distributed over a smaller area which leads to more entrainment and therefore also more wall wetting for these flow conditions. A narrower spray angle leads to the evaporation rates similar to those with a lower dosing unit pressure. The higher dosing frequency gives a somewhat lower evaporation rate for most tested operating conditions. No difference in the radial distribution was observed.

Keywords: Urea-SCR, urea deposits, sprays.

Acknowledgements

This thesis was done at the department for NO_x treatment systems, NMTN, at Scania CV. First of all I want to thank my supervisor, Henrik Birgersson, for his support and input during the project. I would also like to thank everyone at NMTN and nearby departments for an inspiring environment where everyone is always ready to help or answer questions. A special thanks to all those who have helped me with the experimental equipment.

I also want to thank my examiner at Chalmers, Bengt Andersson, who has come with many helpful comments during the project.

Table of Contents

Abstract iii
Acknowledgements v
1 Introduction 1
1.1 Objective 1
1.2 Constraints 2
2 Theory 2
2.1 Emissions and regulations of nitrogen oxides 2
2.1.1 Environmental and health impact 3
2.1.2 Regulations 4
2.2 Urea-SCR 4
2.2.1 Exhaust after-treatment system 4
2.2.2 SCR chemistry 5
2.2.3 Urea decomposition 6
2.2.4 Performance of the Urea-SCR system 7
2.2.5 Issues related to the use of urea 7
2.3 Sprays 8
2.3.1 Atomization 8
2.3.2 Spray characteristics 9
2.3.3 Spray nozzles 9
2.3.4 Secondary atomization 10
2.3.5 Spray-wall interaction 12
2.3.6 Spray evaporation 13
2.4 Previous studies on sprays in Urea-SCR applications 13
2.4.1 Experimental studies 14
2.4.2 CFD studies on sprays 15
2.5 Estimated droplet properties 16
2.6 Statistic analysis 18
2.6.1 ANOVA-tests 18
2.6.2 Tukey’s test 19
3 Experimental method 20
3.1 Urea dosing 21

3.1.1 Bypassing of urea flow ... 21
3.1.2 Correction of urea dosing ... 22
3.2 Temperature corrections ... 23
3.3 Temperature measurements ... 24
3.4 Analysis of gas composition ... 26
4 Results ... 26
4.1 Outlet ammonia concentrations ... 27
4.1.1 Effect of dosing unit pressure and spray angle ... 28
4.1.2 Effect of spray frequency ... 32
4.1.3 Position of FTIR probe ... 33
4.1.4 Performance ... 36
4.2 Temperature measurements ... 37
4.2.1 Temperature drop from urea decomposition ... 37
4.2.2 Reproducibility ... 38
4.2.3 Spray distribution in the pipe ... 41
4.2.4 Statistic evaluation ... 46
4.2.5 Temperature drops along the pipe ... 53
4.3 Wall temperatures ... 55
4.3.1 Effect of dosing unit pressure ... 56
4.3.2 Effect of spray angle ... 57
5 Discussion and conclusions ... 58
6 Recommendations for further work ... 61
Bibliography ... 62
Appendix ... 65
A. Calculations ... 65
Calculation of droplet depletion times ... 65
Calculation of ideal ammonia concentrations ... 66
Calculation of temperature losses due to urea decomposition ... 66
B. Ammonia concentration profiles ... 68
Ammonia concentrations for dosing unit pressure change ... 68
Ammonia concentrations for spray angle change ... 70
Ammonia concentrations for frequency change ... 72
C. Temperature drops ... 74

Temperature drops for repeat runs 74
Temperature drops for different operating conditions 74
Temperature drops along the pipe 76
D. ANOVA-tables 78
Analysis of variance for pressure differences 78
Analysis of variance for angle change 79
Analysis of variance for frequency change 81

1 Introduction

Nitrogen oxides (NO_x) are one of the major pollutants from diesel engines. Since these affect the environment as well as human health, emission restrictions have been introduced for nitrogen oxides as well as for particulate matter. The Euro 6 emission standards will be introduced in 2013[1].

Since the fuel economy is improved with higher NO_x emissions, different after-treatment strategies can be used to decrease the emissions of NO_x while maintaining a good fuel economy. One solution that has been used for several years is selective catalytic reduction (SCR) where the nitrogen oxides are reduced with ammonia over a catalyst. For mobile applications the ammonia is provided as an aqueous urea-solution called AdBlue that decomposes into ammonia and isocyanic acid in the exhaust pipe according to reaction (1):

$$(NH_2)_2CO \rightarrow NH_3 + HNCO \quad (1)$$

The isocyanic acid can then react further to form ammonia and carbon dioxide according to reaction (2):

$$HNCO + H_2O \rightarrow NH_3 + CO_2 \quad (2)$$

One mole of urea can therefore produce two moles of ammonia.

The residence time in the exhaust system is limited and it is important to avoid components that increase the back-pressure in the system since higher back pressures increase the fuel consumption [2]. The exhaust after-treatment system must also be able to reduce emissions for a wide range temperatures and gas flow rates. For these reasons it is important to obtain a well-designed system where the urea evaporates and decomposes quickly. It is also important to avoid deposit formation in the exhaust pipe.

It has been observed that decomposition of urea as well as deposition formation can depend on characteristics of the spray. Even though several studies have been done on urea sprays for SCR applications most of these focus on the location and direction of the spray. Those who consider spray characteristics are limited to two types of sprays with different qualities and often several parameters are changed at the same time. For this reason a more systematic approach could be necessary to clarify the influence of certain spray characteristics on the performance of the spray.

1.1 Objective

The objective of this thesis is to identify spray parameters that affect the decomposition of urea and to give input on suitable spray characteristics to achieve a good decomposition of urea and good mixing of the components while minimizing deposit formation on the pipe walls. The investigated parameters include the dosing unit pressure, the spray angle and the dosing frequency which should all influence the droplet size. Experimental work will be

carried out to verify the significance of these parameters and to find for what gas temperature and gas flow rates these affect the spray.

1.2 Constraints

In the experimental setup the analysis methods are limited to those available at Scania. The outlet ammonia concentration, radial temperature profile and the wall temperatures will be measured to get an indication on the decomposition of urea and the distribution of the spray in the pipe.

In this thesis only the decomposition of urea will be investigated. It will not cover how the spray characteristics affect the conversion of NO_x over the catalyst. Also, it will only cover the characteristics of the spray and not the location or direction of the spray. The experimental rig is constructed to obtain a plug flow and the thesis will only cover how the spray performs under these types of flow conditions. Even though these flow conditions might not resemble those in a real exhaust system the goal is to eliminate effects of turbulent flow conditions on the mixing of the components to isolate the effects of the spray parameters.

2 Theory

This chapter includes the literature review that covers formation of nitrogen oxides, urea-SCR, theory on sprays and previous studies on sprays in urea-SCR. The properties of the droplets will be estimated from earlier experimental data for the relevant temperatures and droplet sizes. The statistic methods that are used to analyze the results are also explained in this chapter.

2.1 Emissions and regulations of nitrogen oxides

Nitrogen oxides are formed during combustion at high temperatures when nitrogen is present. The most common mechanism is thermal NO_x formation, also called the extended Zeldovich mechanism, which occurs through reaction (3-5) [3]:

$$O_2 + N_2 \leftrightarrow NO + N \quad (3)$$

$$N + O_2 \leftrightarrow NO + O \quad (4)$$

$$N + OH \leftrightarrow NO + H \quad (5)$$

Since the nitrogen reacts with oxygen and hydroxyl radicals, the mechanism is strongly temperature dependent. The minimum flame temperature to maintain complete combustion in diesel engines has been identified to 2300 K. This would result in a minimum NO_x production of 5.5 g/kg fuel [4].

In conventional diesel engines there is a trade-off between production of particulate matter (PM) and production of NO_x which allows for different after-treatment strategies. Higher temperatures increase the production of NO_x and reduce the production of PM while the fuel economy is improved [4].

2.1.1 Environmental and health impact

Nitrogen oxides affect the environment as well as human health. They are toxic and therefore dangerous to human health and harmful to vegetation. Nitrogen oxides also contribute to acid rain and formation of ground-level ozone that constitutes the major part of photochemical smog [5].

2.1.1.1 Acid rain

In the atmosphere nitrogen oxides react with oxygen and water to form nitric acid [6]. The mechanism is shown in reaction (6-8).

$$2\ NO + O_2 \rightarrow 2\ NO_2 \quad (6)$$

$$NO + O_3 \rightarrow NO_2 + O_2 \quad (7)$$

$$2\ NO_2 + 2\ H_2O + O_2 \rightarrow 4\ HNO_3 \quad (8)$$

Depending on the season, nitric acid contributes to 30-50 percent of the acidity of rainfall. Acid rain may lead to disruption of ecosystems in lakes, deforestation, leaching of organic materials from soils and increasing concentrations of heavy metals in soils [6].

2.1.1.2 Ground-level ozone

Nitrogen oxides and hydrocarbons are precursors to ground-level ozone that is irritating for the lungs and considered as a phytotoxin. It can also cause damage to crops and forests [5]. In the atmosphere NO_2 forms oxygen radicals in a reaction initiated by sunlight as shown in reaction (9). These react with oxygen and forms ozone as shown in reaction (10) where *M* is a body that removes energy that would make the ozone dissociate [7].

$$NO_2 + h\nu \rightarrow NO + O \quad (9)$$

$$O + O_2 + M \rightarrow O_3 + M \quad (10)$$

Since mainly NO is produced in the diesel engines the emissions of NO_2 in the atmosphere are low. Natural oxidation of NO is slow but NO_2 can be produced in a reaction that involves hydroxyl radicals that in turn are produced from oxidation of hydrocarbons. One of the suggested mechanisms for NO_2 formation is shown in reactions (11-16) [7].

$$OH + RCH_3 \rightarrow H_2O + RCH_2 \quad (11)$$

$$RCH_2 + O_2 \rightarrow RCH_2O_2 \quad (12)$$

$$RCH_2O_2 + NO \rightarrow RCH_2O + NO_2 \quad (13)$$

$$RCH_2O + O_2 \rightarrow RCHO + HO_2 \quad (14)$$

$$HO_2 + NO \rightarrow NO_2 + OH \quad (15)$$

$$RCH_3 + 2\ NO + 2\ O_2 \rightarrow RCHO + 2\ NO_2 + 2\ H_2O \quad (16)$$

High levels of ground-level ozone therefore occur on sunny days when both levels of nitrogen oxides and hydrocarbons are high.

2.1.2 Regulations

In order to reduce the emissions of NO_x and particulate matter (PM), the European Union introduced emission standards for motor vehicles in 1992. Throughout the years these have become stricter as seen in Figure 1 where the European emission limits for PM and NO_x are presented [1]. The Euro 6 emission standards will be implemented in 2013.

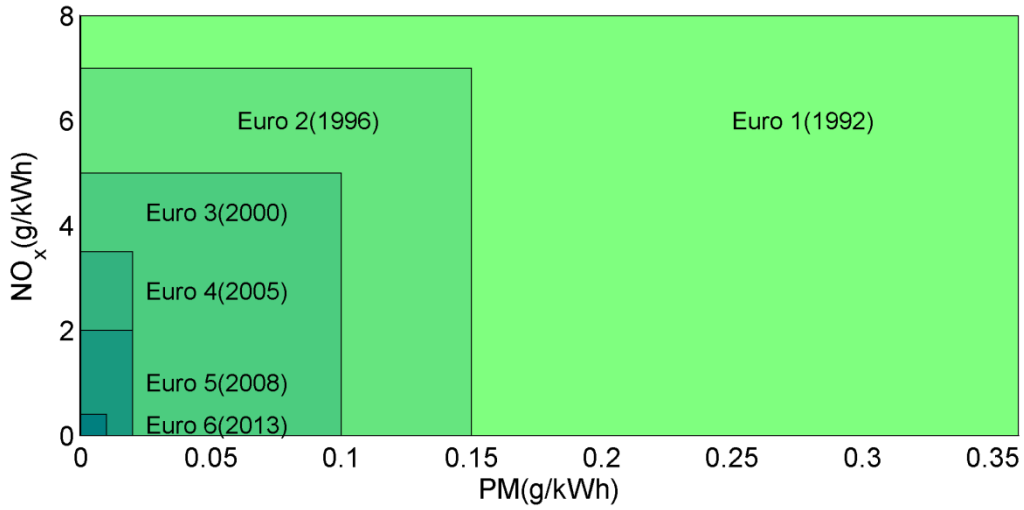

Figure 1: Emission limits for PM and NO_x

2.2 Urea-SCR

Selective catalytic reduction (SCR) is a well-established technique to reduce NO_x emissions from diesel engines. For stationary applications ammonia can be used as a reductant. For mobile applications the ammonia is generated from an aqueous urea solution, AdBlue. Compared to other technologies, such as exhaust gas recirculation (EGR) and NO_x-adsorbers, SCR leads to better fuel economy since more advanced timing of the diesel injection can be used[8]. It is often combined with other technologies to meet specifications on both NO_x and PM [8].

2.2.1 Exhaust after-treatment system

Until now Scania has mainly used SCR for larger engine sizes but for the Euro 6 engines it will be available for all engine sizes. The Scania Euro 6 emission control system is shown in Figure 2.

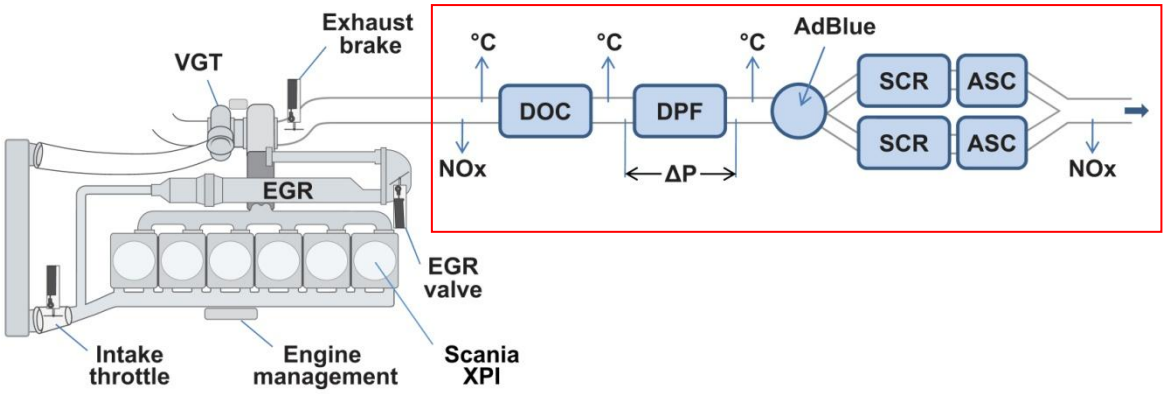

Figure 2: Scania Euro 6 Emission Control System

The exhaust after-treatment system is marked in Figure 2. Except the SCR system it includes catalysts to remove hydrocarbons and filters to remove particulate matter from the exhaust. The urea-water-solution is injected after the diesel particulate filter and the nitrogen oxides are reduced to nitrogen and carbon monoxide over the SCR catalyst. To avoid emissions of ammonia an ammonia slip catalyst (ASC) is included after the SCR catalyst. It is important to minimize the back pressure in the exhaust after-treatment system since higher back pressures will increase the fuel consumption. It will also increase the temperature of the exhaust gas and the emissions of PM, hydrocarbons and carbon monoxide [2].

All these components are integrated in the silencer that is shown with the power train in Figure 3. The AdBlue tank can be seen to the left of the silencer.

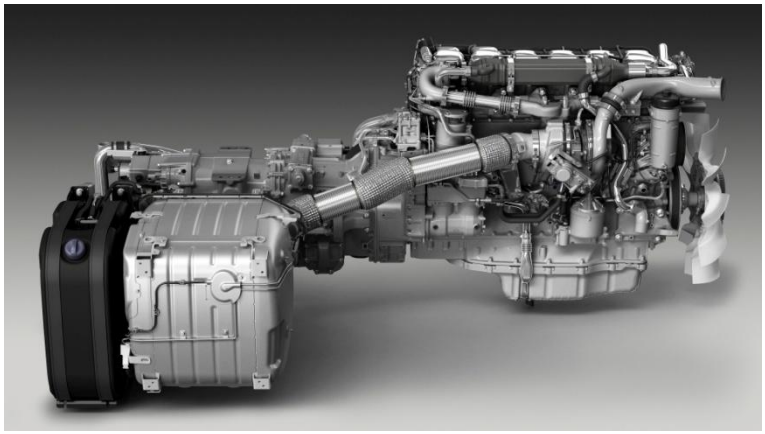

Figure 3: Scania Euro 6 power train with integrated silencer and exhaust after-treatment

2.2.2 SCR chemistry

In the SCR catalyst ammonia reacts with nitrogen oxides in the following reactions [9]:

$$4\,NH_3 + 4\,NO + O_2 \rightarrow 4\,N_2 + 6\,H_2O \quad (17)$$

$$4\,NH_3 + 6\,NO \rightarrow 5\,N_2 + 6\,H_2O \quad (18)$$

$$4\,NH_3 + 2\,NO + 2\,NO_2 \rightarrow 4\,N_2 + 6\,H_2O \quad (19)$$

$$4\,NH_3 + 3\,NO_2 \rightarrow 3.5\,N_2 + 6\,H_2O \quad (20)$$

Reaction (17) is the main SCR reaction. Of these reactions, reaction (19) is the fastest while reaction (18) and (20) are much slower than the other reactions. The conversion of nitrogen oxides is therefore highest when there is an equimolar ratio between NO and NO_2 [10]. This effect can be important to increase conversion for lower temperatures. Since the NO_x of diesel exhausts consists of more than 90 percent NO, pre-oxidation catalysts such as the DOC are often used to increase the concentration of NO_2 [8]. Since all the components are located in the silencer, additional components will lead to shorter residence times before the catalyst. This causes problems with the mixing of the components after the injection of urea [9].

Beside these four reactions two undesirable reactions may occur at higher temperatures [9]. In reaction (21) nitrous oxide is produced, which is considered as a greenhouse gas. In reaction (22), ammonia is oxidized to nitric oxide.

$$4\,NH_3 + 4\,O_2 \rightarrow 2\,N_2O + 6\,H_2O \quad (21)$$

$$4\,NH_3 + 5\,O_2 \rightarrow 4\,NO + 6\,H_2O \quad (22)$$

To avoid ammonia slips an oxidation catalyst could be included after the SCR catalyst [8]. The installation of additional catalysts reduces the residence time as mentioned before. It also increases back pressure in the after-treatment system.

2.2.3 Urea decomposition

For safety reasons ammonia cannot be used for mobile applications. Instead the ammonia is generated in-situ from an aqueous 32.5% urea solution that is sprayed into the exhaust pipe. After the water has evaporated the urea decomposes into ammonia and isocyanic acid according to reaction (23).

$$(NH_2)_2CO \rightarrow NH_3 + HNCO \quad (23)$$

It is not clear whether the urea is in a solid or in a molten state. According to Birkhold et al. the decomposition of urea could occur in two different ways [11]:

- evaporation of urea to gaseous urea, that decomposes into ammonia and isocyanic acid in the gas phase.
- direct decomposition from solid urea to gaseous ammonia and isocyanic acid.

Gaseous urea is unstable which means that the decomposition reaction will take place in the boundary layer of the droplet for both reaction paths. This means that the heat transfer conditions should be the same for both cases [11].

The isocyanic acid produced in reaction (23) is hydrolyzed to ammonia and carbon dioxide as shown in reaction (24).

$$HNCO + H_2O \rightarrow NH_3 + CO_2 \quad (24)$$

Reaction (24) can occur before the catalyst for temperatures above 400°C [12]. During thermal decomposition, the rate of this reaction is slow but the hydrolysis rate increases significantly when a catalyst is present [12].

Since water is one of the reactants in the reaction (24) the decomposition of urea is influenced by the water content of the exhaust stream which has been shown by Fang and DaCosta [13]. The exhaust gases from diesel engines normally contain 5-10 % water [14].

The total enthalpy change for the decomposition of urea depends on the whether the urea is provided as a solid or as water solution since heat is also required to evaporate the water. It also depends on the final temperature and the reaction path. Reaction (24) is exothermic which means that the required heat is lower if reactions (23) and (24) occur simultaneously. The heat required to decompose one mole of urea for different conditions is summarized in Table 1 [15].

Table 1: Heat required to decompose urea (kJ/mol)

	Thermolysis only		Thermohydrolysis	
	T_{final} = 500 K	T_{final} = 600 K	T_{final} = 500 K	T_{final} = 600 K
urea(solid)	203.4	213.4	106.5	116.2
76.93% urea	241.7	255.3	144.8	158.1
50% urea	360.0	382.0	263.1	284.8
32.5% urea	541.5	576.3	444.6	479.1

It has also been suggested that urea and isocyanic acid can react directly with nitric oxide [16]. This is shown in reaction (25) and (26):

$$2\,CO(NH_2)_2 + 6\,NO \rightarrow 5\,N_2 + 2\,CO_2 + 4\,H_2O \quad (25)$$

$$4\,HNCO + 6\,NO \rightarrow 5\,N_2 + 4\,CO_2 + 2\,H_2O \quad (26)$$

2.2.4 Performance of the Urea-SCR system

To achieve a high conversion over the catalyst while avoiding ammonia slips it is important that the components are well-mixed to ensure a good utilization of the catalyst [17]. This can be achieved with a well-designed spray or with different types of static mixers.

It is also important that the urea has enough time to decompose. The distance between the urea injection and the catalyst is short which means that reactions (23) and (24) will not always be complete before the catalyst. This leads to a delayed liberation of NH_3 and decreased SCR performance [9].

2.2.5 Issues related to the use of urea

During some running conditions the urea can react with isocyanic acid and form biuret as shown in reaction (27):

$$(H_2N)_2CO + HNCO \rightarrow (H_2NCO)_2NH \quad (27)$$

This reaction occurs at temperatures from 193 to 250°C [18]. The biuret can react further to form larger compounds such as cyanuric acid, ammelide, ammeline, melamine and other, even more complex, polymeric compounds [19]. The structures of common urea-related byproducts are shown in Figure 4.

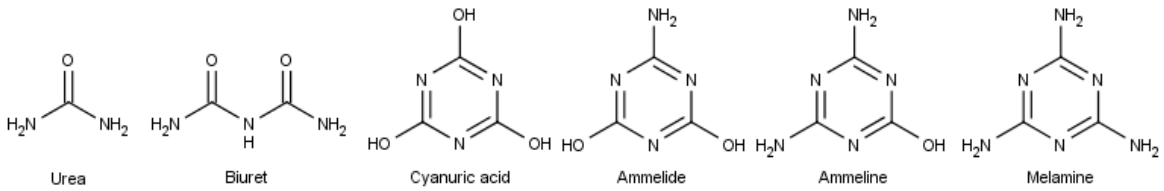

Figure 4: Structures of common urea by-products

Formation of byproducts will result in lower production of ammonia, but also in deposits that are difficult to remove since some of these compounds have higher melting and decomposition temperatures than urea. The composition of urea-related deposits depends on the operating temperature. At temperatures below 150 °C the main component is urea. At temperatures above 300 °C the main component is cyanuric acid [20].

Deposits usually form at the injector tip, the injector house or in the exhaust pipe downstream [17]. If deposits form at the catalyst surface they may contribute to deactivation of the catalyst [13]. Deposit formation is usually dependent on running conditions and increases for low temperatures [19]. It may be avoided with a proper location and direction of the injector, proper pre-injector pipe geometry or with introduction of properly designed mixers [17]. Several authors have shown that deposits can be avoided with a high-quality spray. This will be further discussed in Chapter 2.4.1.

2.3 Sprays

The purpose of a spray is to create a liquid dispersion in a gaseous phase. This means that the interface between the two fluids is increased significantly which is favorable for mass and heat transfer [21].

2.3.1 Atomization

All types of atomizer rely on the principle to create a liquid sheet or column that is unstable because of the surface tension. Any disturbance will then make the liquid break up into droplets [22]. This occurs through different mechanisms depending on the liquid Reynolds number. For circular jets three flow regimes following increasing Reynolds number can be identified [21]:

1) The Rayleigh regime where drop formation occurs through surface tension effects. The sizes of the droplets are fairly equal.

2) The aerodynamic regime where drop formation is influenced by aerodynamic forces. These forces create wave growth on the interface that leads to break-up of the liquid jet.

3) The atomization regime where the liquid disintegrates spontaneously at the nozzle exit.

For liquid sheets instabilities are caused by aerodynamic interactions with the surrounding gas since surface tension forces tend to stabilize the liquid sheet. The spray droplet sizes are generally in the same order as the liquid sheet thickness [23].

2.3.2 Spray characteristics

The sizes of the droplets in a spray are usually described by [21]:

1) A suitable droplet size distribution function
2) The (mean) size parameter
3) The relative width of the distribution

A common way to describe the droplet size distribution is the Sauter mean diameter (SMD). It is defined as the ratio between the mean droplet volume and the mean droplet surface area [21]. Droplet size distributions are also commonly described by the fraction of droplets below a certain diameter. For example DV_{90} is the diameter where 90 percent of the liquid volume consists of droplets below that diameter.

2.3.3 Spray nozzles

Spray nozzles can be divided into several categories [24]:

1) Pressure nozzles (hydraulic)
2) Swirl nozzles
3) Two-fluid nozzles (pneumatic)
4) Rotary devices (spinning cups, disks or vaned wheels)
5) Ultrasonic
6) Electrostatic

The produced spray can then be classified according to the produced spray pattern, i.e. hollow cone, solid cone and flat sprays.

A single nozzle can fall into several categories. The exact design and principle of the spray nozzles used for the Euro 6 trucks is confidential information that is only known by the provider. The principles of two types of spray nozzles might be of interest to try to understand the atomization mechanisms in these types of nozzles.

2.3.3.1 Plain orifice nozzles

In hydraulic nozzles such as the plain orifice nozzle, the liquid is forced through an orifice or a chamber which increases the velocity of the liquid and makes it disintegrate into droplets. The shape and diameter of the orifice is the most important variable to influence the size of

the droplets. These can produce solid or hollow cone sprays if the liquid is swirled at the inlet [24].

Since plain orifice nozzles are often used in fuel combustion most correlations have been developed for these fluids. A summary of correlations for plain orifice nozzles can be found in [24]. Most of these correlations include the liquid density, liquid viscosity, surface tension, liquid flow rate and the pressure drop over the nozzle.

2.3.3.2 Swirl nozzles

Swirl nozzles are a type of pressure nozzle where the fluid experiences a centrifugal force in the nozzle chamber. This results in the formation of a liquid sheet that breaks down into droplets [24]. They can be designed to produce hollow cone sprays as well as solid cone sprays but the hollow cone design is more common since it can produce more fine droplets [24].

Swirl nozzles come in axial and tangential designs. The tangential design has several advantages since it does not require internal vanes, which mean that it is less prone to clogging, and produces sprays with a more stable spray angle [24].

The swirl nozzle comes in three varieties: simplex, duplex and spill-return. The simplex design is most simple and consists of a single swirl chamber. The duplex design consists of two simplex nozzles placed in one chamber where one nozzle surrounds the other. Spill return nozzles are similar to simplex nozzles but contain a passageway where surplus liquid can return to the supply source.

The SMD for a pressure swirl nozzle is proportional to the surface tension, the liquid viscosity, the mass flow rate and the pressure drop [25]. This is shown in equation (28)

$$d_{32} \propto \sigma^a \mu_d^b m_d^c \Delta P^{-d} \tag{28}$$

where d_{32} is the SMD, σ is the surface tension, μ is the viscosity, m_d is the mass flow rate and ΔP is the pressure drop.

A summary of correlations for the SMD in swirl nozzles has been reported by Omer and Ashgriz [24]. Some of these suggest that the droplet SMD decreases with the spray cone angle.

For hollow cone sprays, droplets with small diameters are usually distributed in the center region while larger droplets are found in the outer edges [25]. This can affect the performance of the spray.

2.3.4 Secondary atomization

Secondary atomization can occur if the shear forces acting on a droplet are large. It will then break up into smaller droplets. These forces can be caused by relative velocity between the droplet and the fluid, turbulence or shock structure interaction [21]. Secondary breakup through droplet-wall interaction is further described in Chapter 2.3.5.

Pilch and Erdman identified a critical Weber number below which droplet breakup does not occur. The Weber number describes the ratio between the kinetic energy of the droplet and the surface tension energy of the droplet. It is defined in equation (29):

$$We = \frac{\rho_d U_{rel}{}^2 d_d}{\sigma} \tag{29}$$

where ρ_d is the liquid density, U_{rel} is the relative velocity between the droplet and the gas, d_d is the droplet diameter and σ is the surface tension.

The critical Weber number is a function of the Ohnesorge number that describes the ratio between viscous forces to inertial and surface tension forces. It is defined in equation (30):

$$Oh = \frac{\mu_d}{\sqrt{\rho \sigma d_d}} = \frac{\sqrt{We}}{Re} \tag{30}$$

where μ_d is the liquid viscosity, ρ is the gas density, σ is the surface tension and d_d is the droplet diameter.

The critical Weber number where droplet breakup starts is described by the correlation shown in equation (31)[26]. For low-viscosity fluids (Oh<0.1) the critical Weber number will approach 12.

$$We_c = 12\left(1 + 1{,}077 Oh^{1,6}\right) \tag{31}$$

From this a maximum stable diameter for a droplet in a fluid can be determined with equation (32) [26]:

$$d = We_c \frac{\sigma}{\rho U_{rel}^2} \tag{32}$$

The time required for breakup of a droplet decreases with the Weber number [26]. It should be noted that breakup occurs through acceleration of the droplets. When the velocities of the droplets approach the velocity of the gas breakup of droplets through acceleration should also decrease. This will occur faster for small droplets with low Stokes numbers. The Stokes number is defined as the ratio between the response time for the droplet and a characteristic time for the gas as shown in equation (33):

$$St = \frac{\tau_d}{\tau_c} \tag{33}$$

where τ_d is the response time for the droplet and τ_c is a characteristic time for the gas.

2.3.5 Spray-wall interaction

Depending on the flow conditions, different phenomena may appear when a droplet hits a wall. Chen et al. describes six types of flow regimes for impinging droplets[27]:

- Adhesion: The droplet remains at the wall in a spherical form.
- Rebound: The droplet bounces back from the wall.
- Spread: The droplet spreads out and forms a liquid film.
- Splash: Some of the droplet breaks up and is ejected as smaller droplets while the rest remains at the wall
- Rebound with break-up: The droplet bounces back and breaks up into two or three droplets.
- Break-up: The droplet bounces back and breaks up into a number of small droplets.

The outcome when a droplet hits the wall depends on a number of parameters, grouped in the Weber number (29) and the Laplace number (34):

$$La = \frac{\rho_d \sigma d_d}{\mu_d^2} = \frac{1}{\sqrt{Oh}} \tag{34}$$

The Laplace number describes the quotient of surface tension to viscous forces. The relative velocity used in the Weber number will be the relative velocity between the droplet and the wall.

Liquid deposition also depends on the wall temperature. Film formation can only occur if the wall temperature is lower than the Leidenfrost temperature. Above this temperature the droplets will start to evaporate before they reach the wall. Therefore there will be a vapor film between the droplets and the wall that prevents wetting of the wall [27]. The described wall impingement regimes and during which conditions they appear are summarized in Figure 5.

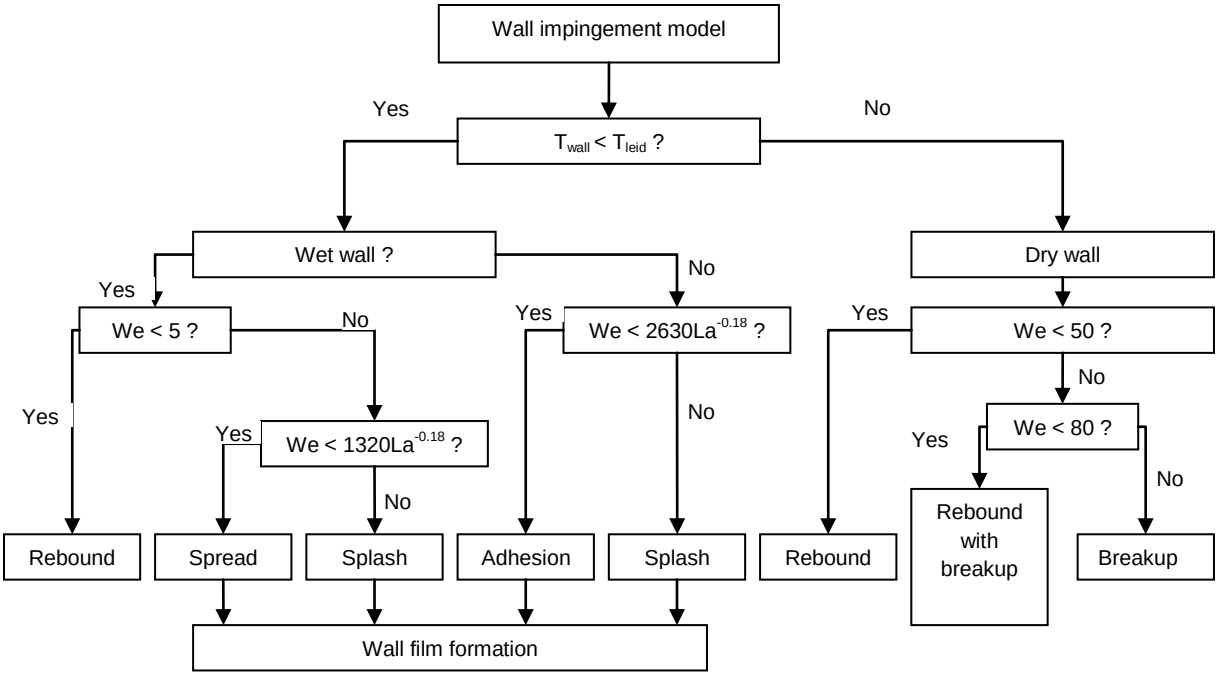

Figure 5: Wall impingement regimes [28]

From Figure 5 it can be observed that film formation only occurs if the temperature is below the Leidenfrost temperature and the Weber number is large enough. At high Weber numbers only part of the droplets will deposit on the wall.

2.3.6 Spray evaporation

Evaporation is a mechanism that is driven by concentration differences as well as temperature differences. Since heat has to be provided for the liquid to evaporate these processes are coupled. The coefficients for mass and heat transfer depend on the fluid properties, flow conditions and droplet sizes.

A common way to model evaporation from liquid droplets is the D-squared law where the drop surface area decreases linearly with time after the initial heat-up period [28].

$$d_d^2(t) = d_{d,0}^2 - \beta t \qquad (35)$$

where d^2_d is the square of the diameter, $d^2_{d,0}$ is square of the initial diameter and β is the rate coefficient.

The heat and mass transfer that a dispersion can produce is often proportional to $1/d^2$. For this reason it is often favorable to have small droplets. Since these have lower Stokes number they are easily entrained with the gas [22].

2.4 Previous studies on sprays in Urea-SCR applications

The literature on spray evaporation mainly covers evaporation for combustion applications and the literature on evaporation from urea-water-solutions is limited. The decomposition of urea has mainly been studied with pure urea and most studies do not cover the influence of the spray characteristics on the decomposition. When the influence of spray quality on the

conversion of NO_x and deposit formation has been investigated only two spray types have been compared and a more systematic approach could be necessary to find suitable spray characteristics for a certain spray type. Also, some of the tested spray types, e.g. air-assisted sprays, might not be available from distributors or suitable for these applications.

2.4.1 Experimental studies

Some experimental studies have been done on the evaporation and decomposition of AdBlue droplets. This has been done for individual droplets as well as droplets in spray systems. The evaporation of the droplets as well as the influence on the conversion of NO_x and the deposition of liquids has been investigated.

2.4.1.1 Individual droplets

Wang et al. investigated evaporation and decomposition of AdBlue droplets for temperatures from 373 to 873 K and initial droplet sizes from 0.7 to 1.4 mm. The obtained data was fitted to a linear equation similar to the D-squared law. They observed two stages in the evaporation history of the droplet, corresponding to water evaporation and urea gasification. It was observed that the rate coefficients for both stages increased with temperature. They also observed that the rate coefficient increased with increasing initial droplet diameter [14].

Even though the rate coefficients for evaporation could be higher for larger droplets as shown by Wang et al., the initial surface area is proportional to the square of the droplet diameter which means that the evaporation time is smaller for smaller droplets unless the differences between the rate constants is considerable. Those experiments were also run under stationary condition where natural convection should be the most important mechanism. In an exhaust pipe the mass and heat transfer should be higher since both the Sherwood and the Nusselt number increase with the Reynolds number. It should also be noted that in SCR applications the temperature in the exhaust pipe will decrease when the urea evaporates.

2.4.1.2 Sprays

Several studies suggest that sprays with a finer atomization will increase the conversion of urea to ammonia, the conversion of NO_x over the catalyst and decrease liquid deposits on the catalyst or in the pipe.

Fang and DaCosta compared two spray systems with different qualities and found that a high-quality spray decreased the deposit formation and improved the conversion of NO_x[13]. In their investigation the DRIFTS spectra for two trials with different spray qualities are compared. They do not report any information concerning droplet size for the tested sprays.

Salanta et al. tried to optimize a urea-SCR system by changing to a spray that gave smaller droplets and a larger cone angle. Their results are shown in Table 2 where Type1 refers to older spray and Type 2 to the new spray. This improved the reduction efficiency for all tested operating points [29]. Since the SMD, the cone angle and the spray offset are changed at the same time it is difficult to determine the influence of each parameter on the reduction efficiency. Moreover actual SMD is not reported; only that it is decreased by 30 percent.

Table 2: Test results for two types of urea injectors

Operating points(OP)	Temperature uniformity Type 1/Type 2	NO_x reduction efficiency Type 1/Type 2	NO_x reduction uniformity Type 1/Type 2
OP1	0.99/0.99	0.82/0.85	0.96/0.98
OP2	0.98/0.99	0.81/0.85	0.96/0.97
OP3	0.98/0.99	0.72/0.76	0.97/0.97

Dong et al. compared the influence of two air-assisted sprays on the conversion of NO and the deposit formation on the SCR catalyst. The properties of the two sprays are summarized in Table 3.

Table 3: Spray parameters

	Number of injector holes	Diameter of injector hole (mm)	Assisted air pressure (MPa)
Low-quality spray	1	0.9	0.2
High-quality spray	4	0.25	0.8

The high-quality spray gave a higher conversion and no deposit formation in contrast to the low-quality spray [18].

2.4.2 CFD studies on sprays

The depletion times for urea-water droplets has been estimated by several authors. The results from two different publications are shown in Figure 6.

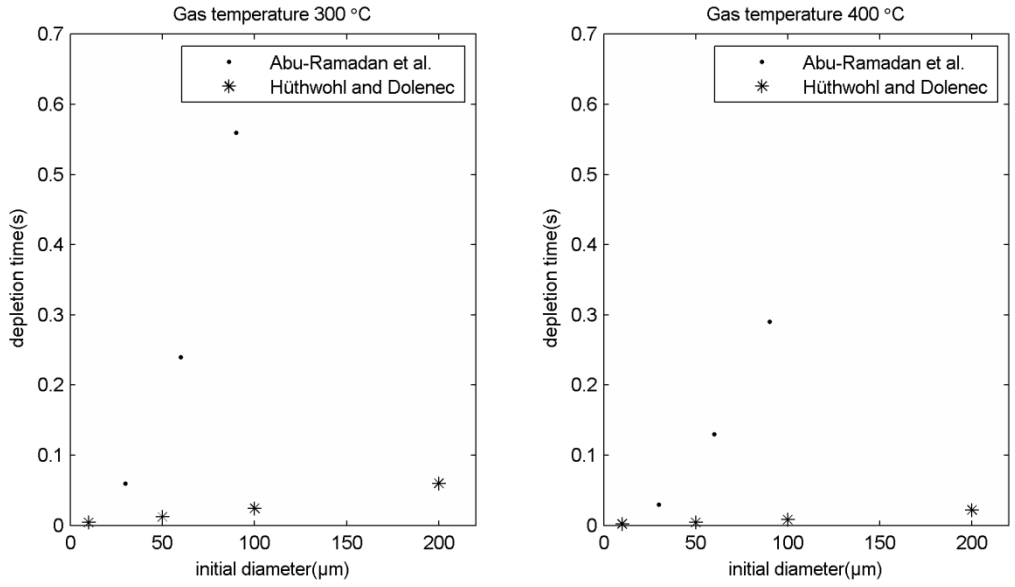

Figure 6: Depletion times of urea-water-droplets [30],[31]

It can be observed that the depletion time decreases with smaller initial droplet diameters and higher temperatures. It can also be observed that Hüthwohl and Dolenec report a much shorter depletion time than Abu-Ramadan et al.

Hüthwohl and Dolenec also found that larger droplets could be allowed for higher gas velocities since secondary break-up takes place for gas velocities above 100 m/s [31]. For this gas velocity a depletion time of less than 0.01 seconds could be observed even for droplets with initial diameters up to 500 µm.

2.5 Estimated droplet properties

The depletion time for urea-water droplets for the relevant droplet sizes in this project has been estimated from data from Wang et al. The SMD and the DV_{90} for the tested dosing unit pressures are shown in Table 4.

Table 4: SMD and DV_{90} for tested dosing unit pressures

Dosing unit pressure (bar)	SMD (µm)	DV_{90} (µm)
9	30	130
6.5	40	150
4	60	220

The depletion times for the tested temperatures and droplet sizes are shown in Table 5. The calculations can be found in section A in the appendix.

Table 5: Depletion times for tested temperatures and droplet sizes

Temperature (°C)	Droplet diameter (µm)	Depletion time(s)	Depletion time according to Abu-Ramadan et al. (s)
200	30	0.42	-
200	60	1.67	-
200	130	7.86	-
200	220	22.51	-
300	30	0.08	0.06
300	60	0.30	0.24
300	130	1.41	-
300	220	4.03	-
400	30	0.03	0.03
400	60	0.13	0.11
400	130	0.62	-
400	220	1.77	-

The depletion times have been estimated from data from Wang et al. Their reported rate coefficients are taken from experimental data for droplets that are considerably larger than the droplets that was used in this project. The used rate coefficients are therefore extrapolated very far from their tested region. Even so, the calculated depletion times shown in Table 5 correspond quite well to the data from simulations provided by Abu-Ramadan et al. that is based on the same experimental data.

The residence times in the pipe for the tested operating conditions are shown in Table 6.

Table 6: Residence time for the tested gas flow rates and temperatures

Temperature (°C)	Gas flow rate(kg/h)	Residence time(s)
200	400	0.29
200	800	0.14
200	1200	0.10
300	400	0.24
300	800	0.12
300	1200	0.08
400	400	0.2
400	800	0.10
400	1200	0.07

If the residence times are compared to the depletion times for the droplets it means that situations should appear where droplets might have enough time to evaporate if the initial droplet size is 30 µm but not if the initial droplet size is 60 µm. It can also be observed that the droplets with a size above DV_{90}, i.e. 10 percent of the injected volume will not be depleted unless the secondary atomization occurs.

The Weber number for relevant initial droplet sizes and relative velocities is shown in Table 7. It is calculated with equation (29) with AdBlue properties taken at room temperature.

Table 7: Weber numbers for relevant initial droplet sizes and relative velocities

		Relative velocity(m/s)			
		1	2	5	10
Droplet diameter (µm)	30	1	2	13	50
	60	1	4	25	101
	130	2	9	55	218
	220	4	15	92	369

Secondary atomization can occur for Weber numbers larger than 12. In Figure 5 it can be seen that break-up of droplets at wall collisions can occur if the Weber number is larger than 50 and the wall temperature is above the Leidenfrost temperature. The sizes of the Weber numbers indicate that secondary atomization can occur for the larger droplet sizes and relative velocities. Also break-up could occur for even larger droplets sizes or velocities.

The droplet Laplace numbers for relevant initial droplet sizes are shown together with the criterions for splashing in Table 8. It is calculated with equation (34) with AdBlue properties taken at room temperature.

Table 8: Laplace numbers for relevant initial droplet sizes with criterions for splashing

Droplet diameter(µm)	Laplace number	Wet wall: $We>1320\cdot La^{-0.18}$ $1320\cdot La^{-0.18}$	Dry wall: $We> 2630\cdot La^{-0.18}$ $2630\cdot La^{-0.18}$
30	1084	375	748
60	2169	331	660
130	4699	288	574
220	7953	262	522

If the Weber numbers in Table 7 are compared to the criterions for splashing when the droplet hits the wall it can be seen that splashing is unlikely unless the relative velocity is very high.

2.6 Statistic analysis

The statistic methods that are used to analyze the results are explained briefly.

2.6.1 ANOVA-tests

The results are analyzed with ANOVA-tests. In the tests the mean sum of squares for each factor is tested against the mean sum of squares for the error. The difference is significant if the value is larger than the statistic F-value for the wanted significance level.

The response for an unreplicated experiment with a combination of factors A, B and C can be written with an effects model:

$$y_{ijk} = \mu + \alpha_i + \beta_j + \gamma_k + (\alpha\beta)_{ij} + (\alpha\gamma)_{ik} + (\beta\gamma)_{jk} + \epsilon_{ijk} \quad (36)$$

where

$$i = 1,2 \dots a \quad (37)$$
$$j = 1,2 \dots b \quad (38)$$
$$k = 1,2 \dots c \quad (39)$$

For each factor the tested hypothesis is

$$H_0: \alpha_1 = \alpha_2 = \cdots \alpha_a = 0 \quad (40)$$
$$H_1: \alpha_i \neq 0 \quad \text{for at least one i} \quad (41)$$

The same hypotheses can be formulated for the other main effects and the interaction effects.

The sum of squares for the main effects is calculated as:

$$SS_A = \frac{1}{bc}\sum_{i=1}^{a} y_{i\bullet\bullet}^2 - \frac{y_{\bullet\bullet\bullet}^2}{abc} \quad (42)$$
$$SS_B = \frac{1}{ac}\sum_{j=1}^{b} y_{\bullet j\bullet}^2 - \frac{y_{\bullet\bullet\bullet}^2}{abc} \quad (43)$$
$$SS_C = \frac{1}{ab}\sum_{k=1}^{c} y_{\bullet\bullet k}^2 - \frac{y_{\bullet\bullet\bullet}^2}{abc} \quad (44)$$

where

$$y_{i\bullet\bullet} = \sum_{j=1}^{b}\sum_{k=1}^{c} y_{ijk} \quad (45)$$
$$y_{ij\bullet} = \sum_{k=1} y_{ijk} \quad (46)$$

$$y_{\bullet\bullet\bullet} = \sum_{i=1}^{a}\sum_{j=1}^{b}\sum_{k=1}^{c} y_{ijk} \tag{47}$$

The sum of squares for interaction effects are calculated as:

$$SS_{AB} = \frac{1}{c}\sum_{i=1}^{a}\sum_{j=1}^{b} y_{ij\bullet}^2 - SS_A - SS_B - \frac{y_{\bullet\bullet\bullet}^2}{abc} \tag{48}$$

$$SS_{AC} = \frac{1}{b}\sum_{i=1}^{a}\sum_{k=1}^{c} y_{i\bullet k}^2 - SS_A - SS_C - \frac{y_{\bullet\bullet\bullet}^2}{abc} \tag{49}$$

$$SS_{BC} = \frac{1}{a}\sum_{j=1}^{b}\sum_{k=1}^{c} y_{\bullet jk}^2 - SS_B - SS_C - \frac{y_{\bullet\bullet\bullet}^2}{abc} \tag{50}$$

The total sum of squares is calculated as:

$$SS_T = \sum_{i=1}^{a}\sum_{j=1}^{b}\sum_{k=1}^{c} y_{ijk}^2 - \frac{y_{\bullet\bullet\bullet}^2}{abc} \tag{51}$$

The error can then be calculated as:

$$SS_E = SS_T - SS_A - SS_B - SS_C - SS_{AB} - SS_{AC} - SS_{BC} \tag{52}$$

2.6.2 Tukey's test

If the ANOVA-test indicates that an effect is significant Tukey's test can be used to find the specific treatment averages for which the difference is significant. The difference between two sample means is significant if it exceeds:

$$T_\alpha = q_\alpha(a, f)\sqrt{\frac{MS_E}{n}} \tag{53}$$

where $q_\alpha(a, f)$ is the upper value of the studentized range statistic for the chosen value of α, a is the number of compared treatment averages, f is the degrees of freedom for the error, MS_E is the mean error from the ANOVA-test and n is the number of observations used to calculate the treatment averages.

3 Experimental method

The experiments were run in a test cell where an electric fan provides air flow rates from 0 to 2500 kg/h with temperatures from 120 to 550°C. These parameters can be controlled through the STP interface in the control room as shown in Figure 7.

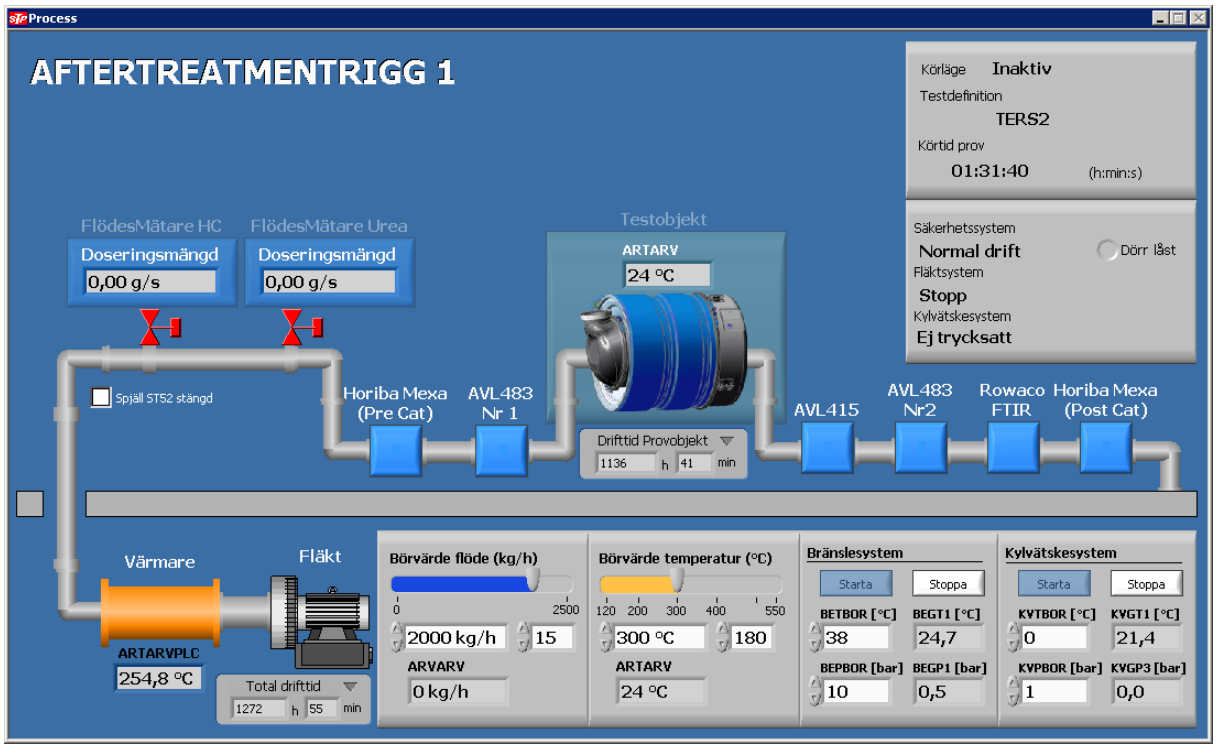

Figure 7: STP interface for control of test cell

A special test object was made for the purpose of this project. It is shown in Figure 8.

Figure 8: Test object

The test object was designed to achieve a plug flow after the injection. The flow has to pass through a perforated plate that should decrease turbulence. The injection point is screened by a perforated cone.

3.1 Urea dosing

In short, the urea dosing system consists of a pump, a urea tank and a dosing unit. The pump and the dosing unit are regulated by the EEC3 control unit which can be controlled from a computer. Since the urea dosing system could not be controlled with STP, the urea dosing was executed with the software EEC3logger on a separate computer. The pressure decrease was obtained by programming the EEC3 control unit with different software. To change the spray angle another dosing unit was used. The frequency increase could be executed from EEC3logger.

3.1.1 Bypassing of urea flow

The return flow rate from the dosing unit is proportional to the square of the pressure in the dosing unit. For low pressures and low dosing rates the total flow rate from the pump may therefore get too low. This can be avoided if a fraction of the flow is by-passed the dosing unit to increase the total flow rate from the pump. This configuration is shown in Figure 9.

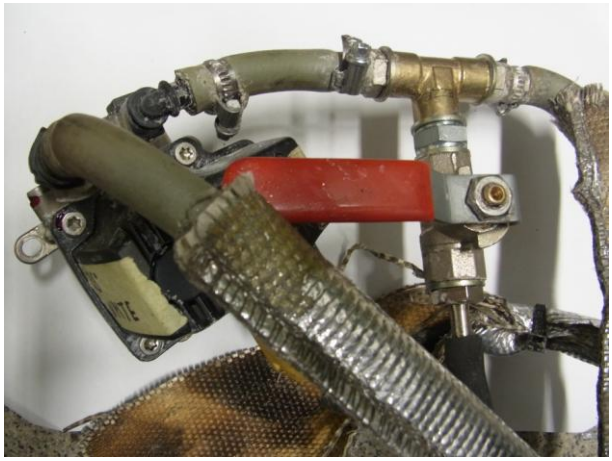

Figure 9: By-passing of urea flow

3.1.2 Correction of urea dosing

Before the experiments were run in the test rig, the dosing accuracy was tested in a separate test rig where the dosing system is controlled with ATI Vision. The amount of dosed AdBlue is weighed and can be compared to the desired amount. For flow rates above 10 g/min this was done with a standard test script where 600 g AdBlue was dosed with the specified flow rate. Since this script could not be used for flow rates of 5 g/min the test was run manually for this flow rate.

The results from the initial tests for dosing accuracy are shown in Figure 10. It can be observed that the dosing error at 3 bar is very high. For this reason the lowest pressure was set to 4 bar.

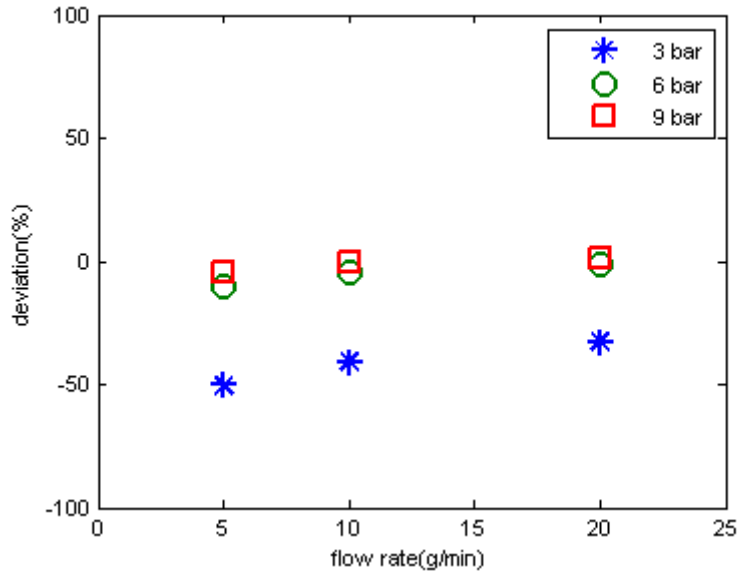

Figure 10: Dosing error for pressures 3, 6 and 9 bar

The results from the next runs are shown in Figure 11. It can be observed that the error is much smaller, although it is larger than the specification.

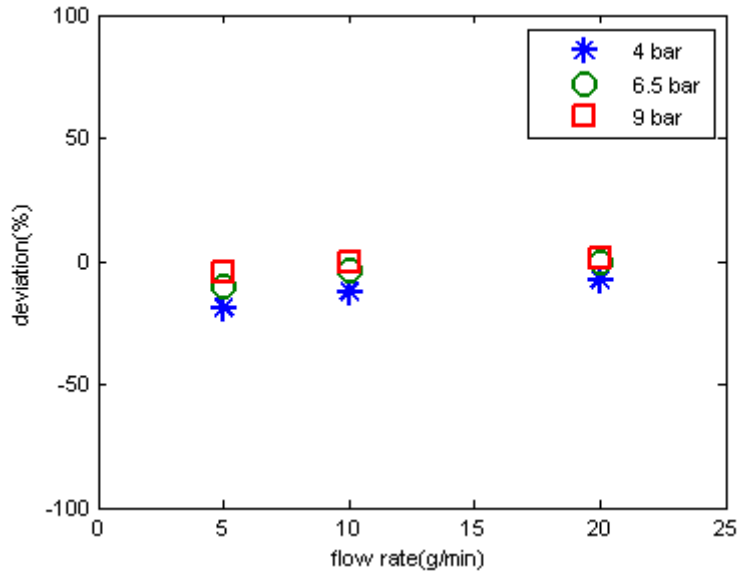

Figure 11: Dosing error for pressures 4, 6.5 and 9 bar

To get an orthogonal experimental design the urea dosing rates were set to 5, 12.5 and 20 grams/min. For each pressure a linear expression was used to calculate the required flow rate to compensate for under-dosing in the points where the error exceeded 5 percent. It was also verified that the correction gave the desired flow rate as shown in Table 9.

Table 9: Verification of urea dosing correction

Pressure(bar)	Desired flow rate (g/min)	Set flow rate (g/min)	Measured flow rate (g/min)	Deviation (%)
4	5	6	5.1	1.5
	12.5	13.8	12.6	1
	20	21.6	20.2	1.2
6.5	5	5.5	5	0.5
	12.5	12.5	-	-
	20	20	-	-
9	5	5	-	-
	12.5	12.5	-	-
	20	20	-	-

The flow rate was also tested for a frequency of 4 Hz and for a spray angle of 35 degrees. Since these parameter changes did not give large errors in the urea dosing no correction was made for these parameters.

3.2 Temperature corrections

During the experiments the gas temperature in front of the injection point cannot be measured since this could disturb the spray. For this reason the temperature at this position (MPTC27) was measured and the set temperature upstream (T1) was adjusted to obtain the desired temperature for each flow rate. The pipe was also insulated to achieve a lower temperature drop over the pipe.

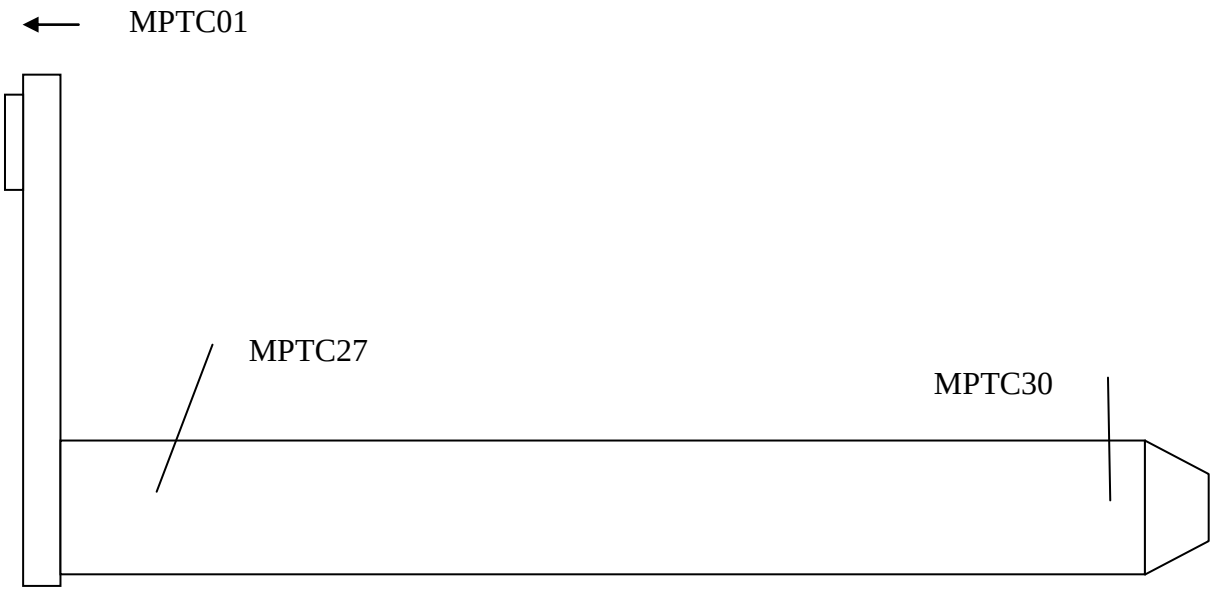

Figure 12: Measurement points for temperature corrections

For lower flow rates a higher temperature is required since the temperature drop before the injection point is higher. Also the temperature drop over the pipe was measured. These results are shown in Table 10.

Table 10: Set and measured temperatures without injection

Gas flow rate (kg/h)	400	800	1200
T1(set) (°C)	212	207	206
MPTC01 (°C)	211.9	207.2	206.1
MPTC27 (°C)	200	200.1	200.4
MPTC 27-MPTC30 (°C)	10	7	6
T1(set) (°C)	319	308	304
MPTC01 (°C)	319.1	308.3	304.3
MPTC27 (°C)	299.6	300.1	300.3
MPTC 27-MPTC30 (°C)	17	12	10
T1(set) (°C)	415	415	409
MPTC01 (°C)	415.0	415.0	409.1
MPTC27 (°C)	385	400.2	399.9
MPTC 27-MPTC30 (°C)	25	17	14

At the lowest flow rate it was difficult to obtain a temperature above 415 degrees. For this reason this temperature was used even though a temperature of 400 degrees is not obtained at the spray.

3.3 Temperature measurements

The wall temperature after the injection is measured with thermo element at the positions shown in Table 11.

Table 11: Position of thermo elements on the pipe wall

	0 degrees	90 degrees	180 degrees	270 degrees
12 cm	MPTC31	MPTC37	MPTC43	MPTC49
15 cm	MPTC32	MPTC38	MPTC44	MPTC50
18 cm	MPTC33	MPTC39	MPTC45	MPTC51
21 cm	MPTC34	MPTC40	MPTC46	MPTC52
24 cm	MPTC35	MPTC41	MPTC47	MPTC53
27 cm	MPTC36	MPTC42	MPTC48	MPTC54

The temperature is also measured on a separate pipe part that consists of a wheel with thermo elements as shown in Figure 13.

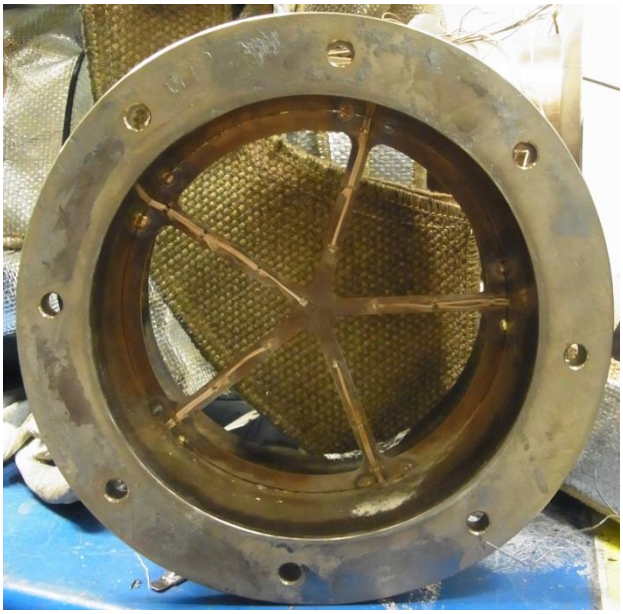

Figure 13: Wheel with thermo elements

The position of the thermo elements on the wheel as it is mounted in the pipe is shown in Figure 14. The direction is towards the outlet of the pipe.

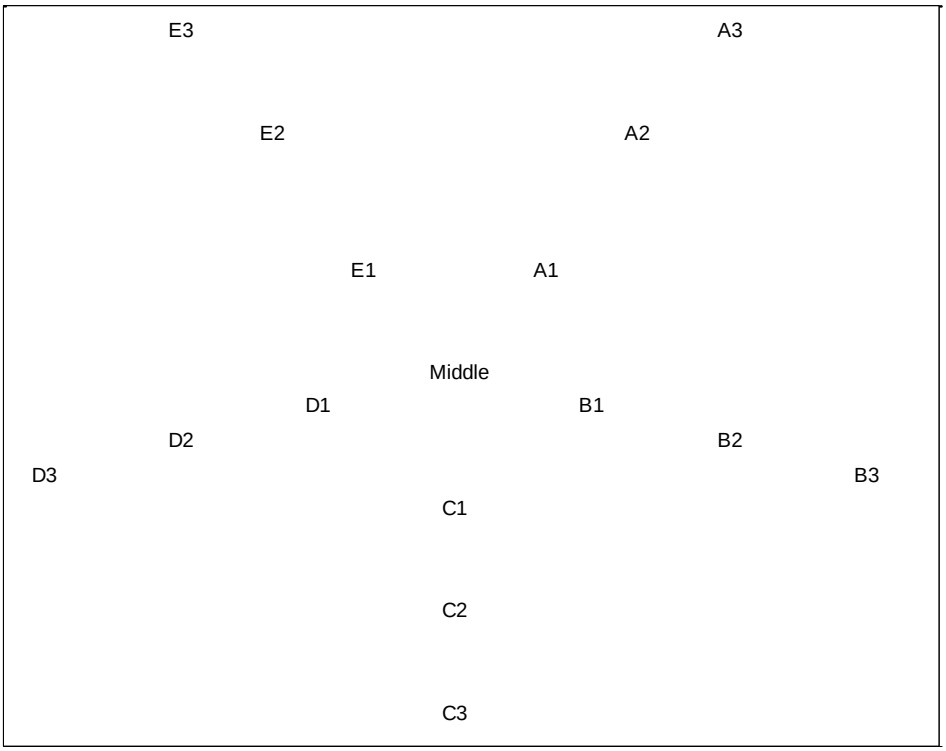

Figure 14: Position of thermo elements on the wheel

3.4 Analysis of gas composition

The composition of the outlet gas is measured with an FTIR instrument. The function of the instrument relies on the principle that a molecule will absorb radiation with specific wavelengths that makes it possible to detect a specific component. The amount of absorbed radiation is proportional to the concentration of the component. Two different FTIR probes were used. For most of the measurements a 13.5 cm FTIR probe was used. This was inserted 8 cm into the pipe. For some measurements a 9.5 cm probe that was inserted 4 cm into the pipe was used.

4 Results

The tested spray parameters are summarized in Table 12.

Table 12: Tested spray parameters

Dosing unit pressure(bar)	Spray angle(degrees)	Dosing frequency(Hz)
4	50	1
6.5	35	4
9		

Each spray parameter is tested for the operating conditions shown in Table 13 for urea dosing rates of 5, 12.5 and 20 g/min. Each dosing period is executed for 5 minutes with a 5 minute pause between the dosing periods. An exception is the higher dosing unit frequency that could only be run with a dosing rate of 20 g/min.

Table 13: Tested operating conditions

Operating point	Gas temperature (°C)	Gas flow rate(kg/h)
1	200	400
2	200	1200
3	300	800
4	385	400
5	400	1200

4.1 Outlet ammonia concentrations

The outlet concentration of concentration of ammonia was measured for the different pressures, frequencies and spray angles. To get an indication of the repeatability of the experiments multiple runs were done in the center point. These are shown in Figure 15.

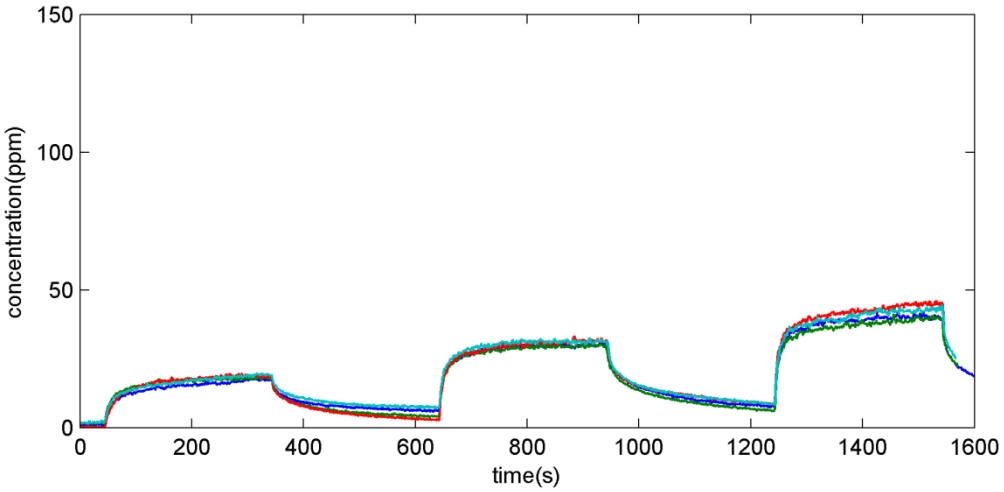

Figure 15: Repeated measurements at 300 ºC, 800 kg/h 6.5 bar.

In Figure 15 it can be seen that there is some difference between the runs. This can also be confirmed from an ANOVA-test that is done for the mean concentrations for the last 10 seconds that are shown in Table 14.

Table 14: Outlet ammonia concentrations for repeated runs

Run	Urea dosing rate(g/min)	NH_3 concentration(ppm)
1	5	17.4
1	12.5	30.2
1	20	39.7
2	5	19.3
2	12.5	31.5
2	20	43.0
3	5	18.6
3	12.5	31.5
3	20	45.0
4	5	18.0
4	12.5	29.8
4	20	39.6

The ANOVA-test shown in Table 15 shows that the difference between the different runs is significant on a 93 percent confidence level. The significance level with which the null hypothesis can be rejected can be found by subtracting the p-value in the column to the right from one. A 95 percent confidence level therefore requires a p-value of less than 0.05.

Table 15: Analysis of variance for repeated runs

Source	Sum of squares	DOF	Mean sum of squares	F	Prob>F
Run	16.90	3	5.63	4.11	0.07
Urea dosing rate	1107.24	2	553.62	403.64	0.00
Error	8.23	6	1.37		
Total	1132.37	11			

4.1.1 Effect of dosing unit pressure and spray angle

The results for the different dosing unit pressures and the different spray angle will be presented together for comparison. The results for the spray frequency will be presented separately. The largest differences are observed at a gas temperature of 200 °C and a gas flow rate of 400 kg/h that is shown in Figure 16 and Figure 17. The slope of the ammonia curves is much steeper than those for the repeat runs which indicates that the FTIR-instruments samples liquid urea that disturbs the FTIR signal which was confirmed from the temperature measurements. This is shown in Chapter 4.2.5. Moreover, the filter in the FTIR instrument can catalyze reactions that change the composition of the gas [32]. For this reason it could be more appropriate to use an earlier value of the ammonia concentration, e.g. 30 seconds after the urea dosing has been started, where little urea has accumulated in the filter. It can be observed that for the pressure of 4 bar the concentration does not increase more after a certain point for the highest dosing rate. For the spray angle of 35 degrees the concentration is higher for all flow rates. Since the spray distributions are similar and the droplet sizes are larger for these parameters it is difficult to tell what could be the reason for the higher ammonia concentration for the spray angle of 35 degrees.

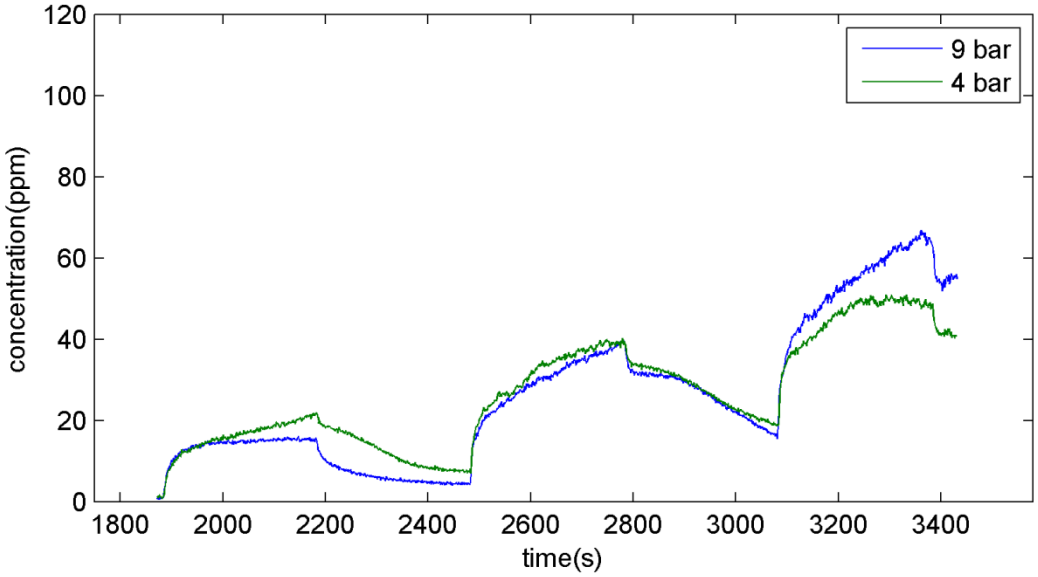

Figure 16: Outlet ammonia concentrations for a gas temperature of 200 °C and a gas flow rate of 400 kg/h with urea dosing rates of 5,12.5 and 20 g/min.

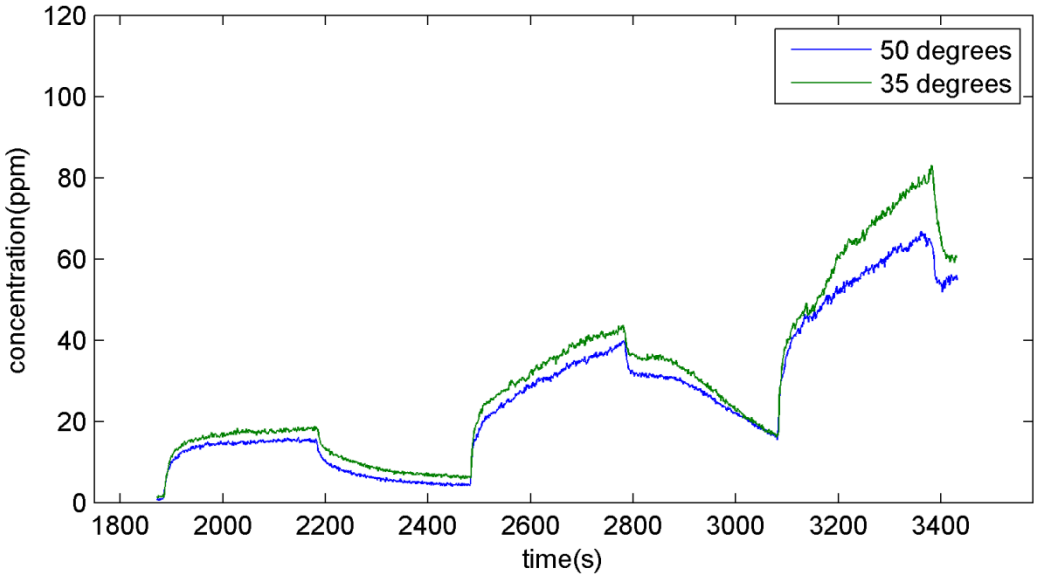

Figure 17: Outlet ammonia concentrations for a gas temperature of 200 °C and a gas flow rate of 400 kg/h with urea dosing rates of 5, 12.5 and 20 g/min.

For the rest of the operating conditions the differences are very small for the different parameters and the curves are more similar to those for the repeated runs. The results are therefore only presented in table form. The outlet concentration is obtained from a mean for the last ten seconds of dosing for each urea dosing rate. The ammonia concentration profiles are available in section B in the appendix.

The outlet ammonia concentrations for the tested dosing unit pressures are shown in Table 16.

Table 16: Outlet ammonia concentrations for tested dosing unit pressures

Gas temperature (°C)	Gas flow rate (kg/h)	Urea dosing rate(g/min)	Ammonia concentration(ppm) 9 bar	4 bar
200	400	5	15.2	21.3
		12.5	39.2	39.1
		20	64.2	48.3
200	1200	5	9.8	10.3
		12.5	15.6	17.3
		20	24.0	28.0
300	800	5	17.1	18.6
		12.5	31.1	31.3
		20	42.7	43.4
385	400	5	41.8	40.5
		12.5	77.2	73.3
		20	105.9	103.8
400	1200	5	20.2	25.4
		12.5	43.2	45.2
		20	58.2	60.6

The outlet ammonia concentrations for the tested spray angles are shown in Table 17.

Table 17: Outlet ammonia concentrations for tested spray angles

Gas temperature (°C)	Gas flow rate (kg/h)	Urea dosing rate(g/min)	Ammonia concentration (ppm) 50 degrees	35 degrees
200	400	5	15.2	18.3
		12.5	39.2	43.1
		20	64.2	80.0
200	1200	5	9.8	11.7
		12.5	15.6	18.4
		20	24.0	26.2
300	800	5	17.1	17.1
		12.5	31.1	31.1
		20	42.7	42.9
385	400	5	41.8	43.1
		12.5	77.2	74.5
		20	105.9	104.7
400	1200	5	20.2	21.9
		12.5	43.2	42.4
		20	58.2	57.8

From the values of the outlet ammonia concentrations it is difficult to observe trends concerning the conversion of urea to ammonia. For some operating conditions the higher pressure gives a higher outlet ammonia concentration which can be expected, but for other operating conditions the lower pressure gives a higher outlet ammonia concentration.

A statistic evaluation was done to investigate the significance of the each parameter for the tested operating conditions. The operating point, the urea dosing rate and the dosing unit

pressure/spray angle were chosen as parameters. The result for the change in dosing unit pressure is presented in Table 18.

Table 18: ANOVA-test for ammonia concentrations for a changed dosing unit pressure

Source	Sum of squares	DOF	Mean sum of squares	F	Prob>F
Operating point	10439.31	4	2609.83	187.27	0.00
Urea dosing rate	6463.47	2	3231.74	231.89	0.00
Dosing unit pressure	0.03	1	0.03	0.00	0.96
Operating point·Urea dosing rate	1307.91	8	163.49	11.73	0.00
Operating point·Dosing unit pressure	48.03	4	12.01	0.86	0.53
Urea dosing rate · Dosing unit pressure	26.11	2	13.06	0.94	0.43
Error	111.49	8	13.94		
Total	18396.35	29			

The result from the ANOVA-test indicates that the effect of the dosing unit pressure is not significant since this gives a very low F-value. The p-values shown in the right column shows that a very low significance level would be required to reject the null hypothesis. The F-values for the interaction terms that include the dosing unit pressure are larger but still not significant.

The result from the ANOVA-test for the spray angle is shown in Table 19.

Table 19: ANOVA-test for ammonia concentration for a changed spray angle

Source	Sum of squares	DOF	Mean sum of squares	F	Prob>F
Operating point	10741.06	4	2685.26	451.57	0.00
Urea dosing rate	7626.14	2	3813.07	641.22	0.00
Spray angle	25.71	1	25.71	4.32	0.07
Operating point·Urea dosing rate	1660.88	8	207.61	34.91	0.00
Operating point·Spray angle	69.71	4	17.43	2.93	0.09
Urea dosing rate · Spray angle	9.09	2	4.55	0.76	0.50
Error	47.57	8	5.95		
Total	20180.16	29			

For the spray angle the ANOVA-test shows that the F-value is higher. The effect of the spray angle and the interaction effects including the spray angle is however not significant of a 95 percent confidence level. It should also be noted that the main reason why the value is significant is the results at the lowest temperature and the lowest gas flow rate that are not very reliable.

4.1.2 Effect of spray frequency

The spray frequency gave lower concentrations of ammonia for most operating conditions. The results are however difficult to compare since the base case is taken from the last dosing rate from an entire cycle that the ammonia concentration is higher when the dosing starts. This can be seen in Figure 18 that shows the ammonia concentrations for a gas temperature of 200 °C and a gas flow rate of 400 kg/h. The concentration for the frequency of 1 Hz is higher since the start concentration is higher. The increase is however similar for both frequencies. To be able to compare the results better it could therefore be necessary to subtract the start concentration.

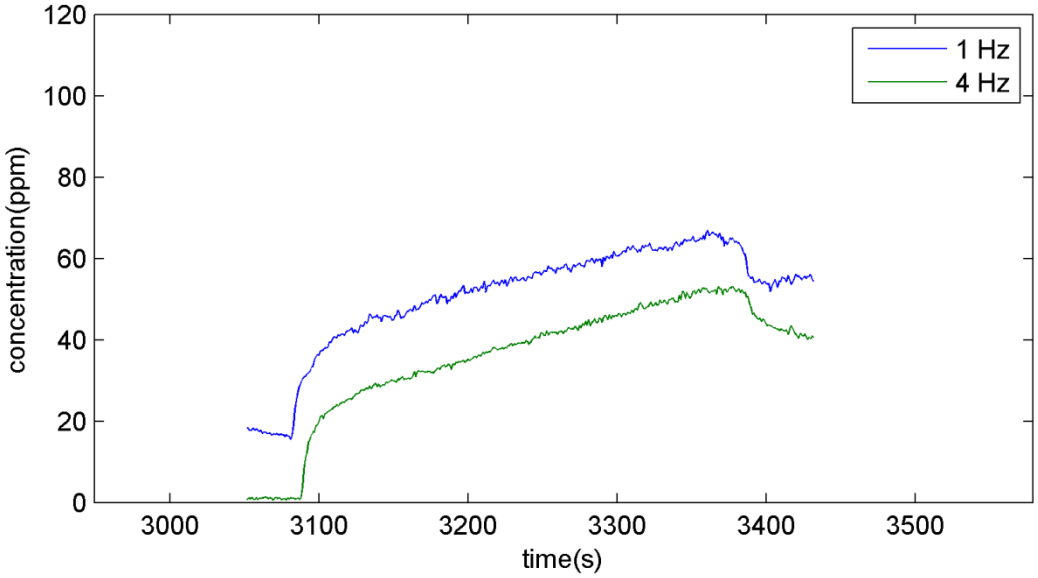

Figure 18: Outlet ammonia concentrations for a gas flow rate of 400 kg/h and a gas temperature of 200 °C with a urea dosing rate of 20 g/min.

The ammonia concentration profiles for the other operating points can be found in section B in the appendix. The outlet ammonia concentrations without compensation for the start concentration offset are shown in Table 20.

Table 20:Outlet ammonia concentrations for tested frequencies without compensation for offset

Gas temperature (°C)	Gas flow rate (kg/h)	Ammonia concentration (ppm)	
		1 Hz	4 Hz
200	400	64.2	52.4
200	1200	24.0	29.7
300	800	42.7	40.3
385	400	105.9	110.3
400	1200	58.2	59.0

The outlet ammonia concentrations with a compensation for the start concentration offset are shown in Table 21.

Table 21:Outlet ammonia concentrations for tested frequencies with compensation for start concentration offset

Gas temperature (°C)	Gas flow rate (kg/h)	Ammonia concentration (ppm)	
		1 Hz	4 Hz
200	400	47.7	51.5
200	1200	18.2	27.5
300	800	34.6	38.6
385	400	100.3	108.3
400	1200	55.1	57.0

The result from the ANOVA-test for spray frequency is shown in Table 22 and

Table 23. Without the subtraction of the start concentration the effect of the dosing unit frequency is not significant. When the start concentration is subtracted the effect of the frequency is significant on a high confidence level. It is difficult to decide which of these results that is most reliable but it could at least be safe to assume that a higher frequency does not lead to lower ammonia concentrations.

Table 22: ANOVA-test for ammonia concentration without compensation for concentration offset

Source	Sum of squares	DOF	Mean sum of squares	F	Prob>F
Operating point	7505.24	4	1876.31	77.26	0.00
Frequency	1.26	1	1.26	0.05	0.83
Error	97.15	4	24.29		
Total	7603.65	9			

Table 23: ANOVA-test for ammonia concentration with compensation for offset

Source	Sum of squares	DOF	Mean sum of squares	F	Prob>F
Operating point	7661.22	4	1915.31	340.06	0.00
Frequency	126.17	1	126.17	22.40	0.01
Error	22.53	4	5.63		
Total	7809.92	9			

4.1.3 Position of FTIR probe

To get an idea of the radial variation of the ammonia concentration some experiments were done with a shorter FTIR probe that samples gas closer to the wall. In the plots position 1 refers to the experiments with the usual FTIR probe and position 2 refers to the experiments with the shorter FTIR probe.

For a dosing unit pressure of 9 bar the ammonia concentration is lower closer to the wall as seen in Figure 19.

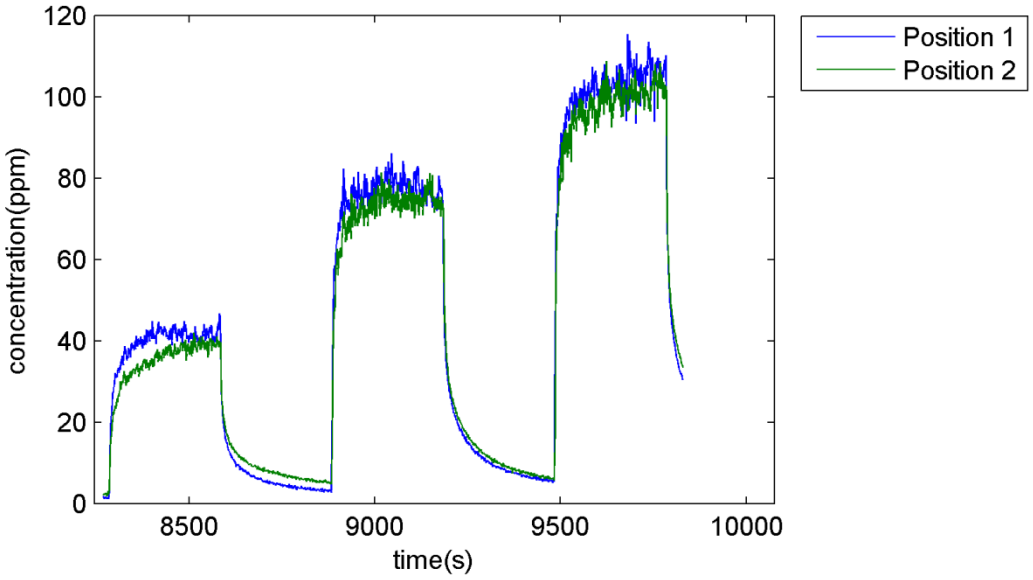

Figure 19: Ammonia concentrations at a gas temperature of 385 °C and a gas flow rate of 400 kg/h for a dosing unit pressure of 9 bar for two different positions of the FTIR probe

For a dosing unit pressure of 4 bar the concentration is higher closer to the wall as seen in Figure 20. In the plots of the spray distribution it can be seen that the distribution of the spray is uneven, probably because a plug flow has not been obtained. This effect is more prominent for the lower dosing unit pressure which could be one explanation for the difference in ammonia concentration.

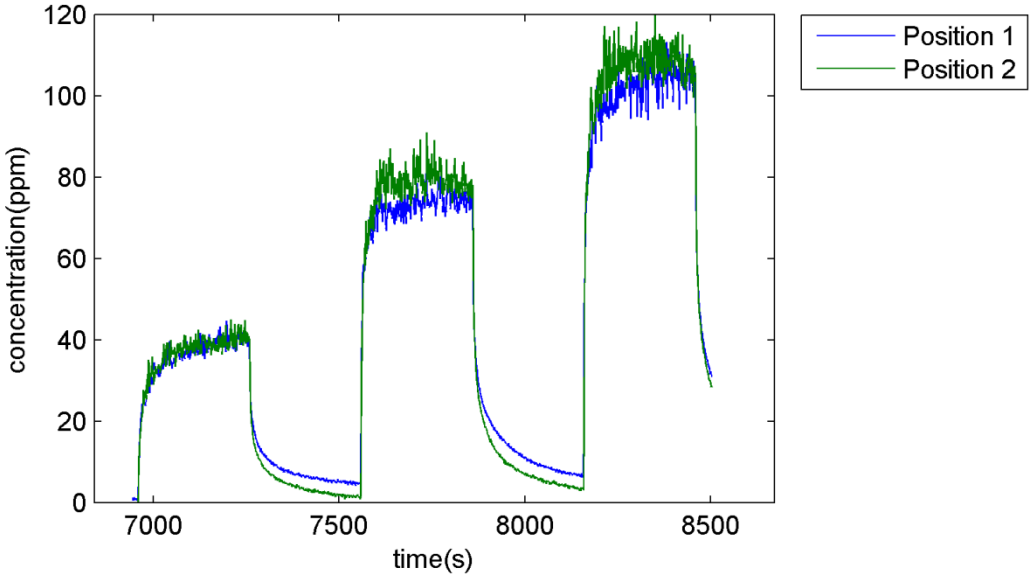

Figure 20: Outlet ammonia concentrations at a gas temperature of 385 °C and a gas flow rate of 400 kg/h for a dosing unit pressure of 4 bar for two different positions of the FTIR probe

For a higher flow rate, the concentrations for both dosing unit pressures are higher closer to the wall as seen in Figure 21 and Figure 22. This is probably because there is much

entrainment of droplets towards the upper part of the pipe for both dosing unit pressures.

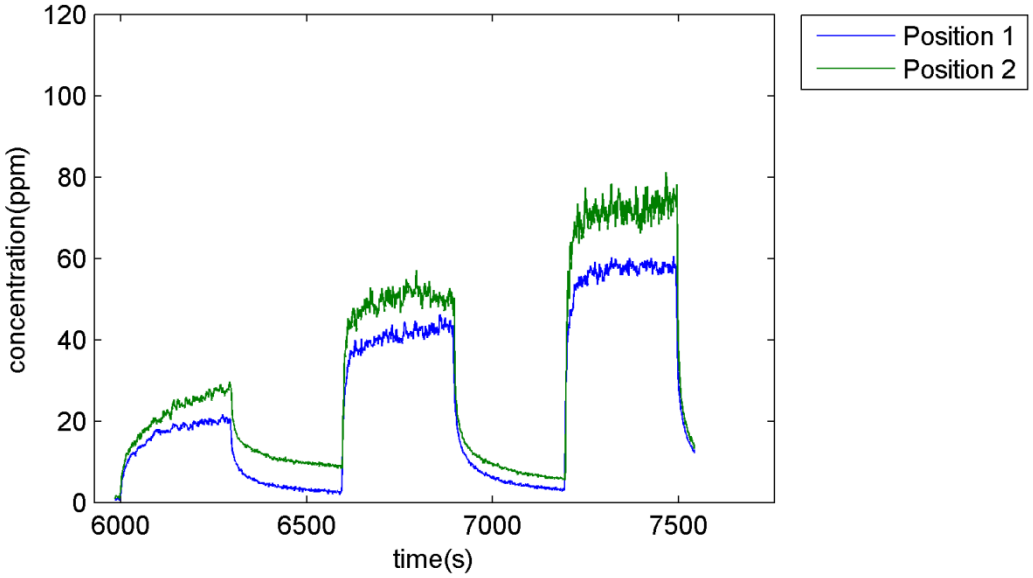

Figure 21: Outlet ammonia concentrations at a gas temperature of 400 °C and a gas flow rate of 1200 kg/h for a dosing unit pressure of 9 bar for two different positions of the FTIR probe

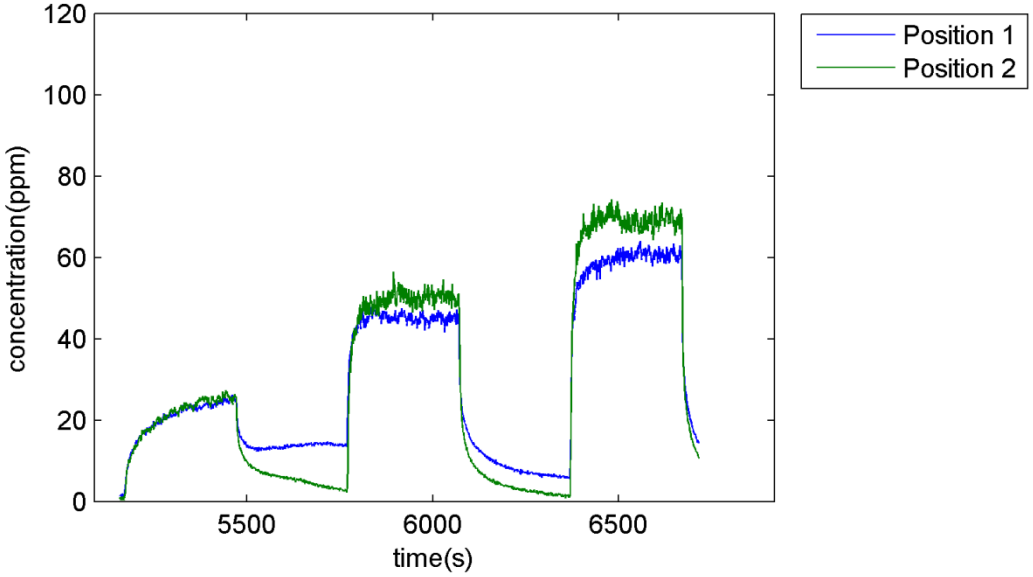

Figure 22: Outlet ammonia concentrations at a gas temperature of 400 °C and a gas flow rate of 1200 kg/h for a dosing unit pressure of 4 bar for two different positions of the FTIR probe

Even though there is a difference in the radial distribution of ammonia the mean ammonia concentration for the two positions is similar for the two dosing unit pressures as can be seen in Table 24. This could be an indication that the observed differences are due to radial differences in the ammonia distribution rather than different evaporation rates.

Table 24: Ammonia concentrations for the two tested positions

Gas temperature(°C)	Gas flow rate(kg/h)	Dosing unit pressure(bar)	Urea dosing rate (g/min)	Ammonia concentration(ppm) Position 1	Position 2	Mean
385	400	9	5	41.8	39.2	40.5
385	400	9	12.5	77.2	73.3	75.2
385	400	9	20	105.9	102.5	104.2
385	400	4	5	40.5	41.3	40.9
385	400	4	12.5	73.3	76.9	75.1
385	400	4	20	103.8	106.2	105.0
400	1200	9	5	20.2	28.2	24.2
400	1200	9	12.5	43.2	50.0	46.6
400	1200	9	20	58.2	74.7	66.5
400	1200	4	5	25.4	25.1	25.3
400	1200	4	12.5	45.2	48.7	47.0
400	1200	4	20	60.6	69.2	64.9

4.1.4 Performance

To estimate the efficiency of the spray the outlet ammonia concentration is compared to the ideal concentration. It is assumed that the only reaction (23) takes place so that the ratio between urea and ammonia is one to one. The calculations can be found in section A in the appendix.

The ideal ammonia concentrations can be found in Table 25.

Table 25: Ideal ammonia concentrations

Gas flow rate (kg/h)	Urea dosing rate(g/min)	Ammonia concentration(ppm)
400	5	117.8
400	12.5	294.5
400	20	471.3
800	5	58.9
800	12.5	147.3
800	20	235.6
1200	5	39.3
1200	12.5	98.2
1200	20	157.1

In Figure 23 it can be observed that the efficiency decreases with increased dosing amounts and with decreased flow rates. Since this behavior is similar for all tested parameters the spray efficiency is only reported for the base case. Even though the residence time is lower for a higher gas flow rate the higher energy content in the gas and the lower temperature drop over the pipe seems to compensate for this. Other contributing reasons could also be the lower inlet temperature of the gas for the highest temperatures and more break-up of droplets for the higher gas flow rates. Another reason could be differences in the radial distribution. From the temperature measurements it can be observed that more droplets are distributed in the upper

part of the pipe for the higher gas flow rates while the distribution is more even for the lower gas flow rates.

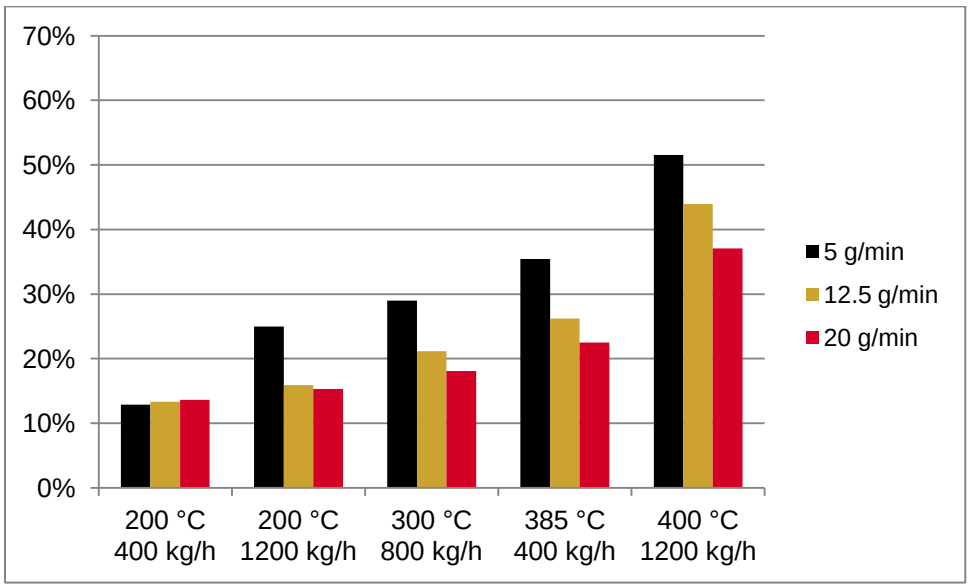

Figure 23: Percent ammonia of theoretical amount for a dosing unit pressure of 9 bar

Since the conversion of urea to ammonia is low only the smallest droplets have time to evaporate. Since most of the energy is required for water evaporation it could be likely that the increase in ammonia concentration is very slow in the first part of the pipe while the concentration increases remarkably in the end. This means that the results are obtained in a region where the ammonia concentration increases rather fast. If the sampling could have been done just a little bit downstream the concentrations should be much higher.

4.2 Temperature measurements

The evaporation rate in the pipe was also estimated from the temperature drop when the spray hits the wheel that is inserted in the pipe. The more droplets that hit the wheel, the more the temperature will drop since heat is required to evaporate the liquid film. It should be noted that the smallest droplets with low Stokes numbers will not hit the wheel. These will instead follow the gas flow past the wheel. For most experiments the wheel is located 30 cm from the injection point.

4.2.1 Temperature drop from urea decomposition

When the urea-water-solution evaporates the gas temperature will decrease since heat is required to evaporate the water and since the thermolysis reaction is endothermic. The temperature drops on the wheel is therefore a combination of the temperature loss as a result of film formation and the temperature loss due to the gas temperature decrease. Since the conversion is not known the exact temperature drop cannot be estimated.

The gas temperature decreases for complete decomposition of urea for the tested operating conditions are shown in Table 26. The calculations can be found in section A in the appendix.

The temperature drops will be higher for lower gas flow rates since less heat is available from the gas.

Table 26: Gas temperature drops for tested operating conditions

Gas temperature (°C)	Gas flow rate(kg/h)	Urea dosing rate(g/min)	Temperature drop(°C)
200	400	5	2.1
200	400	12.5	5.3
200	400	20	8.4
200	1200	5	0.7
200	1200	12.5	1.8
200	1200	20	2.8
300	800	5	1.1
300	800	12.5	2.7
300	800	20	4.4
385	400	5	2.3
385	400	12.5	5.7
385	400	20	9.1
400	1200	5	0.7
400	1200	12.5	1.9
400	1200	20	3.0

4.2.2 Reproducibility

The results from three repeated measurements made in the beginning, middle and the end of a 7-cycle run are shown in Figure 24. It can be observed that there are some fluctuations in the temperature due to fluctuations in the gas temperature.

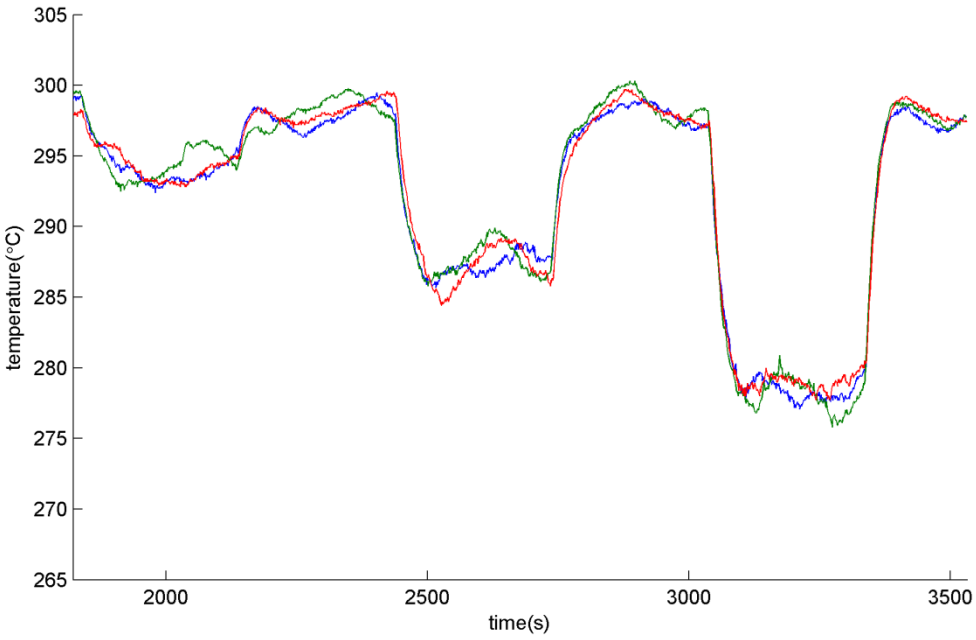

Figure 24: Repeated measurements at the middle position for 300 °C, 800 kg/h and dosing unit pressure 6.5 bar for urea dosing rates of 5, 12.5 and 20 g/min

For other positions (i.e. the bottom position that is shown in Figure 25) the temperature drops are hard to distinguish for lower dosing amounts. The fluctuations are caused by fluctuations in the inlet gas temperature that increase for high temperatures and high gas flow rates. It can also be seen that there are some differences in the starting temperature.

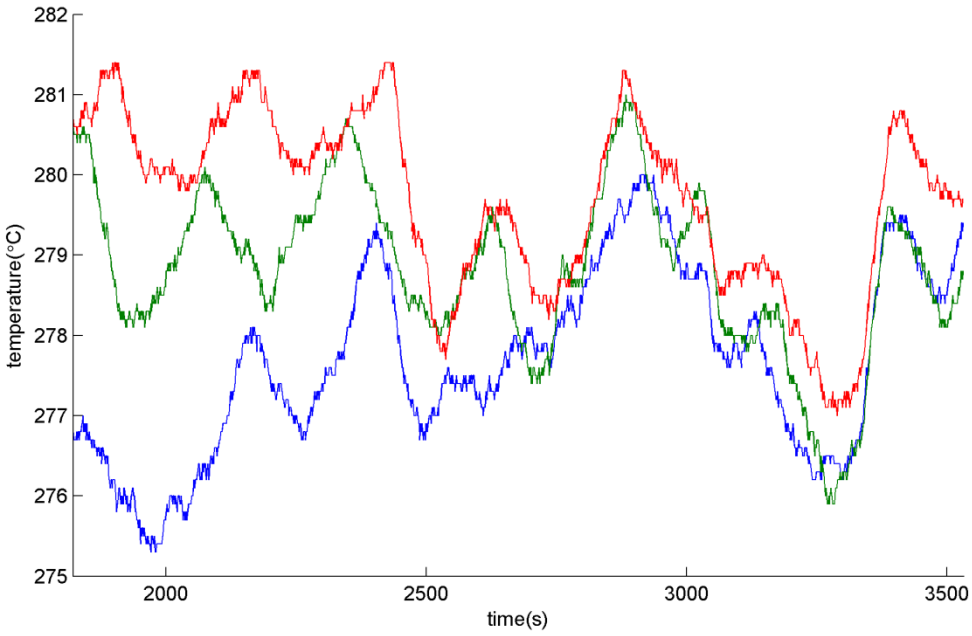

Figure 25: Repeated measurements at position C1 for 300 °C, 800 kg/h and dosing unit pressure 6.5 bar for urea dosing rates of 5,12.5 and 20 g/min

The analysis of variance for the repeated runs is shown in Table 27. It is done for the mean temperature drop that is calculated from the mean temperature during the last 100 seconds of dosing and the mean temperature 30 seconds before dosing. To compensate for the temperature fluctuations the temperature is corrected with the deviation from the set temperature. All temperature drops can be found in section C in the appendix. A significant effect for the runs indicates that one or more of the means for all flow rates and positions in one run is different from the other runs. A significant effect for the interaction between the position and runs indicates that there are positions where the mean temperature drops for all flow rates differs from the mean temperature drops at the same point for one or more of the others runs. A significant interaction between urea dosing rate and runs indicates that there are urea dosing rates for which the mean temperature drops for all positions differs from one or more of the means for the same urea dosing rates for the other runs. It can be observed that the effects of the runs and the interaction between urea dosing rate and runs are significant.

Table 27: Analysis of variance for repeated measurements

Source	Sum of squares	DOF	Mean sum of squares	F	Prob>F
Position	17685.30	15	1179.02	1370.80	0.00
Urea dosing rate	10060.14	2	5030.07	5848.27	0.00
Run	14.78	2	7.39	8.59	0.00
Position·Urea dosing rate	7456.75	30	248.56	288.99	0.00
Position·Run	29.71	30	0.99	1.15	0.32
Urea dosing rate · Run	14.02	4	3.50	4.07	0.01
Error	51.61	60	0.86		
Total	35312.31	143			

In Table 28 and it can be seen that the confidence interval for the mean temperature drop for run 2 does not overlap with the one for run 1 and 3, although the differences are rather small.

Table 28: Mean temperature drop for repeat runs

Run	Confidence interval for mean temperature drop (°C)		
	Lower bound	Mean	Upper bound
1	13.4	13.6	13.8
2	14.1	14.4	14.6
3	13.5	13.8	14.0

In Table 29 it can be seen that the confidence interval for the mean temperature drop for run 2 and 3 do not overlap for the highest flow rate.

Table 29: Confidence intervals for temperature drop for each urea dosing rate and run

Urea dosing rate(g/min)	Run	Confidence interval for mean temperature drop (°C)		
		Lower bound	Mean	Upper bound
5	1	3.7	4.2	4.7
	2	4.3	4.8	5.3
	3	4.3	4.8	5.3
12.5	1	11.2	11.7	12.3
	2	12.1	12.6	13.2
	3	11.9	12.4	12.9
20	1	24.3	24.9	25.4
	2	25.1	25.6	26.1
	3	23.6	24.1	24.7

For the interpretation of the results it might be necessary to be careful since some effects can appear because of experimental error and how the data is treated. It could also be good to consider the confidence intervals between the means as well as the significance and not draw conclusions from differences that are very small. From the repeated measurements it can be seen that differences of about 1-2 °C can appear for the mean temperatures.

4.2.3 Spray distribution in the pipe

To get an overview of the spray distribution in the pipe and of the evaporation rate the mean temperature drop in each point is estimated. The temperature drop in one point is calculated from the mean temperature during the last 100 seconds of dosing and the mean temperature 30 seconds before dosing. To compensate for the temperature fluctuations the temperature is corrected with the deviation from the set temperature. The temperature drop for each position can be found in section C in the appendix.

The temperature drops in each point for a gas temperature of 200 °C and a gas flow rate of 400 kg/h are shown in Figure 26. Since the temperature drops are larger than what would occur through urea decomposition the main reason is liquid droplets hitting the wheel. The temperature drop is much larger for the dosing unit pressure of 4 bar and for a spray angle of 35 degrees which indicates that the droplet sizes for these parameters could be similar. It can be observed that a plug flow has not been obtained since more of the spray is directed towards the upper part of the wheel. It can also be seen that the distribution is slightly different for the different parameters. For the dosing unit pressure of 4 bar little of the spray hits the edges at the lower part of the wheel. This is probably because the droplets are ejected with a lower velocity and therefore travel a shorter distance before they are entrained with the flow. This makes the spray distribution similar to that for a spray angle of 35 degrees. The distributions with different frequencies are similar.

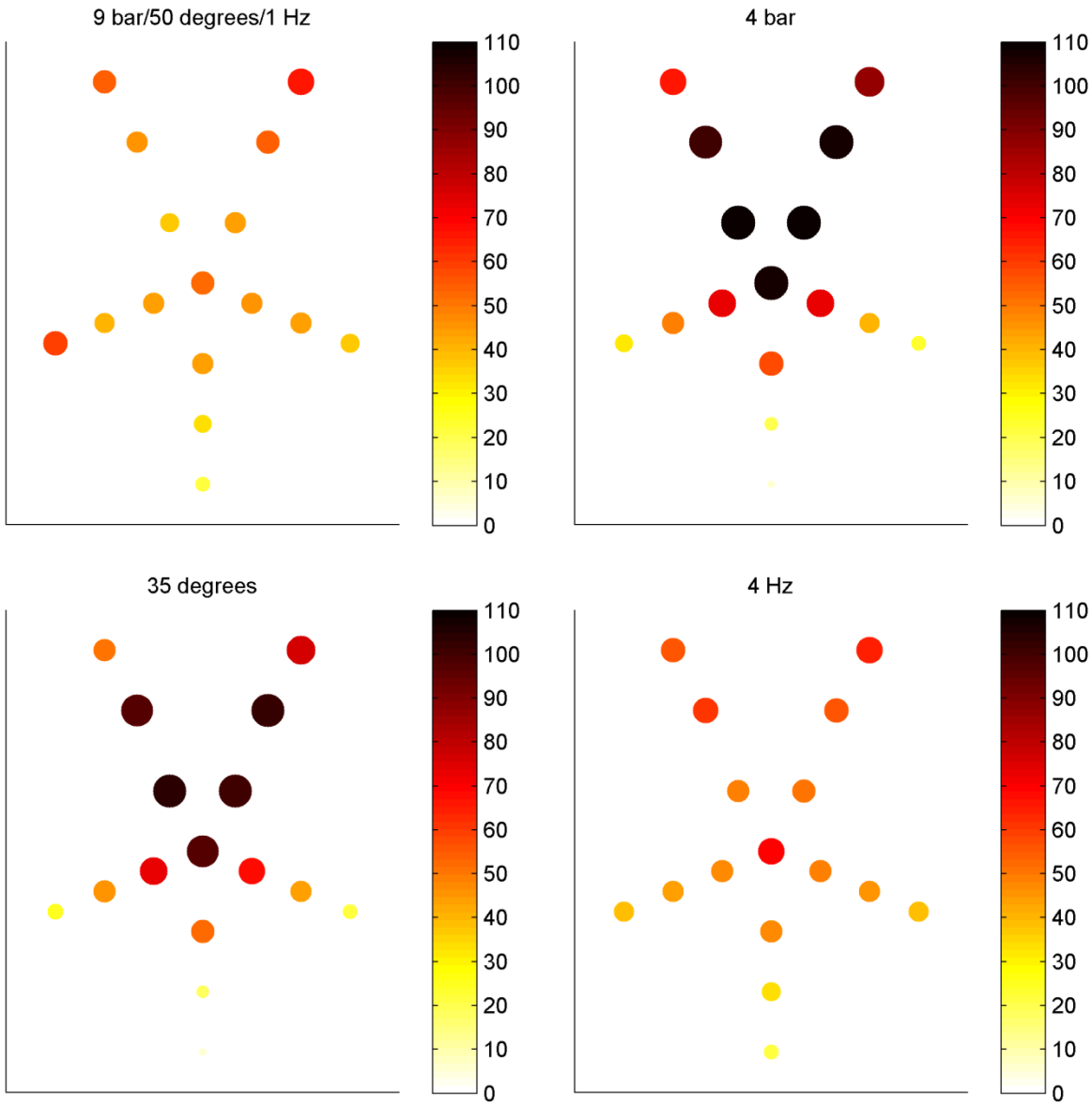

Figure 26: Temperature drops for a gas temperature of 200 °C and a gas flow rate of 400 kg/h with a urea dosing rate of 20 g/min

For a higher flow rate that is shown in Figure 27, the temperature drops are still higher than they would be for urea decomposition. It can be seen that very little of the spray hits the lower part of the wheel, especially for the dosing unit pressure of 4 bar and for the spray angle of 35 degrees. The distribution of the spray is very uneven and it seems like a lot of the spray hits the wall. Since the distributions are very different it is difficult to tell what the effect is on the overall evaporation rate. The distributions for the different frequencies are similar.

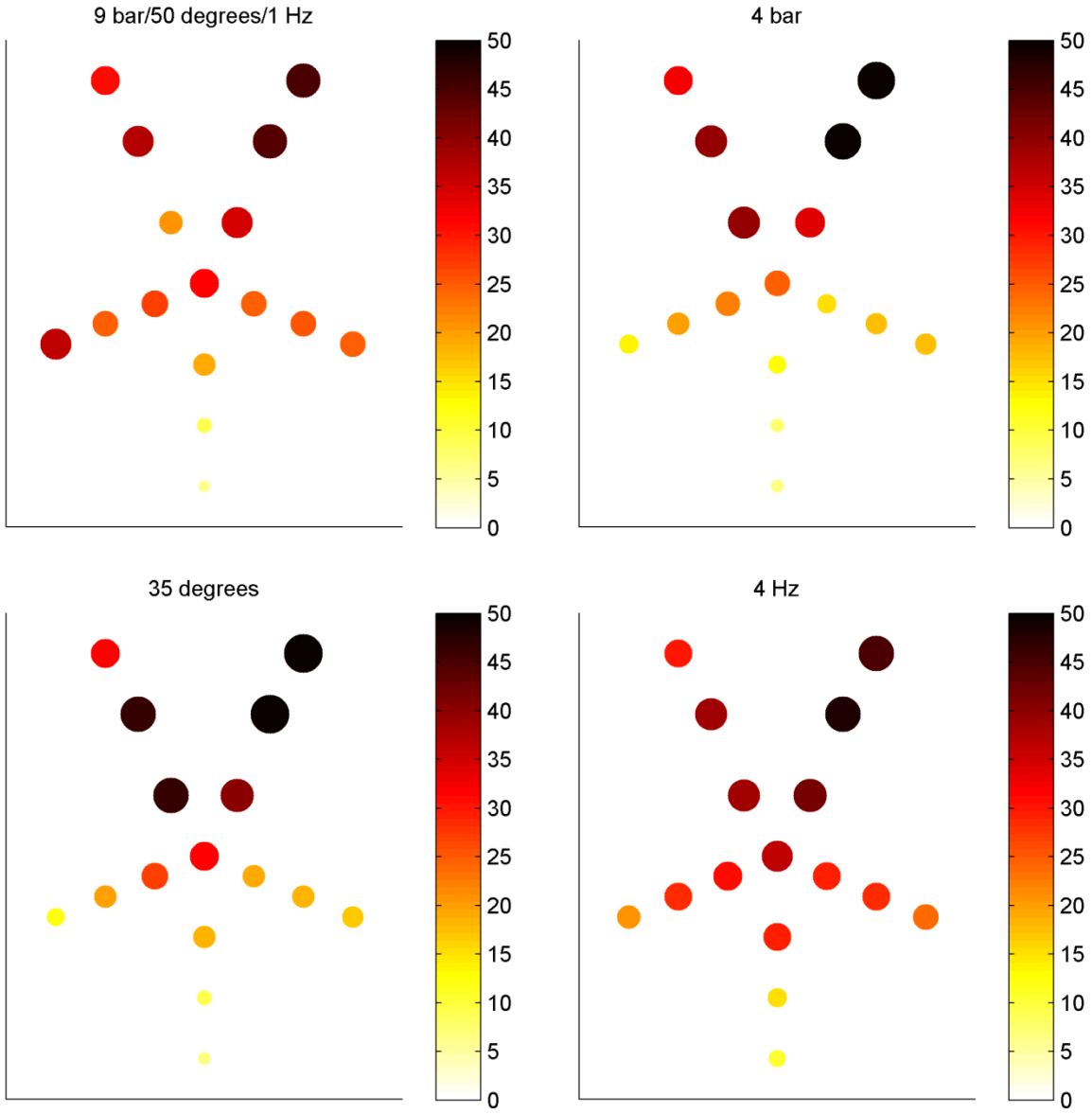

Figure 27: Temperature drops for a gas temperature of 200 °C and a gas flow rate of 1200 kg/h with a urea dosing rate of 20 g/min

The temperature drops for a gas temperature of 300 °C and a gas flow rate of 800 kg/h are shown in Figure 28. The temperature drops are larger than they would be for urea decomposition. As before the distribution of the spray is very uneven. A lot of droplets still remain in the upper part of the pipe for the dosing unit pressure of 4 bar and for the spray angle of 35 degrees which indicates that the evaporation rate is lower for these parameters. The distributions for the different frequencies are similar.

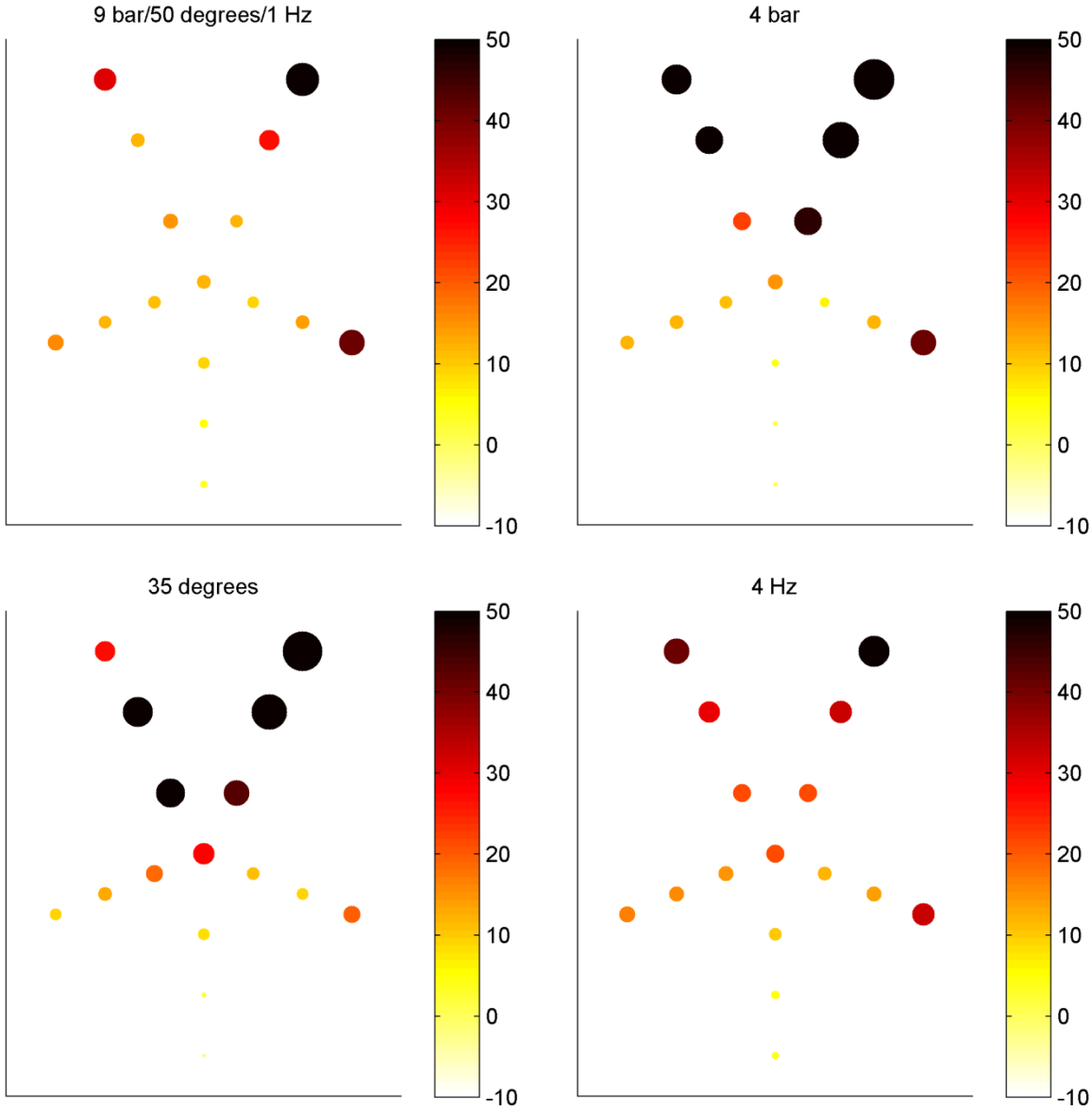

Figure 28: Temperature drops for a gas temperature of 300 °C and a gas flow rate of 800 kg/h with a urea dosing rate of 20 g/min

The temperature drops for a gas temperature of 385 °C and a gas flow rate of 400 kg/h are shown in Figure 29. For this operating condition the differences are much smaller and the values of the temperature drops starts to approach those that could be due to urea decomposition. The distributions are similar but it can be seen that the temperature drops on the upper part of the wheel are somewhat higher for a spray angle of 35 degrees. If these results are compared to those for a lower temperature it can be seen that the temperature drops in the middle are smaller while they are larger at the edges. One reason could be that the small droplets that should be found in the middle evaporate faster when the temperature is increased.

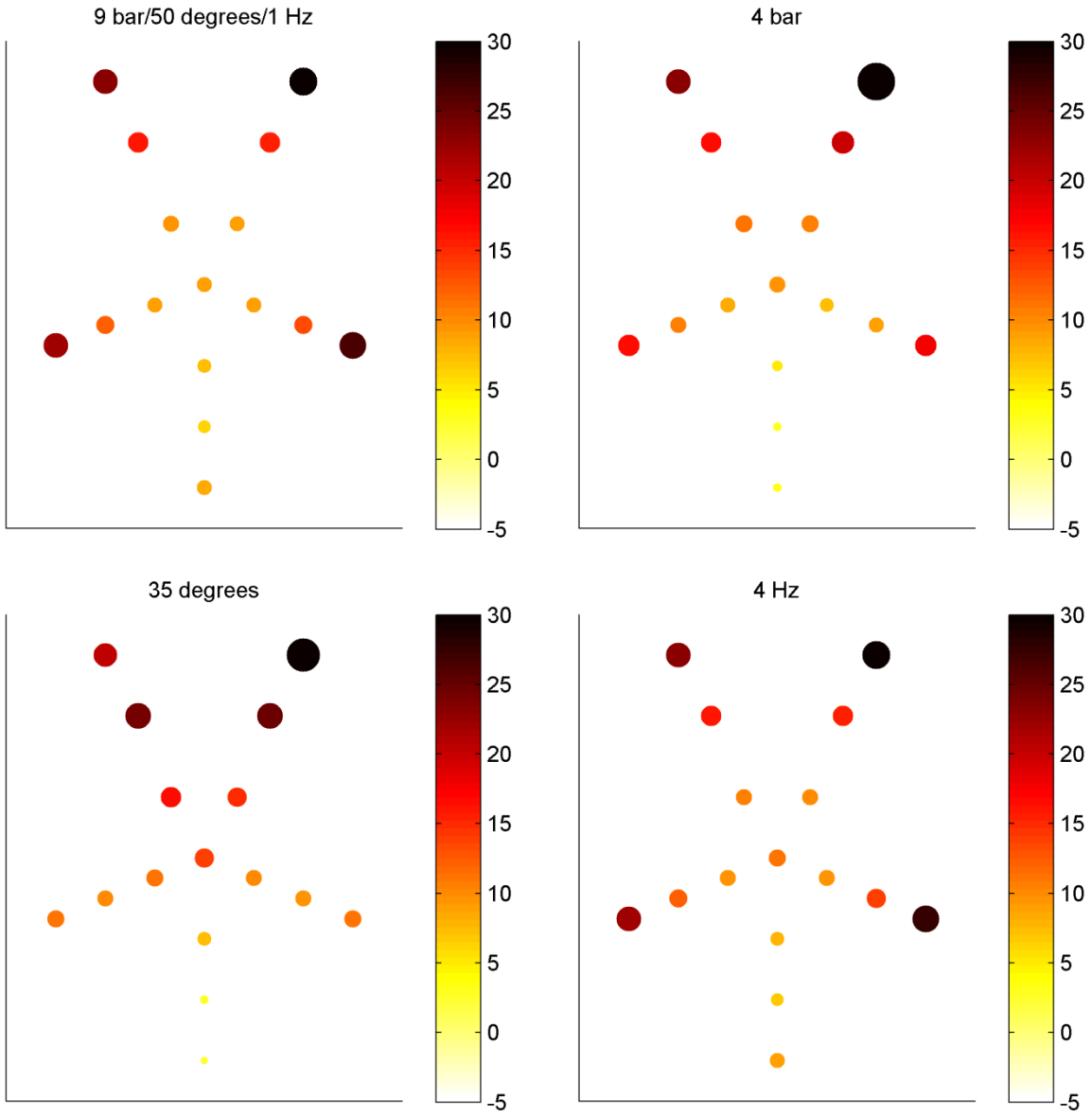

Figure 29: Temperature drops for a gas temperature of 385 °C and a gas flow rate of 400 kg/h with a urea dosing rate of 20 g/min

The temperature drops for a gas temperature of 400 °C and a gas flow rate of 1200 kg/h are shown in Figure 30. The temperature drops and the distribution are similar for all parameters. In the middle the values of the temperature drops start to approach those for urea decomposition but it can be seen that droplets remain towards the edges.

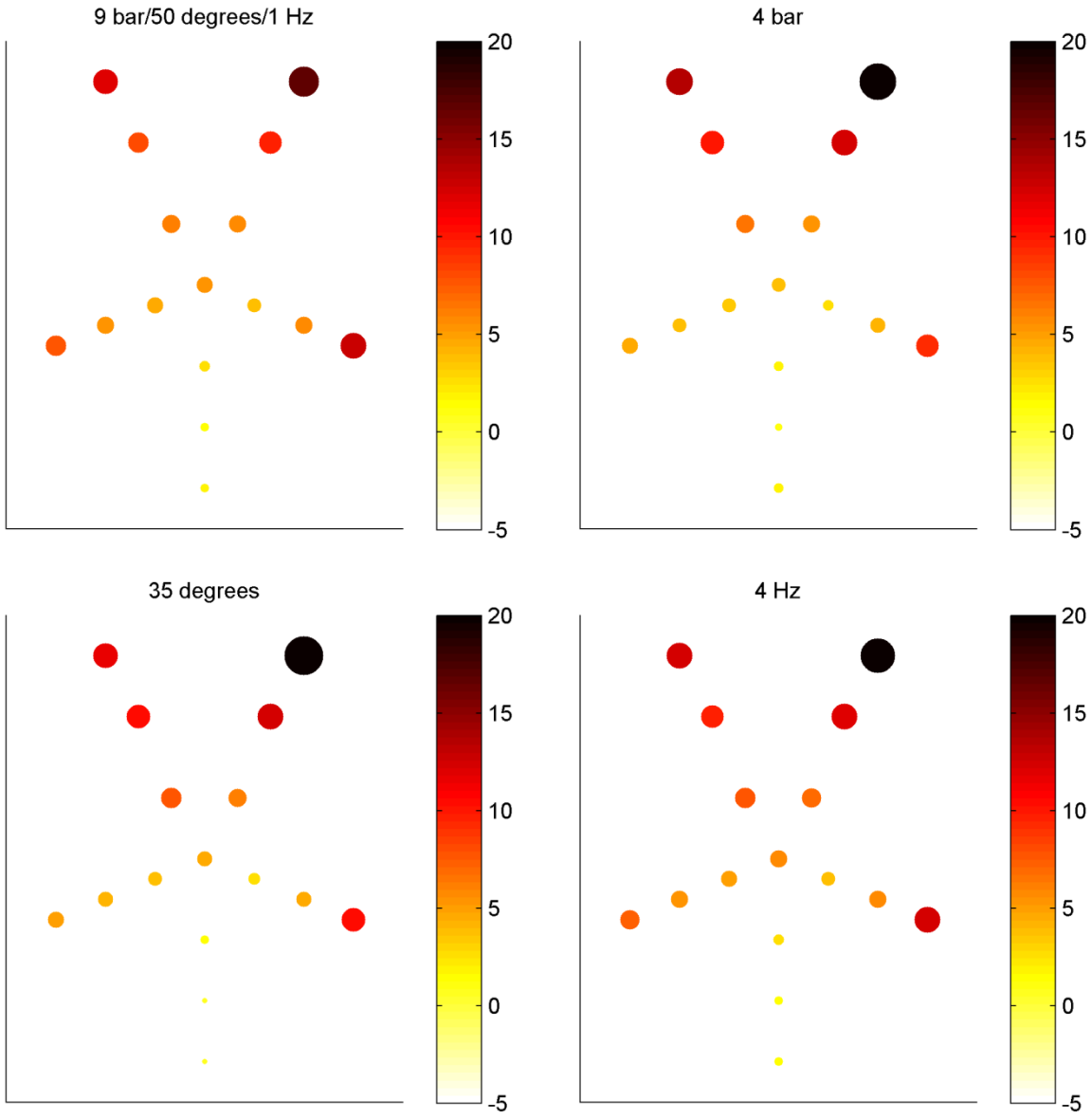

Figure 30: Temperature drops for a gas temperature of 400 ° and a gas flow rate of 1200 kg/h with a urea dosing rate of 20 g/min

4.2.4 Statistic evaluation

A statistic evaluation was done to investigate the influence for each parameter on the overall evaporation rate and the distribution. This was done with an ANOVA-test that is followed by investigation of the confidence intervals for the parameters where significant differences appear. A significant effect of the dosing unit pressure indicates that there is a significant difference for all positions and flow rates which indicates that the overall evaporation rate is

lower. A significant difference for the interaction between position and dosing unit pressure is an indication on a different distribution or different evaporation rate. A significant difference for the interaction between dosing unit pressure and urea dosing rate also indicates differences in the evaporation rate but that there is a difference depending on the urea dosing rate.

4.2.4.1 Effect of dosing unit pressure

The results from the ANOVA-test for all operating conditions are summarized in Table 30. The complete ANOVA-tests can be found in section D in the appendix. It can be observed that the effect of the dosing unit pressure is significant on a 95 percent confidence level for all operating points except for a gas flow rate of 400 kg/h and a temperature of 385 °C. Also, the interaction effect between dosing unit pressure and the position is significant which indicates that the distribution of the spray is different for the two pressures. The interaction between dosing unit pressure and urea dosing rate is significant for some operating conditions.

Table 30: Summary of ANOVA-tests for pressure change

Temperature (°C)	Gas flow rate (kg/h)	Dosing unit pressure		Dosing unit pressure · Position		Dosing unit pressure · Urea dosing rate	
		F0	Prob>F	F0	Prob>F	F0	Prob>F
200	400	87.92	0.00	12.96	0.00	6.06	0.01
200	1200	8.40	0.01	13.93	0.00	1.33	0.28
300	800	13.32	0.00	3.32	0.00	4.74	0.02
385	400	0.06	0.81	2.20	0.03	0.03	0.97
400	1200	4.64	0.04	6.44	0.00	4.24	0.02

Even though a parameter does give a significant effect it does not necessarily mean that the differences between the mean temperature drops are large. The confidence intervals for the mean temperature drops for the tested dosing unit pressures for each operating condition can be seen in Table 31.

Table 31: Confidence intervals for mean temperature drops for different dosing unit pressures

Temperature (°C)	Gas flow rate(kg/h)	Dosing unit pressure (bar)	Confidence interval for mean temperature drop(°C)		
			Lower bound	Mean	Upper bound
200	400	9	28.2	29.7	31.3
		4	42.3	43.9	45.4
200	1200	9	16.5	17.0	17.4
		4	15.2	15.7	16.1
300	800	9	9.1	10.7	12.1
		4	14.4	15.9	17.4
385	400	9	8.0	8.5	9.0
		4	7.9	8.4	8.9
400	1200	9	3.7	3.9	4.00
		4	4.02	4.2	4.3

For the points where the difference is significant a dosing unit pressure of 4 bar gives higher mean temperature drops for all operating points except for a gas temperature of 200 °C and a

flow rate of 1200 kg/h. The difference is largest for a temperature of 200 °C and a flow rate of 400 kg/h which indicates that the droplet size has more impact on the evaporation rate at low temperatures and low flow rates, i.e. when the available energy content to evaporate the urea is limited.

The points where Tukey's test indicates that the differences are significant on a 95 percent level are shown in Table 32. It can be observed that the number is highest for a gas temperature of 200 °C and a gas flow rate of 400 kg/h. The positions of the thermo elements on the wheel are shown in Figure 35. The test corresponds well to the contour plot although it is rather conservative.

Table 32: Points with significant differences

Temperature (°C)	Gas flow rate (kg/h)	Positions with significant differences
200	400	Middle, A1, A2, E1, E2
200	1200	D3,E1
300	800	A1,A2
385	400	A3
400	1200	A3

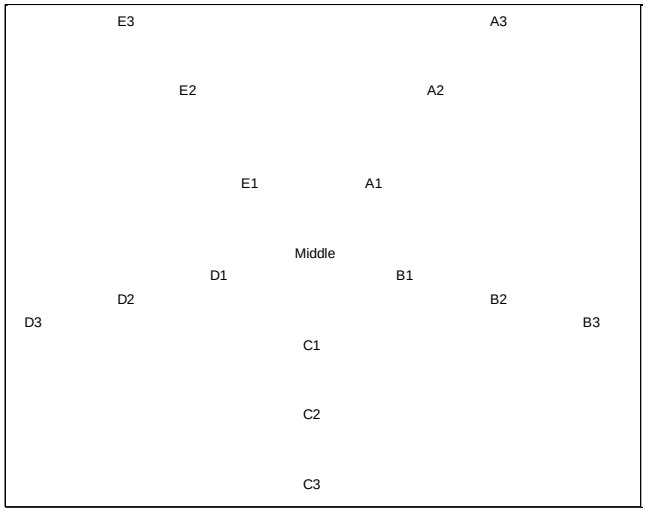

Figure 31: Positions of thermo elements on the wheel

The confidence intervals for the mean temperature drops at each dosing unit pressure and urea dosing rate for a gas temperature of 200 °C and a gas flow rate of 1200 kg/h are shown in Figure 32. The confidence intervals are more separated for higher urea dosing rates which could be an indication that the droplet size is more important when the heat required to evaporate all urea increases. This agrees with the suggestion that the droplet size is more important when the energy content of the gas is low.

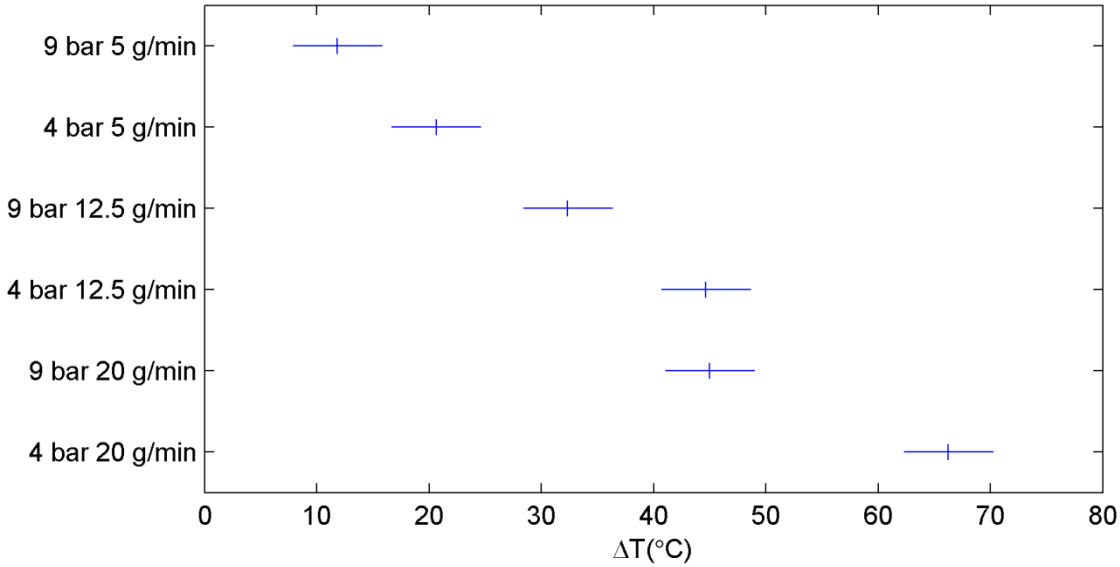

Figure 32: Confidence intervals for the mean temperature for all positions drops at a gas temperature of 200 °C and a gas flow rate of 400 kg/h

The confidence intervals for the mean temperature drops for each flow rate at a gas temperature of 300 °C and a gas flow rate of 800 kg/h are shown in Figure 33. The difference is only significant for the highest urea dosing rate but it can be seen that the distance between the means increase with the dosing rate. Again, this could be an indication that the droplet size is important when the available energy to evaporate all urea is limited.

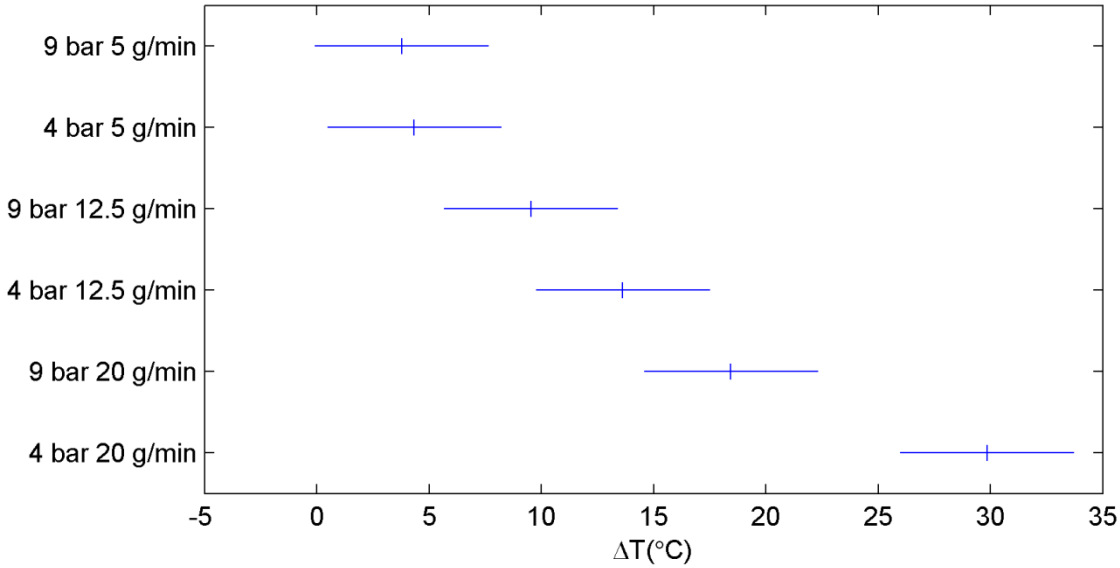

Figure 33: Confidence intervals for the mean temperature drops for all positions at a gas temperature of 300 °C and a gas flow rate of 800 kg/h

The confidence intervals for the mean temperature drops for each flow rate at a gas temperature of 300 °C and a gas flow rate of 800 kg/h are shown in Figure 34. The reason why the difference is significant for the lowest flow rate is probably difficulties calculating a

correct mean temperature since the temperature fluctuations are large while the temperature drops are small.

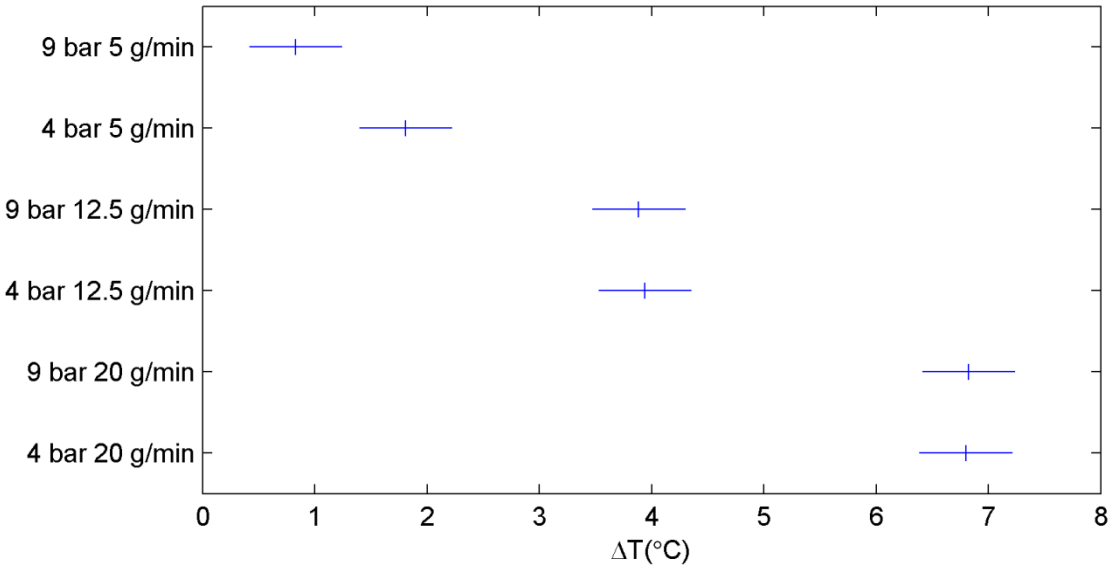

Figure 34: Confidence intervals for the mean temperature drops for all positions at a gas temperature of 400 °C and a gas flow rate of 1200 kg/h

4.2.4.2 Effect of spray angle

The results from the ANOVA-test with different spray angles are summarized in Table 33. The complete ANOVA-tests can be found in section D in the appendix. Again the only point where the effect of the spray angle does not give significant results for the mean temperature drop for all flow rates and positions is a flow rate of 400 kg/h with a gas temperature of 385 °C. The interaction between spray angle and position is significant for all operating conditions. The interaction between spray angle and urea dosing rate only gives significant differences for the temperature of 300 °C and a flow rate of 800 kg/h.

Table 33: Summary of ANOVA-tests for angle changes

Temperature (°C)	Gas flow rate (kg/h)	Spray angle		Spray angle · Position		Spray angle ·Urea dosing rate	
		F0	Prob>F	F0	Prob>F	F0	Prob>F
200	400	51.47	0.00	10.41	0.00	2.90	0.07
200	1200	6.41	0.02	13.82	0.00	0.12	0.89
300	800	24.04	0.00	5.37	0.00	4.07	0.03
385	400	1.03	0.32	4.55	0.00	0.12	0.89
400	1200	14.03	0.00	5.44	0.00	1.29	0.29

The confidence intervals for the different angles are shown in Table 34. The 35 degree spray gives higher temperature drops for all operating conditions. The largest differences appear for the same operating conditions as for the dosing unit pressure.

Table 34: Confidence intervals for mean temperature drops for spray angles

Temperature (°C)	Gas flow rate (kg/h)	Spray angle (degrees)	Confidence interval for mean temperature drop (°C)		
			Lower bound	Mean	Upper bound
200	400	50	28.1	29.7	31.3
		35	39.4	41.0	42.6
200	1200	50	16.4	17.0	17.5
		35	17.8	18.3	18.8
300	800	50	9.3	10.6	11.9
		35	15.7	17.0	18.4
385	400	50	8.0	8.5	9.0
		35	8.5	9.00	9.5
400	1200	50	3.6	3.9	4.1
		35	4.4	4.6	4.8

The positions where Tukey's test indicates that the differences are significant are shown in Table 35. The positions are shown in Figure 35. There are significant differences for more points for lower flow rates and temperatures. The test corresponds quite well to what can be seen in the contour plots although it is conservative.

Table 35: Points with significant differences

Temperature (°C)	Gas flow rate (kg/h)	Positions with significant differences
200	400	Middle, A1, A2, E1, E2
200	1200	A2, A3, D3, E1
300	800	A2, A3, E2
385	400	B3
400	1200	A3

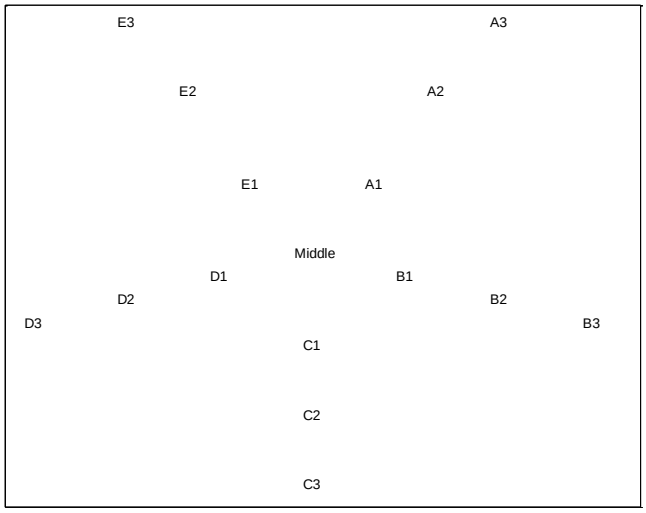

Figure 35: Positions of thermo elements on the wheel

The confidence intervals for the mean temperature drops for each flow rate at a gas temperature of 200 °C and a gas flow rate of 400 kg/h are shown in Figure 36. There is a

significant difference for the two highest urea dosing rates. Also, it can be seen that the differences increase with the urea dosing rate. This is similar to the runs where the dosing unit pressure is changed.

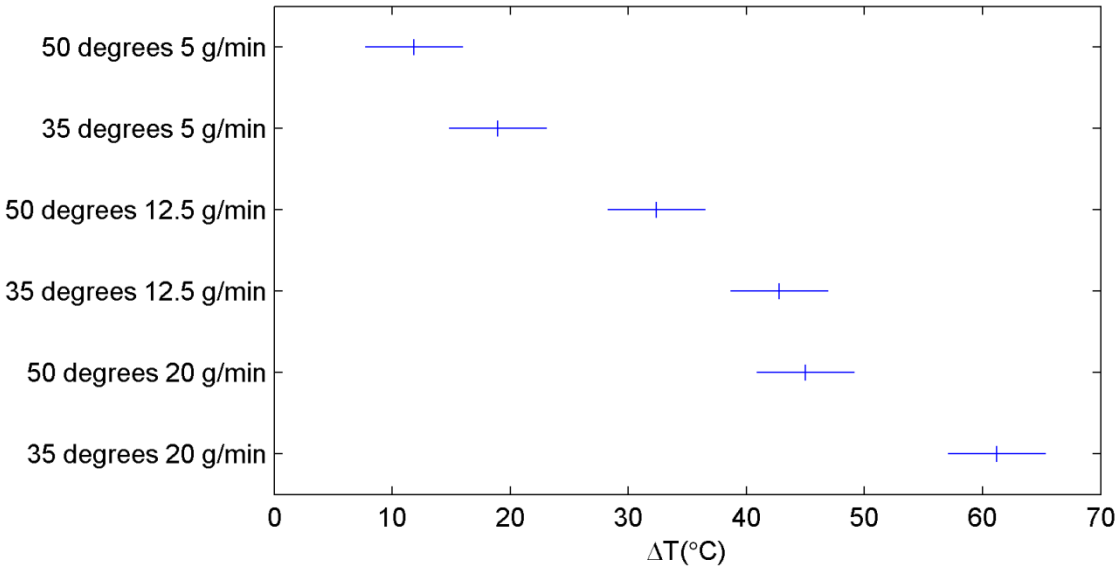

Figure 36: Confidence intervals for the mean temperature drops for all positions at a gas temperature of 200 °C and a gas flow rate of 400 kg/h

The confidence intervals for the mean temperature drops for each flow rate at a gas temperature of 300 °C and a gas flow rate of 800 kg/h are shown in Figure 37. The difference is significant for the highest urea dosing rate as for the change in dosing unit pressure.

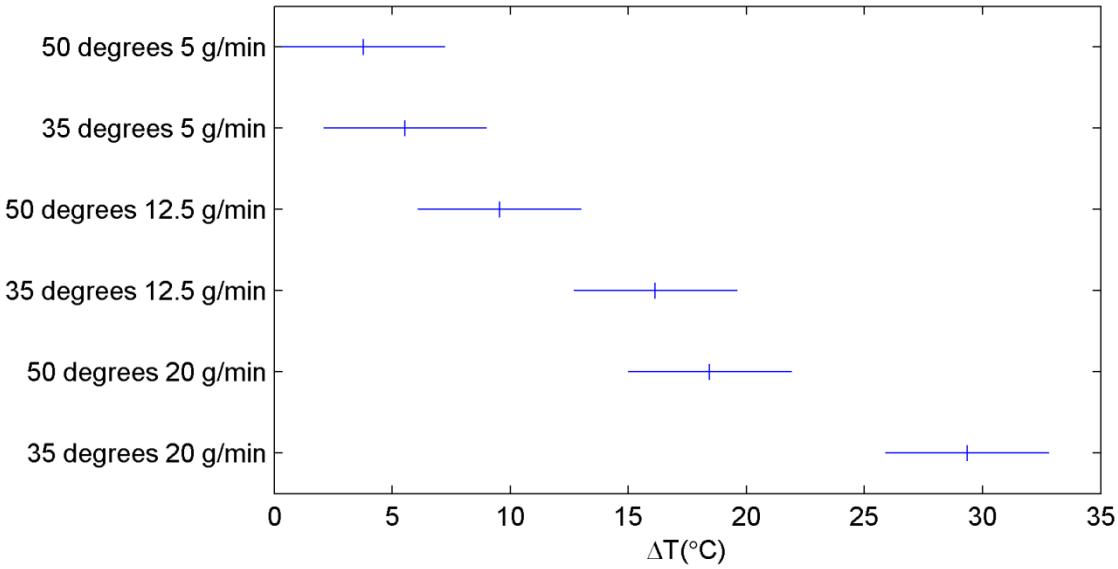

Figure 37: Confidence intervals for the mean temperature drops for all positions at a gas temperature of 300 °C and a gas flow rate of 800 kg/h

4.2.4.3 Effect of frequency

The results from the statistic evaluation in the different operating points are summarized in Table 36. The complete results are available in section D in the appendix. The frequency gives significant differences for the higher temperatures but the differences in the temperature drops are small compared to the differences for the other parameters. Even though the difference for the different frequencies is larger for the lower temperature the variance is larger which means that the null hypothesis cannot be rejected. Since the runs were only done for one dosing rate the interaction effects cannot be estimated.

Table 36: Summary of ANOVA-tests for frequency changes

Temperature (°C)	Gas flow rate(kg/h)	F0	Prob>F	Frequency (Hz)	Confidence interval for mean temperature drop (°C)		
					Lower bound	Mean	Upper bound
200	400	2.50	0.13	1	42.8	45.0	47.3
				4	46.1	48.4	50.7
200	1200	3.92	0.07	1	25.6	27.5	29.3
				4	29.1	30.9	32.8
300	800	5.16	0.04	1	16.8	18.5	20.1
				4	20.4	22.1	23.7
385	400	20.76	0.00	1	13.9	14.0	14.2
				4	14.5	14.7	14.8
400	1200	4.41	0.05	1	6.5	6.8	7.2
				4	7.2	7.5	7.9

4.2.5 Temperature drops along the pipe

For the operating point 200 °C and 400 kg/h the temperature drops on the wheel was measured at four positions along the pipe. This operating point was chosen since this gave the lowest evaporation rate for all parameters. The FTIR results also indicate that there are droplets left in the end of the pipe which was confirmed from the temperature measurements.

The mean temperature drop for all positions on the wheel for four residence times along the pipe is shown in Figure 38.

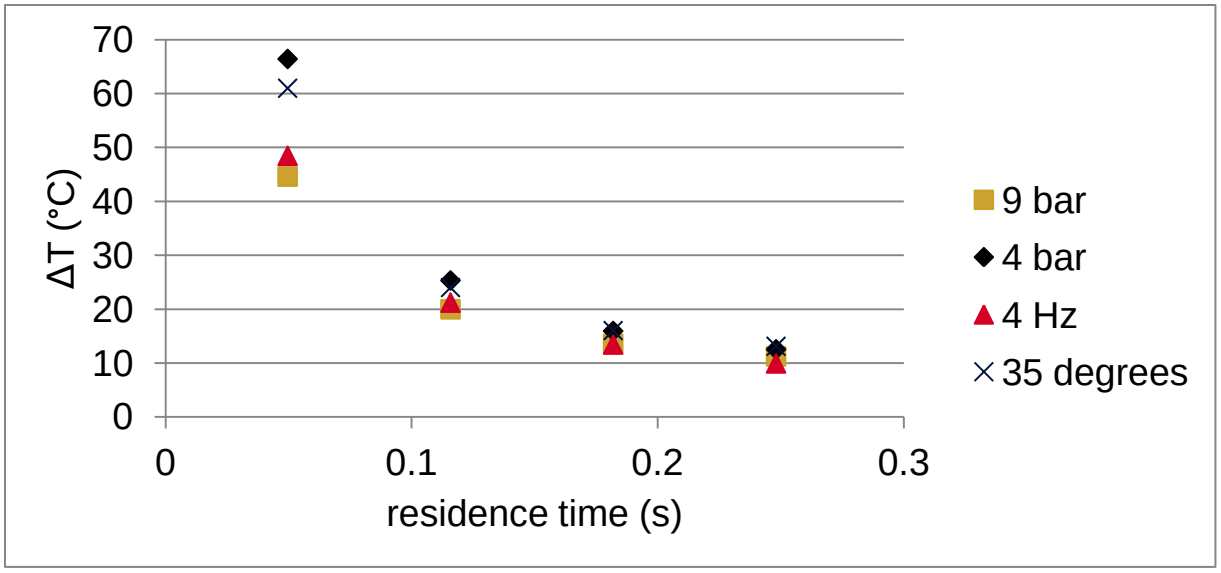

Figure 38: Mean temperature drop for a gas flow rate of 400 kg/h and a gas temperature of 200 °C with a urea dosing rate of 20 g/min

In Figure 38 it can be observed that the droplets break up and evaporate quickly in the beginning but that the rate decreases along the pipe. The difference for each parameter change gets smaller along the pipe. The value will not approach a value of zero since the temperature drop is also caused by a combination of evaporation of urea from the surface and the decrease of the gas temperature caused by urea evaporation and decomposition. In Table 26 it can be seen that the temperature drop for this operating point and urea dosing rate should be 8.4 degrees if all urea is evaporated.

The result from the ANOVA-test for the dosing unit pressure is shown in Table 37. These show that all effects that include the dosing unit pressure are significant.

Table 37: Analysis of variance for change of dosing unit pressure in the end of the pipe

Source	Sum of squares	DOF	Mean sum of squares	F	Prob>F
Position	278.72	15	18.58	20.81	0.00
Urea dosing rate	1186.21	2	593.11	664.19	0.00
Dosing unit pressure	142.95	1	142.95	160.09	0.00
Position·Urea dosing rate	78.98	30	2.63	2.95	0.00
Position·Dosing unit pressure	36.39	15	2.43	2.72	0.01
Urea dosing rate · Dosing unit pressure	7.52	2	3.76	4.21	0.02
Error	26.79	30	0.89		
Total	1757.55	95			

The result from the ANOVA-test for dosing unit angle is shown in Table 38. The test shows that all effects that includes the dosing unit pressure are significant.

Table 38: Analysis of variance for change of dosing unit angle in the end of the pipe

Source	Sum of squares	DOF	Mean sum of squares	F	Prob>F
Position	188.14	15	12.54	34.36	0.00
Urea dosing rate	1250.49	2	625.24	1713.01	0.00
Angle	116.50	1	116.50	319.18	0.00
Position·Urea dosing rate	93.22	30	3.11	8.51	0.00
Position·Angle	18.65	15	1.24	3.41	0.00
Urea dosing rate · Angle	12.39	2	6.20	16.98	0.00
Error	10.95	30	0.37		
Total	1690.35	95			

The result from the ANOVA-test for frequency is shown in Table 39. The test shows that the effect of the dosing frequency is significant.

Table 39: Analysis of variance for change of frequency in the end of the pipe

Source	Sum of squares	DOF	Mean sum of squares	F	Prob>F
Position	190.66	15	12.71	23.89	0.00
Frequency	3.12	1	3.12	5.87	0.03
Error	7.98	15	0.53		
Total	201.77	31			

Even though the effects are smaller the difference is significant for all parameters. This is because the variance in the end of the pipe is smaller and the confidence intervals are narrower as can be seen in Table 40.

Table 40: Confidence intervals for the mean temperature drop in the end of the pipe

		Confidence interval for mean temperature drop(°C)		
		Lower bound	Mean	Upper bound
Dosing unit	9	6.0	6.2	6.4
pressure(bar)	4	8.5	8.7	8.9
Spray angle	50	6.1	6.2	6.4
(degrees)	35	8.3	8.4	8.6
Frequency	1	9.9	10.2	10.5
(Hz)	4	9.3	9.6	9.9

4.3 Wall temperatures

The temperature measurements on the wall correspond quite well to those on the wheel. The largest differences occur for lower temperatures which will be shown in this report. For the higher temperatures the differences are very small or difficult to distinguish because of temperature fluctuations. The minimum temperature that is reached during the dosing cycle are shown for the thermo elements at 0 degrees and for a urea dosing rate of 20 g/min. A lower temperature indicates that more film formation occurs at that position. The reference shows the temperature for that position without dosing.

4.3.1 Effect of dosing unit pressure

The minimum temperature for during the dosing unit period for a gas flow rate of 400 kg/h is presented in Figure 39. For a dosing unit pressure of 4 bar the spray hits the wall further down the pipe. This is probably due to a lower droplet velocity. When the spray hits the wall more film formation occurs since more droplets remain in the spray. The reason why the temperature for the reference is lower for the first three positions is probably that the insulation is somewhat better for the positions further down the pipe.

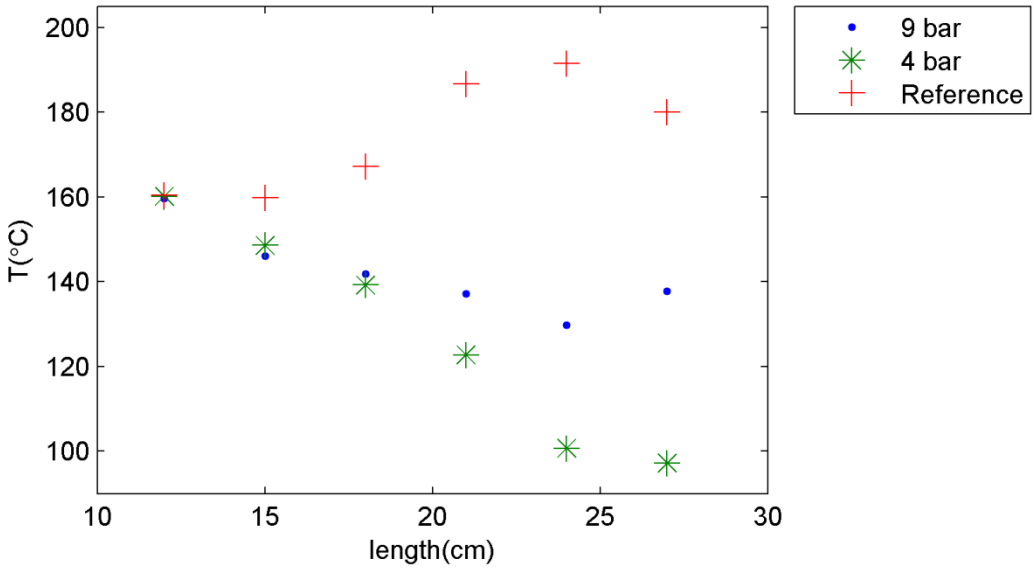

Figure 39: Minimum wall temperature during the dosing period for a gas temperature of 200 °C and a gas flow rate of 400 kg/h with a urea dosing rate of 20 g/min

For the higher flow rate somewhat more film formation occurs for the lower dosing unit pressure as seen in Figure 40. The reason is probably that more droplets are entrained towards the upper part of the pipe which could be seen in the contour plots.

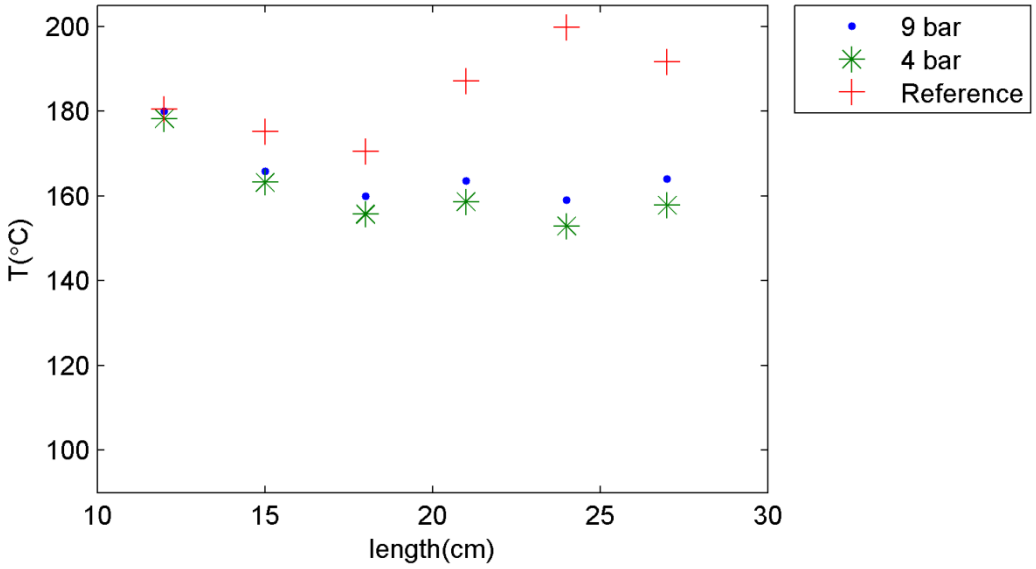

Figure 40: Minimum wall temperatures during the dosing period for a gas temperature of 200 °C and a gas flow rate of 1200 kg/h with a urea dosing rate of 20 g/min

4.3.2 Effect of spray angle

The minimum wall temperatures during the dosing period for a gas flow rate of 400 kg/ h are presented in Figure 41. The spray hits the wall later since the spray angle is more narrow. When it does more film formation occurs although it is less than for the lower dosing unit pressure. The reason is probably that more droplets remain in the spray which could be seen in the contour plots.

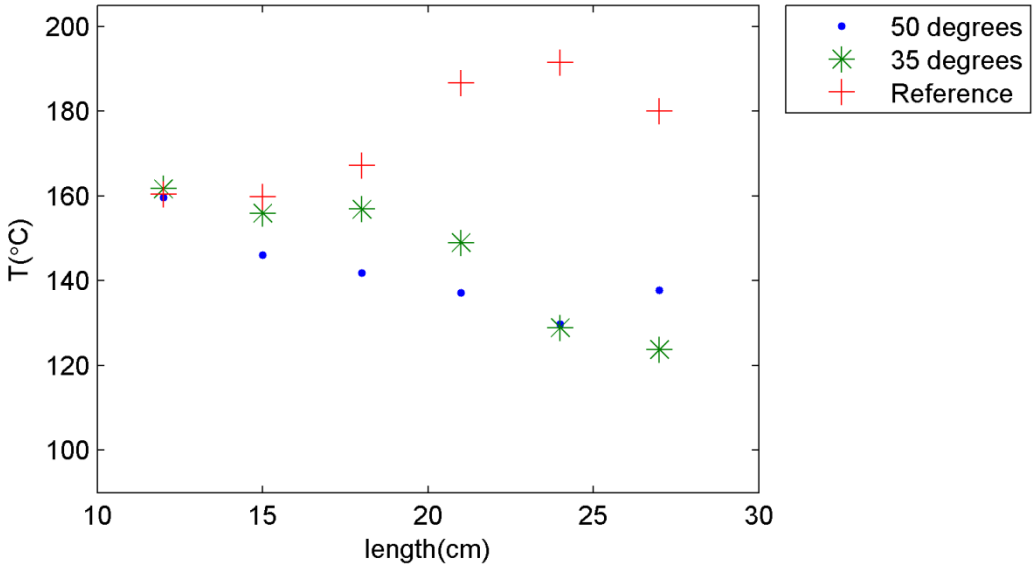

Figure 41: Minimum wall temperatures during the dosing period for a gas temperature of 200 °C and a gas flow rate of 400 kg/h with a urea dosing rate of 20 g/min

For a higher gas flow rate, somewhat more film formation occurs further down the pipe for the spray angle of 35 degrees as seen in Figure 42. The reason is probably that more droplets remain in the spray and that there is more entrainment of droplets as could be seen in the contour plots.

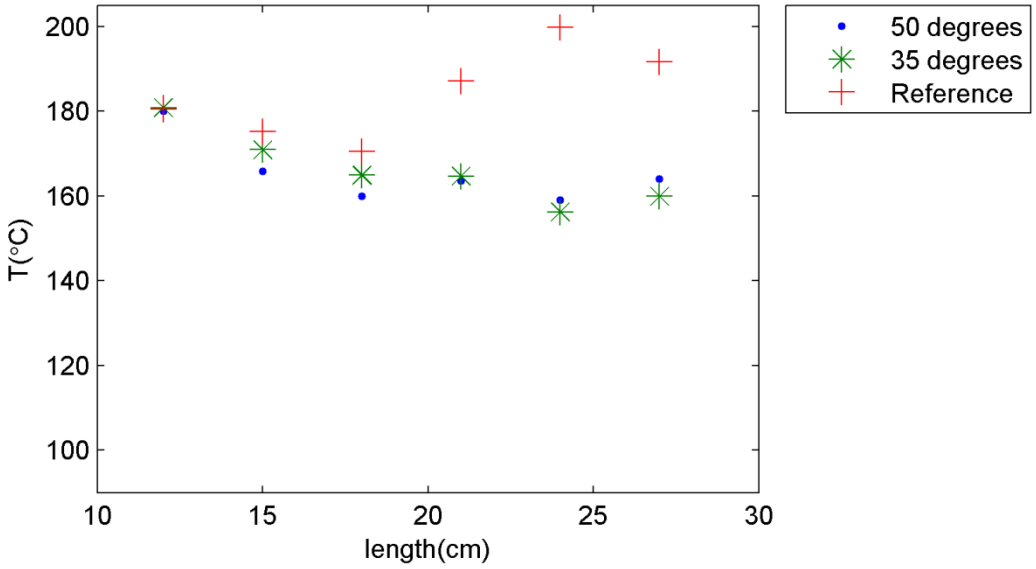

Figure 42: Minimum wall temperatures during the dosing period for a gas temperature of 200 °C and a gas flow rate of 1200 kg/h with a urea dosing rate of 20 g/min

5 Discussion and conclusions

From the estimated depletion time for AdBlue droplets it could be expected that the differences in ammonia concentration would be large since there are operating conditions where the droplets should have enough time to evaporate for the higher dosing unit pressure but not for the lower dosing unit pressure. The differences in the outlet ammonia concentration are however small for most operating conditions and for most of the cases the reason could be the difference in radial distribution rather than a different evaporation rate. The sizes of the Weber numbers indicate that secondary atomization can occur which could be one reason why the differences are smaller than expected. Even though an evaporation time cannot be determined they should be longer than those reported by Abu-Ramadan et al. and Hüthwohl and Dolenec since quite little of the AdBlue is evaporated.

The operating point where the largest differences are observed is for a gas temperature of 200 °C and a gas flow rate of 400 kg/h. For these conditions droplets still remain in the outlet of the pipe. Since the FTIR instrument samples liquid components as well as gas component this analysis method might not be suitable to capture the decomposition at these low temperatures accurately.

The statistic evaluations for the ammonia do not indicate significant effects for the dosing unit pressure and the spray angle but indicates significant effects for the dosing frequency if the start concentration is subtracted from the mean concentration. Even though it is difficult to say which of the evaluations is most reliable it seems safe to conclude that a frequency increase does not lead to decreased outlet concentrations of ammonia.

The decomposition was better captured with the temperature measurements in the pipe since this showed the radial distribution and since it was not affected by remaining liquids. The disadvantage is that these measurements are difficult to correlate to the conversion of urea. A plug flow is not obtained in the pipe since most of the droplets are entrained towards the upper part of the pipe. The droplets seem to be affected by the flow to a larger extent for the dosing unit pressure of 4 bar. This might seem unreasonable since large droplets should have higher response times. One explanation could be that the droplets are ejected with a lower velocity and are therefore spread over a smaller area before they are entrained with the flow. For this reason the distribution for the dosing unit pressure of 4 bar and for the spray angle of 35 degrees is very uneven for higher flow rates

The consequences of each parameter change are summarized in Table 41.

Table 41: Consequences of parameter changes from the base case

Gas temperature (°C)	Gas flow rate (kg/h)	Decreased dosing unit pressure	Decreased spray angle	Increased dosing unit frequency
200	400	• Large decrease in evaporation rate for low residence times • More wall wetting further down the pipe • Moderate decrease in evaporation rate for high residence times	• Large decrease in evaporation rate for low residence times • More wall wetting further down the pipe • Moderate decrease in evaporation rate for high residence times	• Moderate but not significant decrease in evaporation rate for low residence times • Small increase in evaporation rate for high residence times
200	1200	• Difficult to estimate the effect on the overall evaporation rate • Uneven distribution of droplets in the pipe • Somewhat more wall wetting for all positions	• Small decrease in evaporation rate for low residence times • Uneven distribution of droplets in the pipe • Somewhat more wall wetting further down the pipe	• Moderate but not significant decrease in evaporation rate for low residence times
300	800	• Large decrease in evaporation rate for low residence times • Uneven distribution of droplets in the pipe	• Large decrease in evaporation rate for low residence times • Uneven distribution of droplets in the pipe	• Moderate decrease in evaporation rate for low residence times
385	400	• No significant effect on evaporation rate for low residence times	• No significant effect on evaporation rate for low residence times	• Small decrease in evaporation rate for low residence times
400	1200	• Small decrease in evaporation rate for low residence times	• Small decrease in evaporation rate for low residence times	• Small decrease in evaporation rate for low residence times

For the dosing unit pressure and for the dosing unit angle, the largest differences were observed for a gas temperature of 200 °C with a gas flow rate of 400 kg/h and for a gas temperature of 300 °C with a gas flow rate of 800 kg/h. For the other operating conditions, the differences are small or not significant. It seems like the droplet size is more important when the energy content in the gas is low due to a low temperature and/or flow rate. This is indicated by the operating conditions for which significant differences appear. Another indication is that the differences in mean temperature drop increase with the urea dosing rate. Significant effects could therefore appear for the other tested operating conditions evaporation rate if the urea dosing rate is increased.

For the frequency the differences are significant for the higher temperatures even though the differences between the mean temperature drops are smaller than for lower temperatures. In the outlet the mean temperature drop was somewhat lower for the higher frequency.

For these flow conditions the results do not indicate that there could be any disadvantages in using a spray with smaller droplets. In contrast, there seems to be more entrainment of droplets and therefore more wall film formation with large droplets.

6 Recommendations for further work

In the project it has been verified that all tested parameters have significant effect for some of the tested operating conditions. It is however difficult to quantify the evaporation rate from the temperature measurements. Since the largest differences were observed for low temperatures where it is difficult to obtain a reliable FTIR signal a different analysis method could be suitable. For example Kröscher et al. describes an analysis method that is suitable for dirty exhaust gases [32]. Relevant temperatures to investigate further includes gas temperatures below 300 °C. It also seems like lower gas flow rates could be more relevant. Since the largest effects were observed as the urea dosing rate was increased it could be relevant to study the effects for higher urea dosing rates than those used in this thesis. The pressure chosen in this project are pressures for which the SMD for the dosing unit were available. Since the evaporation rate increased with higher dosing unit pressures it could be relevant to increase it. It could also be relevant to test other spray types, e.g. air-assisted sprays.

To be able to compare the results for different sprays more accurately it is desirable to obtain a plug flow in the pipe. One way to do this could be to decrease the size of the perforation on the plate in the inlet of the pipe. To avoid differences because of the radial distribution a mixer could be inserted before the sampling point.

Bibliography

1. Emission Standards: Europe: Heavy-Duty Diesel Truck and Bus Engines. [Online]. 2009 [cited 2012 01 27]. Available from: http://www.dieselnet.com/standards/eu/hd.php.

2. Jääskeläinen H. Engine Exhaust Back Pressure. [Online]. 2007 [cited 2012 02 16]. Available from: http://www.dieselnet.com/tech/diesel_exh_pres.php.

3. Khair MK, Jääskeläinen H. Emission Formation in Diesel Engines. [Online]. 2008 [cited 2012 02 06]. Available from: http://www.dieselnet.com/tech/diesel_emiform.php.

4. Majewski WA, Jääskeläinen H. Engine Design for Low Emissions. [Online]. 2009 [cited 2002 02 06]. Available from: http://www.dieselnet.com/tech/engine_design.php.

5. Allen DT. Air Pollution. In Kirk-Othmer Encyclopedia of Chemical Technology. New York: Wiley; 2002.

6. Sutton WM, Ziegler E. Nitrogen Oxides Reduction. In Encyclopedia of Environmental Science and Engineering. Boca Ranton, FL: CRC Press; 2006. p. 746-768.

7. Twigg MV. Progress and future challenges in controlling automotive exhaust gas emissions. Applied Catalysis B: Environmental. 2007: p. 2-15.

8. Majewski WA. SCR Systems for Mobile Engines. [Online]. 2005 [cited 2012 02 02]. Available from: http://www.dieselnet.com/tech/cat_scr_mobile.php.

9. Koebel M, Elsener M, Kleemann M. Urea-SCR: a promising technique to reduce NOx emissions from automotive diesel engines. Catalysis Today. 2000: p. 335-345.

10. Koebel M, Madia G, Elsener M. Selective catalytic reduction of NO and NO2 at low temperatures. Catalysis Today. 2007: p. 239-247.

11. Birkhold F, Meingast U, Peter W. Modeling and simulation of the injection of urea-water solution for automotive SCR DeNOx-systems. Applied Catalysis B: Environmental. 2007: p. 119-127.

12. Yim SD, Kim SJ, Baik JH, Nam IS, Mok YS, Lee JH, et al. Decomposition of Urea into NH3 for the SCR Process. Ind. Eng. Chem. Res. 2004: p. 4856-4863.

13. Fang H, Dacosta H. Urea thermolysis and NOx reduction with and without SCR catalysts. Applied Catalysis B: Environmental. 2003: p. 17-34.

14. Wang TJ, Baek SW, Lee SY. Experimental investigation of Urea-Water-Solution Droplet for SCR applications. AIChe Journal. 2009: p. 3267-3276.

15. Koebel M, Strutz EO. Thermal and Hydrolytic Decomposition of Urea for Automotive

Selective Catalytic Reduction Systems: Thermochemical and Practical Aspects. Ind. Eng. Chem. Res. 2003: p. 2093-2100.

16. Seke E, Yasyerli NGE, Christine L, Hammerle RH. NOx reduction by urea under lean conditions over single step sol-gel Pt/alumina catalyst. Applied Catalysis B: Environmental. 2002: p. 27-35.

17. Zheng G, Gardner T, Motrba A, Golin M. Development of Urea SCR Systems for Large Diesel Engines. SAE Technical Paper 2011-01-2204. 2011.

18. Dong H, Shuai S, Wang J. Effect of Urea Thermal Decomposition on Diesel NOx-SCR After Treatment Systems. SAE Technical Paper 2008-01-1544. 2008.

19. Strots V, Santhanam S, Adelman B, Griffin G, Derybowski A. Deposit Formation in Urea-SCR Systems. SAE Int. J. Fuels Lubr. 2010: p. 283-289.

20. Xu L, Watkings W, Snow R, Graham G, McCabe R, Lambert C, et al. Systems, Laboratory and Engine Study of Urea-Related Deposits in Diesel Urea-SCR After-Treatment. SAE Technical Paper 2007-01-1582. 2007.

21. Fritsching U. Spray Systems. In Crowe CT. Multiphase flow handbook. Boca Ranton, FL: Taylor & Francis; 2006.

22. Kister HZ, Mathias PM, Steinmeyer DE, Penney WR, Crocker BB, Fair JR. Equipment for distillation, gas absorption, phase dispersion, and phase separation. In Green DW, Perry RH. Perry's chemical engineers' handbook. New York: McGraw-Hill Professional; 2007. p. 1529-1658.

23. Ashgriz N, Li X, Sarchami A. Instability of liquid sheets. In Ashgriz N. Handbook of Atomization and Sprays. New York: Springer; 2011.

24. Omer K, Ashgriz N. Spray Nozzles. In Ashgriz N. Handbook of Atomization and Sprays. New York: Springer; 2011.

25. Sprays. In Kirk-Othmer Encyclopedia of Chemical Technology. New York: John Wiley & Sons, Inc; 1999.

26. Pilch M, Erdman CA. Use of breakup time data and velocity history data to predict the maximum sixe of stable fragments for acceleration-induced break-up of a liquid drop. International Journal of Multiphase Flow. 1987: p. 741-757.

27. Chen C, Amlee DR, Johns RJR, Zeng Y. Detailed Modelling of Liquid Fuel Sprays in One-Dimensional Gas Flow Simulation. SAE Technical Paper 2004-01-3000. 2004.

28. Tanner FX. Evaporating Sprays. In Agriz N. Handbook of Atomization and Sprays.:

Springer; 2011.

29. Salanta G, Zheng G, Kortba A, Rampazzo R, Bergantim L. Optimization of a Urea SCR System for On-Highway Truck Applications. SAE Technical Paper 2010-01-1938. 2010.

30. Abu-Ramadan E, Saha K, Li X. Modeling of the Injection and Decomposition Processes of Urea-Water-Solution Spray in Automotive SCR Systems. SAE Technical Paper 2011-01-1317. 2011.

31. Hüthwohl G, Dolenec S. A new Approach in AdBlue Dosing to Improve Performance and Durability of SCR Systems for the Use in Passanger Cars up to Heavy Duty Vehicles. SAE Technical Paper 2011-01-2095. 2011.

32. Kröscher O, Elsener M, Koebel M. An ammonia and isocyanic acid measuring method for soot containing exhaust gases. Analytica Chimica Acta. 2005: p. 393-400.

Appendix

A. Calculations

Calculation of droplet depletion times

The rate coefficients that are used to calculate the depletion times are shown in

Table 42: Rate coefficients for evaporation of a urea-water-solution [14]

Temperature(°C)	Diameter(mm)	Rate coefficient (mm^2/s)
200	0.72	0.0085
200	1.02	0.012
200	1.3	0.014
300	0.9	0.0195
300	1.1	0.02
300	1.28	0.0225
400	0.7	0.036
400	1	0.039
400	1.34	0.044

The rate coefficient for the relevant droplet sizes are then calculated with a linear equation. The calculated rate coefficients are shown in Table 43.

Table 43: Estimated rate coefficients

Temperature (°C)	Diameter(µm)	Rate coefficient(mm^2/s)
200	30	0.0021
200	60	0.0024
200	130	0.0031
200	220	0.004
300	30	0.012
300	60	0.013
300	130	0.013
300	220	0.014
400	30	0.027
400	60	0.028
400	130	0.029
400	220	0.030

The square of the diameter can then be calculated with the D-squared law as shown in equation (54):

$$d_d^2(t) = d_{d,0}^2 - \beta t \qquad (54)$$

where d^2_d is the square of the diameter, $d^2_{d,0}$ is the square of the initial diameter and β is the rate coefficient. The depletion time can be found by setting this equation to zero.

Calculation of ideal ammonia concentrations

The molar flow of ammonia can be calculated from the AdBlue flow as shown in equation (55):

$$n_{NH_3} = \frac{m_{AdBlue} X_{urea}}{M_{urea}} \quad (55)$$

where X_{Urea} is the weight percent of urea and M_{Urea} is the molar mass of urea.

The molar flow of air is calculated as shown in equation (56):

$$n_{air} = \frac{m_{air}}{M_{air}} \quad (56)$$

where M_{air} is the molar mass of air.

The ammonia concentration is then calculated as the ratio between the molar flows and converted to ppm.

Calculation of temperature losses due to urea decomposition

The enthalpy required to decompose one mole of urea in a 32.5% water solution and heat it to the temperature of the gas is listed in Table 44.

Table 44: Required heat to decompose one mole of urea in a 32.5 water solution

Gas temperature (°C)	ΔH(kJ/mol urea)
200	532.1
300	567.0
385	596.6
400	601.8

For each flow rate the heat required to evaporate the urea is calculated with equation (57):

$$\Delta H_{Urea} = \frac{X_{Urea} \cdot m_{AdBlue} \cdot \Delta H}{M_{Urea}} \quad (57)$$

where X_{Urea} is the weight percent of urea, ΔH is the heat to decompose one mole of urea, and M_{Urea} is the molar mass of urea.

The enthalpy change in the gas can be calculated with equation (58):

$$\Delta H_{gas} = m_{gas} \cdot C_{P,gas} \cdot (T_1 - T_2) \quad (58)$$

where $C_{P,gas}$ is the specific heat capacity of the gas, T_1 is the start temperature of the gas and T_2 is the end temperature of the gas.

The heat capacity for the gas at the listed temperatures are shown in

Gas temperature (°C)	$C_{P,gas}$(kJ/kg·K)
200	1.026
300	1.047
385	1.065
400	1.068

Since the enthalpy change in the gas is the same as the heat required to evaporate the urea the temperature drop can be calculated with equation (59):

$$(T_1 - T_2) = \frac{X_{Urea} \cdot m_{AdBlue} \cdot \Delta H}{m_{gas} \cdot C_{P,gas} M_{Urea}} \quad (59)$$

B. Ammonia concentration profiles

Ammonia concentrations for dosing unit pressure change

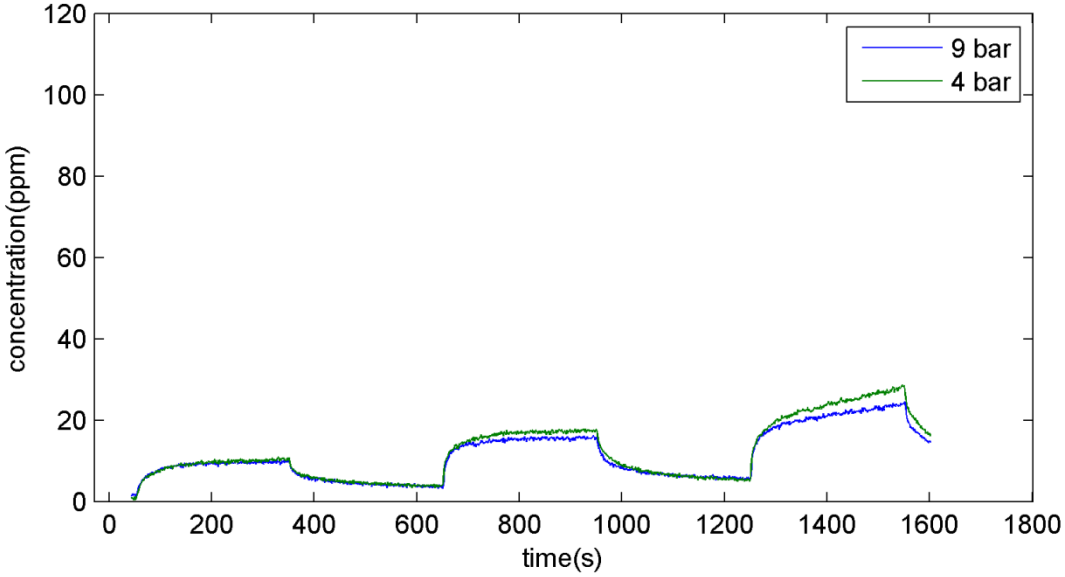

Figure 43: Outlet ammonia concentrations for a gas temperature of 200 °C and a gas flow rate of 1200 kg/h with urea dosing rates of 5, 12.5 and 20 g/min.

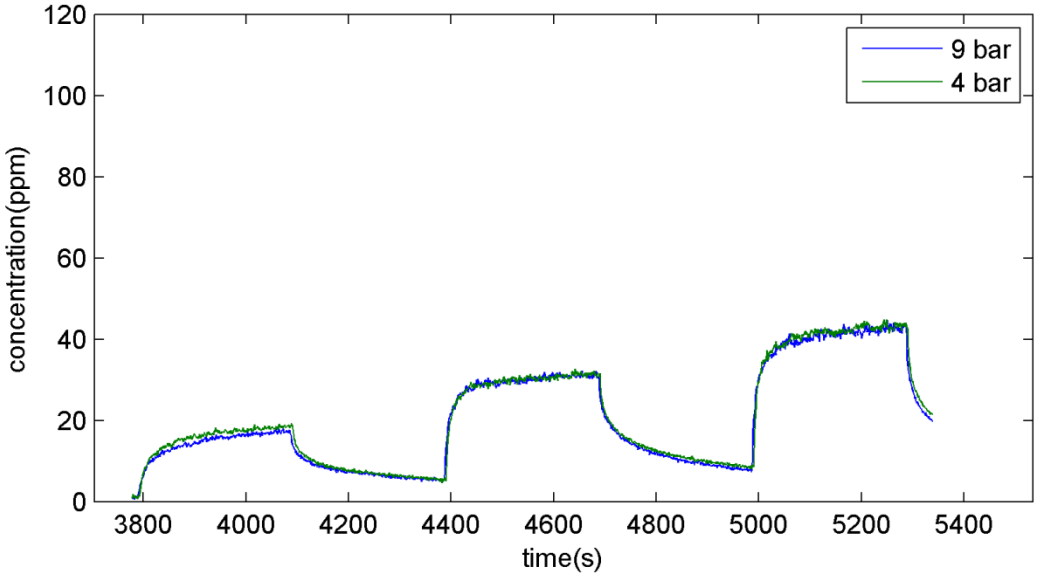

Figure 44: Outlet ammonia concentrations for a gas temperature of 300 °C and a gas flow rate of 800 kg/h with urea dosing rates of 5, 12.5 and 20 g/min.

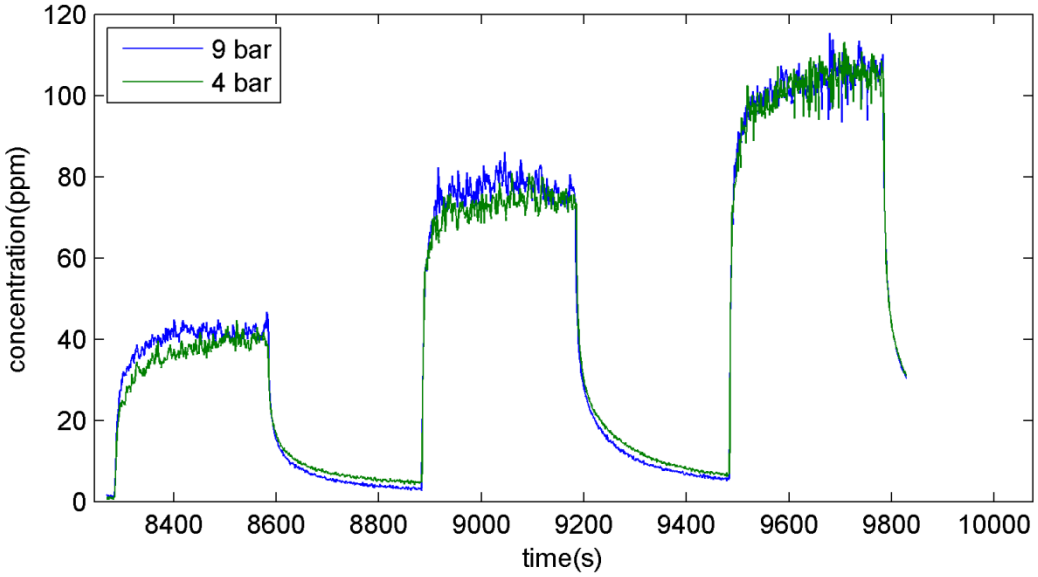

Figure 45: Outlet ammonia concentrations for a gas flow rate of 400 kg/h and a gas temperature of 385 °C with urea dosing rates of 5, 12.5 and 20 g/min.

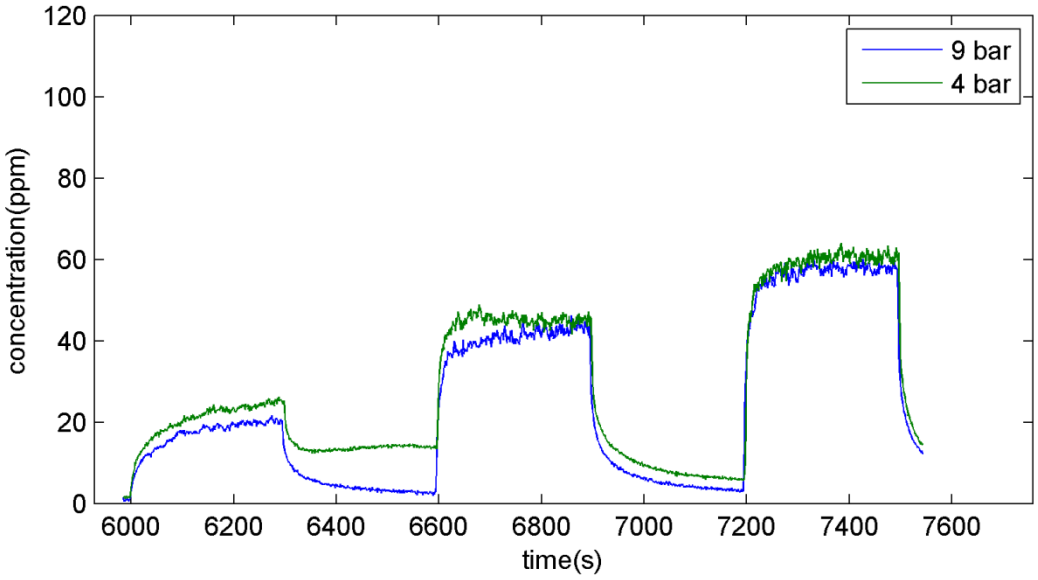

Figure 46: Outlet ammonia concentrations for a gas temperature of 400 °C and a gas flow rate of 1200 kg/h with urea dosing rates of 5, 12.5 and 20 g/min

Ammonia concentrations for spray angle change

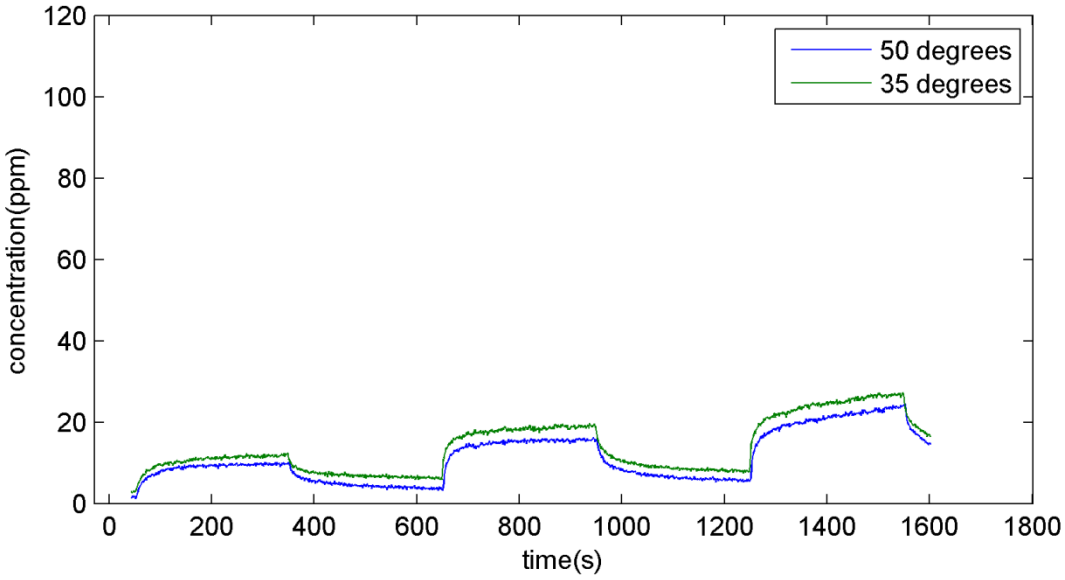

Figure 47: Outlet ammonia concentrations for a gas temperature of 200 °C and a gas flow rate of 1200 kg/h with urea dosing rates of 5, 12.5 and 20 g/min.

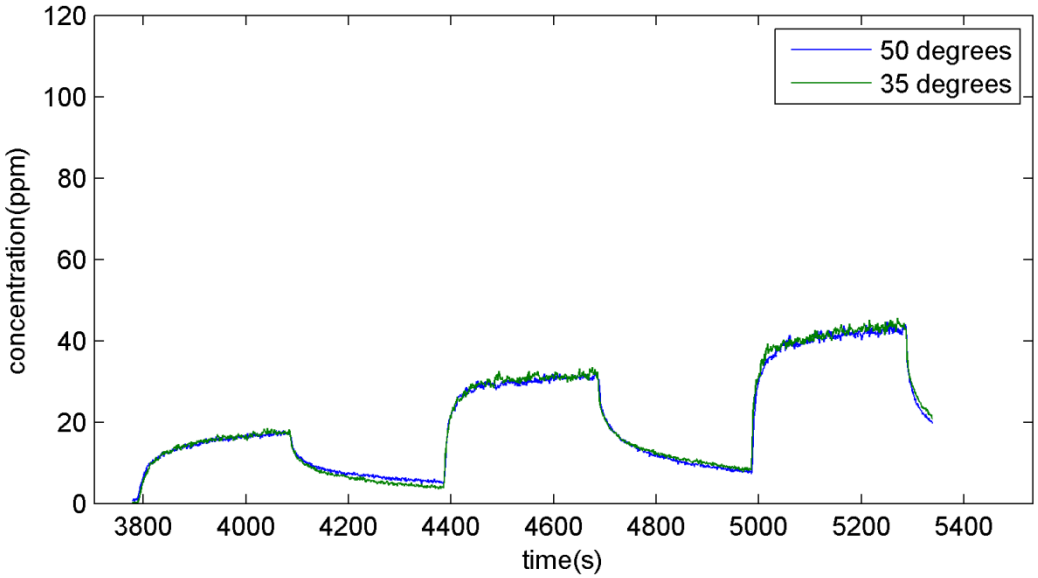

Figure 48: Outlet ammonia concentrations for a gas temperature of 300 °C and a gas flow rate of 800 kg/h with urea dosing rates of 5, 12.5 and 20 g/min.

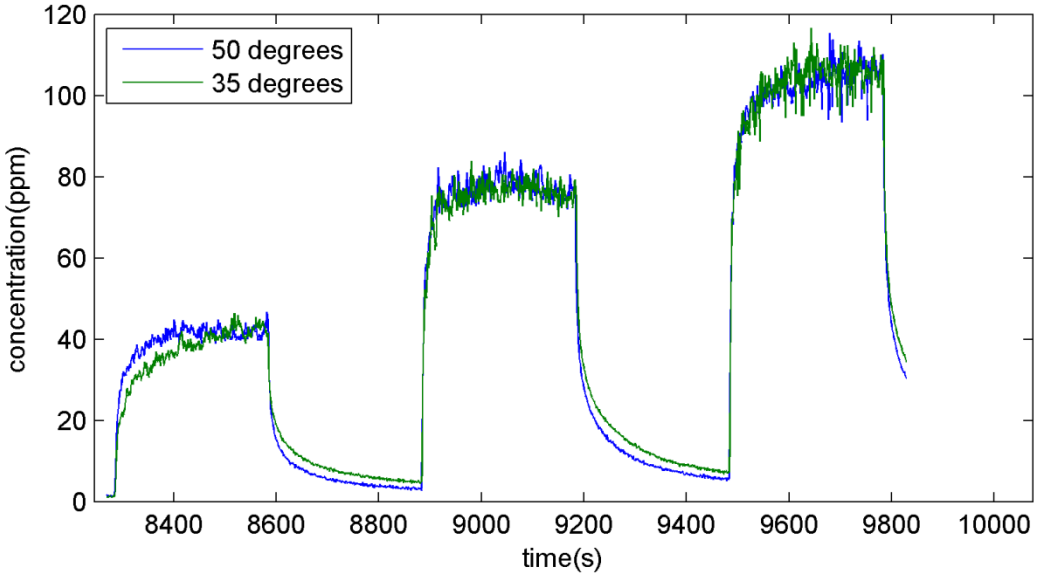

Figure 49: Outlet ammonia concentrations for a gas temperature of 385 °C and a gas flow rate of 400 kg/h with urea dosing rates of 5,12.5 and 20 g/min.

.

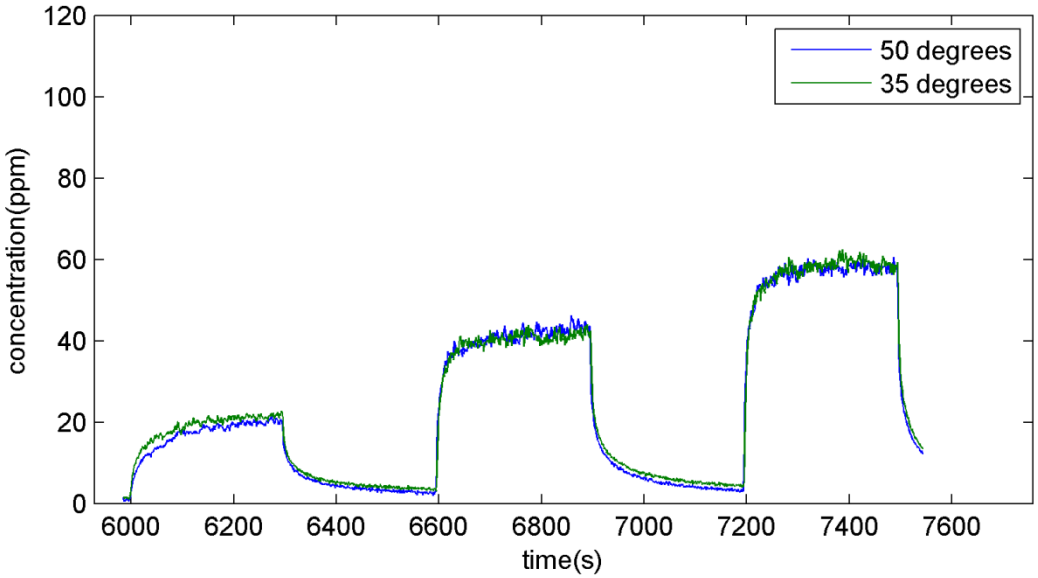

Figure 50: Outlet ammonia concentrations for a gas temperature of 400 °C and a gas flow rate of 1200 kg/h with urea dosing rates of 5, 12.5 and 20 g/min.

Ammonia concentrations for frequency change

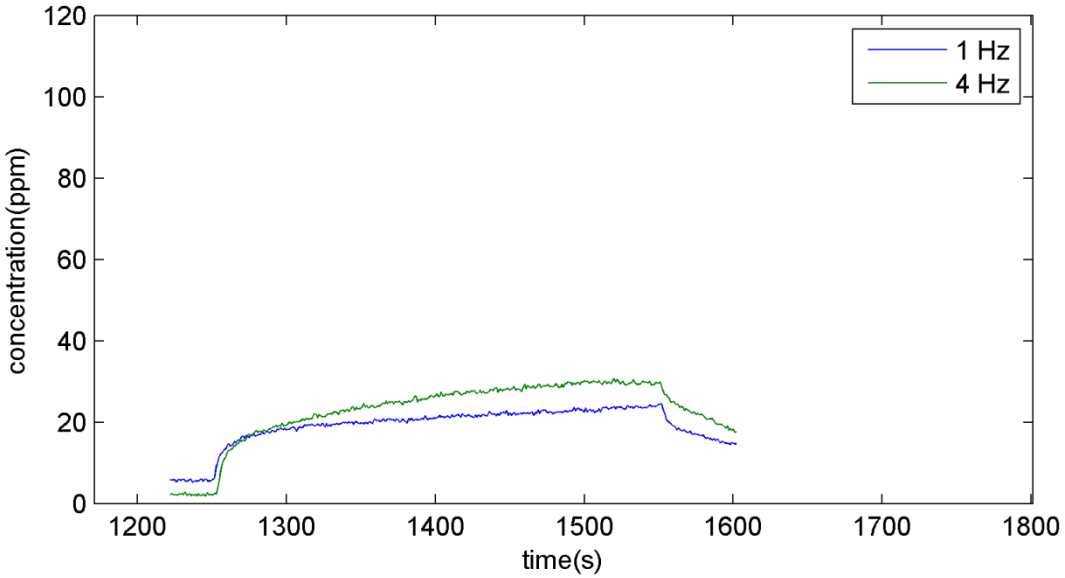

Figure 51: Outlet ammonia concentrations for a gas flow rate of 1200 kg/h and a gas temperature of 200 °C with a urea dosing rate of 20 g/min.

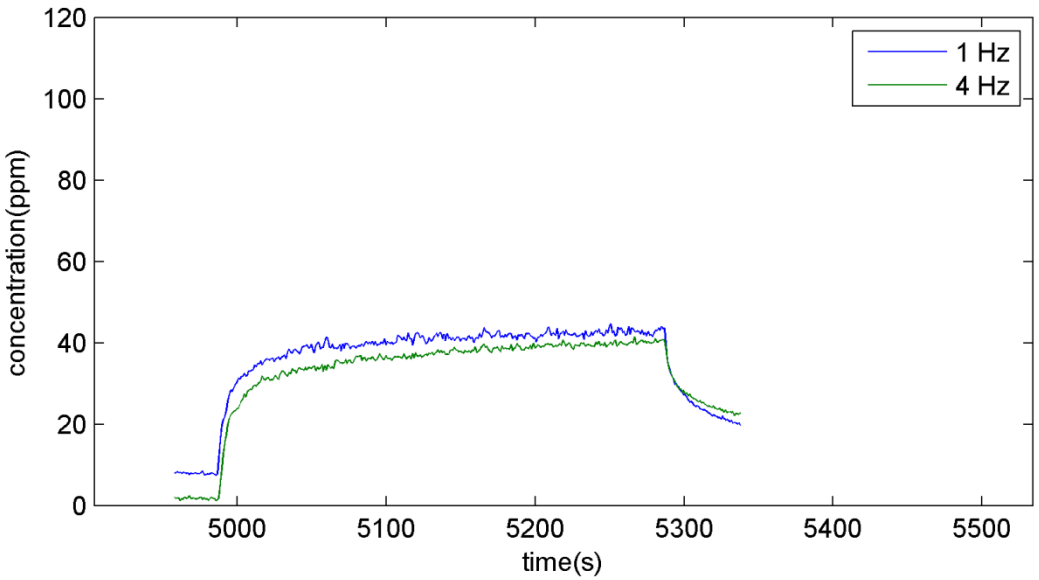

Figure 52: Outlet ammonia concentrations for a gas flow rate of 800 kg/h and a gas temperature of 300 °C with a urea dosing rate of 20 g/min.

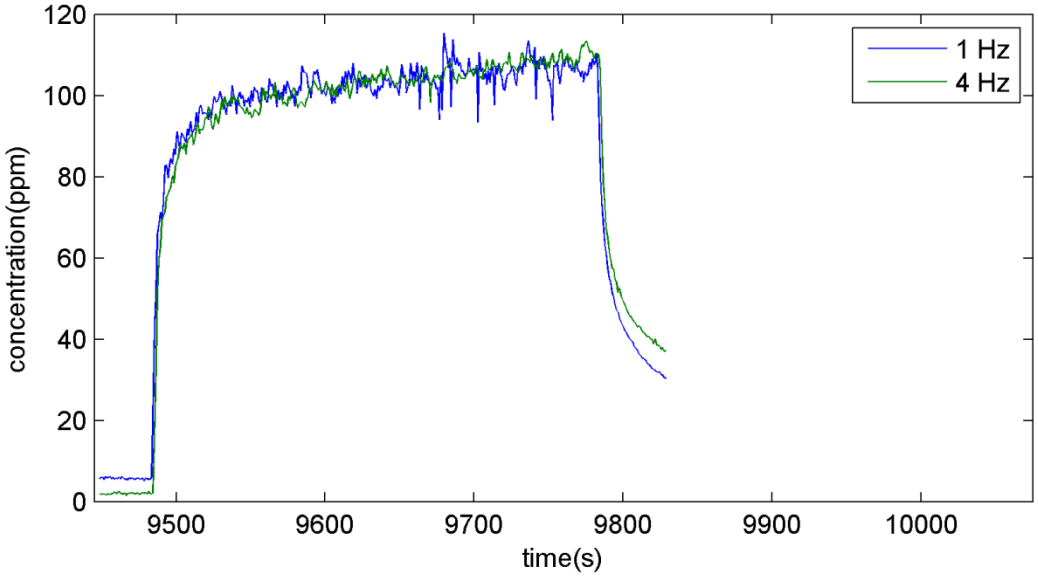

Figure 53: Outlet ammonia concentrations for a gas flow rate of 400 kg/h and a gas temperature of 385 °C with a urea dosing rate of 20 g/min.

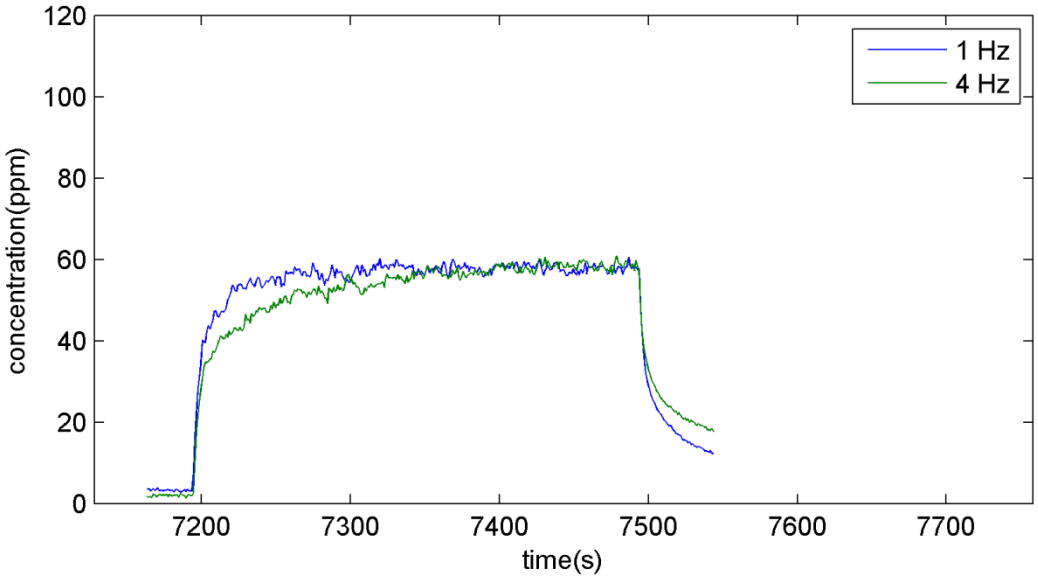

Figure 54: Outlet ammonia concentrations for a gas flow rate of 1200 kg/h and a gas temperature of 400 °C with a urea dosing rate of 20 g/min.

C. Temperature drops

Temperature drops for repeated runs

Table 45: Temperature drops for each position for repeated runs at a gas temperature of 300 °C, a gas flow rate of 800 kg/h and a dosing unit pressure of 6.5 bar.

Run	1			2			3		
Urea dosing rate	5.00	12.50	20.00	5.00	12.50	20.00	5.00	12.50	20.00
Middle	4.04	10.24	19.19	3.83	10.63	20.39	4.01	10.44	17.69
A1	4.86	11.92	24.21	4.62	12.55	25.72	4.85	12.25	22.24
A2	8.07	22.87	62.28	8.43	23.13	65.22	8.97	23.57	56.66
A3	14.03	42.60	82.89	15.35	44.05	79.37	14.86	40.90	77.18
B1	2.31	5.68	11.03	2.40	6.14	12.11	2.26	6.05	10.89
B2	2.06	5.77	12.75	2.83	6.41	13.08	2.55	6.36	12.40
B3	3.60	10.03	37.21	5.73	11.91	36.00	5.80	12.02	36.63
C1	1.71	4.26	8.35	1.91	5.00	9.43	1.70	4.83	7.89
C2	0.22	1.76	3.40	0.84	2.29	4.08	0.67	2.22	3.41
C3	-0.91	0.61	2.73	0.68	1.57	2.77	0.54	1.47	2.44
D1	3.28	8.10	14.80	3.34	8.86	16.24	3.37	8.84	14.16
D2	2.96	7.99	13.72	3.45	9.05	15.24	3.38	8.90	13.59
D3	2.26	7.97	13.08	3.86	9.31	14.17	3.77	9.65	13.89
E1	5.61	13.63	23.15	5.26	14.36	24.52	5.36	14.18	21.87
E2	7.11	18.15	30.04	7.12	18.95	31.97	7.54	19.05	32.80
E3	5.83	15.96	38.87	7.07	18.04	39.58	7.01	17.81	42.16

Temperature drops for different operating conditions

Table 46: Temperature drops for each position for a dosing unit pressure of 9 bar

Temperature	200			200			300			385			400		
Flow rate	400			1200			800			400			1200		
Urea dosing rate	5	12.5	20	5	12.5	20	5	12.5	20	5	12.5	20	5	12.5	20
Middle	11.92	32.71	44.49	9.08	22.00	35.06	2.95	7.44	11.58	2.60	5.47	8.90	1.05	3.47	5.80
A1	13.95	36.69	53.93	11.16	28.95	43.91	4.81	12.66	26.67	3.51	9.06	15.25	1.84	5.80	9.63
A2	19.29	44.48	66.18	11.07	30.91	44.90	9.22	24.97	66.59	6.09	17.53	29.96	3.05	9.64	16.55
A3	10.44	33.95	44.88	6.23	14.56	24.65	2.18	5.89	9.59	2.48	5.36	8.91	0.48	2.25	3.81
B1	10.04	32.30	43.67	5.47	14.93	25.58	3.00	7.47	13.48	3.08	7.70	13.05	0.64	3.42	5.89
B2	11.12	27.55	36.72	4.20	16.19	24.61	6.82	15.72	40.88	5.29	15.11	26.43	1.56	7.46	12.82
B3	9.38	32.33	44.54	4.59	9.82	18.87	2.17	5.59	8.81	2.00	4.23	7.05	0.09	1.24	2.48
C1	6.86	22.92	33.33	1.73	3.65	8.89	1.34	3.46	5.44	1.44	3.42	6.06	-0.49	0.53	1.45
C2	5.97	14.19	20.70	-0.13	1.25	5.94	1.22	2.52	4.00	1.25	4.32	8.20	-1.43	0.18	1.67
C3	10.26	31.24	42.98	6.94	17.44	26.79	2.77	6.95	10.70	2.44	5.43	8.69	0.60	2.71	4.70
D1	9.64	30.58	40.86	5.65	14.26	24.36	3.24	7.78	11.59	2.82	7.40	12.07	0.48	3.08	5.45
D2	15.28	40.95	59.43	9.07	24.94	36.69	4.53	11.62	16.08	4.18	12.91	22.16	0.35	4.22	7.58
D3	10.02	27.25	36.82	3.61	10.83	20.42	4.55	10.29	15.24	2.75	5.81	9.34	1.14	3.62	6.23
E1	11.88	32.57	44.76	9.40	24.98	36.90	3.13	8.08	11.76	3.82	9.35	15.88	1.38	4.75	8.02
E2	15.04	36.91	54.54	5.92	20.02	30.70	5.65	14.49	30.56	5.01	13.47	23.09	1.75	6.81	11.92
E3	11.92	32.71	44.49	9.08	22.00	35.06	2.95	7.44	11.58	2.60	5.47	8.90	1.05	3.47	5.80

Table 47: Temperature drops for each position for a dosing unit pressure of 4 bar

Temperature	200			200			300			385			400		
Flow rate	400			1200			800			400			1200		
Urea dosing rate	5	12.5	20	5	12.5	20	5	12.5	20	5	12.5	20	5	12.5	20
Middle	40.43	72.74	107.21	5.45	16.30	24.93	2.92	8.01	14.56	2.71	6.13	9.46	1.11	2.23	3.88
A1	37.63	74.30	109.73	8.73	22.57	33.90	3.95	10.76	47.01	2.77	6.82	10.83	1.52	3.28	5.41
A2	35.45	72.70	107.14	15.57	34.77	49.97	8.11	28.19	82.36	4.22	10.86	19.92	3.16	7.38	12.19
A3	29.05	60.43	86.01	16.45	36.66	52.68	18.38	71.62	100.87	7.60	20.09	52.67	5.96	14.18	24.26
B1	19.46	41.69	73.27	2.52	6.95	14.89	1.39	3.59	6.66	1.82	4.73	7.28	0.76	1.49	2.50
B2	7.46	24.90	40.13	2.34	7.40	17.37	1.66	4.52	12.47	2.27	5.88	9.05	1.23	2.51	4.20
B3	4.59	16.48	22.98	2.35	10.17	17.35	4.12	10.45	41.16	4.39	10.91	17.53	2.55	5.49	9.35
C1	16.54	33.76	57.45	1.16	5.67	12.86	1.03	2.89	4.33	1.31	3.25	4.86	0.57	0.87	1.71
C2	6.21	13.22	19.35	-0.06	1.85	7.66	0.48	1.56	1.82	0.72	2.04	2.94	0.47	0.52	1.19
C3	1.80	5.77	6.25	-0.49	0.91	6.56	-0.07	1.55	1.61	0.89	2.20	3.27	0.66	0.55	1.73
D1	21.72	48.49	72.47	4.97	14.28	22.04	2.67	7.20	11.49	2.22	5.56	8.45	1.01	2.02	3.56
D2	12.20	35.26	48.27	4.16	11.85	19.66	2.73	7.73	11.97	2.62	6.87	10.41	1.05	2.07	3.82
D3	6.55	23.81	31.42	2.62	7.41	13.59	3.08	8.51	12.10	4.11	10.66	16.68	1.30	2.55	4.67
E1	36.81	76.33	112.16	10.24	26.86	39.07	5.04	13.97	21.92	2.95	7.27	11.24	1.82	3.91	6.64
E2	33.75	71.39	100.72	11.14	27.69	39.82	7.17	19.11	49.84	4.02	10.19	16.52	2.46	5.92	10.05
E3	20.54	43.42	65.61	7.62	22.00	32.22	6.78	18.43	57.37	5.65	14.12	22.93	3.30	8.08	13.60

Table 48: Temperature drops for each position for a spray angle of 35 degrees

Temperature	200			200			300			385			400		
Flow rate	400			1200			800			400			1200		
Urea dosing rate	5	12.5	20	5	12.5	20	5	12.5	20	5	12.5	20	5	12.5	20
Middle	29.68	64.74	96.38	8.92	19.54	31.38	4.44	14.09	28.08	3.88	8.31	13.67	1.28	3.19	4.08
A1	30.82	70.41	100.63	13.49	29.41	39.94	5.89	20.04	42.43	3.69	8.81	14.91	1.67	4.29	5.55
A2	32.20	69.93	102.14	17.44	38.11	55.50	12.83	38.79	76.15	5.69	13.97	25.00	2.98	8.00	11.43
A3	25.49	52.06	76.52	17.89	40.03	56.42	20.89	58.75	94.96	8.71	22.24	42.28	5.43	14.95	25.48
B1	20.78	45.74	68.05	5.34	12.02	19.34	2.23	6.09	10.96	2.99	6.15	10.12	0.72	2.01	2.34
B2	13.00	31.13	43.90	3.95	10.16	18.56	2.10	5.22	9.30	3.21	6.02	9.56	1.00	2.86	4.05
B3	6.27	15.10	20.70	2.71	10.31	16.96	3.38	8.16	19.75	4.07	7.25	11.03	2.20	6.17	9.84
C1	14.08	34.05	52.17	2.93	6.70	18.66	1.67	4.45	8.31	2.39	4.29	7.10	0.39	1.30	1.22
C2	4.61	13.94	17.62	0.29	1.30	8.92	0.53	1.24	1.89	1.58	1.86	3.20	0.16	0.77	0.57
C3	2.42	5.90	5.37	-0.45	1.16	6.64	0.25	0.59	0.95	1.91	1.24	2.64	-0.01	0.74	0.75
D1	21.67	47.74	72.94	7.35	19.22	26.74	3.60	9.75	17.96	3.09	6.61	11.10	1.12	2.85	3.55
D2	13.92	32.73	45.98	5.58	13.85	20.08	3.02	7.57	12.56	2.96	5.94	10.08	1.06	2.85	3.73
D3	6.89	18.34	25.21	3.00	7.75	12.34	2.38	5.88	8.95	3.61	6.56	11.17	1.25	3.66	4.78
E1	31.61	73.46	104.75	14.39	32.04	46.53	7.77	24.68	49.87	4.11	9.75	16.59	2.01	5.09	6.89
E2	32.18	72.16	97.29	14.75	32.98	46.15	10.26	29.58	54.09	5.66	13.89	24.27	2.44	6.42	9.25
E3	17.12	36.78	49.93	8.65	22.02	31.80	6.06	17.59	27.10	5.62	12.05	20.36	2.67	7.27	10.51

Table 49: Temperature drops for each position for a spray frequency of 4 Hz

Temperature	200	200	300	385	400
Flow rate	400	1200	800	400	1200
Middle	69.14	36.68	21.07	11.34	5.52
A1	51.24	42.21	21.46	9.97	6.96
A2	56.17	47.73	32.42	15.46	12.00

A3	65.19	45.22	61.57	30.04	21.20
B1	49.39	28.93	12.50	9.62	3.93
B2	45.50	28.24	14.08	13.63	5.86
B3	38.14	24.11	32.55	27.28	12.54
C1	47.01	29.07	9.97	7.83	2.51
C2	33.78	14.95	4.92	6.60	1.40
C3	21.85	10.87	3.56	8.75	1.37
D1	47.96	30.62	14.76	9.36	4.91
D2	43.75	28.37	15.40	12.36	5.39
D3	39.13	20.55	16.90	21.94	7.15
E1	49.59	38.98	21.02	10.26	7.57
E2	61.90	38.31	29.56	15.89	9.55
E3	55.32	30.16	49.93	8.65	22.02

Temperature drops along the pipe

Table 50: Temperature drops at each position for a dosing unit pressure of 9 bar

Length(m)	0.3			0.7			1.1			1.5		
Urea dosing rate	5	12.5	20	5	12.5	20	5	12.5	20	5	12.5	20
Middle	18.39	41.05	52.36	8.03	19.01	25.39	3.63	8.18	16.36	2.52	6.67	13.90
A1	11.92	32.71	44.49	7.06	17.75	23.35	5.08	11.33	16.73	3.07	7.88	14.26
A2	13.95	36.69	53.93	5.62	18.15	21.17	4.81	12.87	16.12	2.91	8.43	12.38
A3	19.29	44.48	66.18	6.53	17.29	20.58	4.57	10.39	12.51	2.68	7.53	8.49
B1	10.44	33.95	44.87	4.85	13.39	22.77	2.74	8.06	15.25	2.44	6.59	11.97
B2	10.04	32.30	43.67	3.39	11.09	19.49	2.67	9.16	15.04	2.03	6.61	11.20
B3	11.12	27.55	36.72	3.30	12.82	16.30	3.33	9.09	12.41	1.76	6.83	8.05
C1	9.38	32.33	44.54	4.15	13.47	21.22	2.62	6.04	13.36	1.66	5.44	11.99
C2	6.86	22.92	33.33	2.71	9.20	17.03	2.68	5.84	11.43	1.28	4.79	8.81
C3	5.97	14.19	20.70	2.75	7.80	12.16	2.77	5.47	9.10	1.03	3.76	5.26
D1	10.26	31.24	42.98	4.48	15.18	21.09	2.71	6.63	12.40	2.12	5.85	11.58
D2	9.64	30.58	40.86	3.46	13.09	17.97	2.65	6.82	11.68	1.86	5.94	10.49
D3	15.28	40.95	59.43	3.33	12.44	15.61	2.49	7.68	10.95	1.79	4.96	7.73
E1	10.02	27.25	36.82	5.85	17.79	21.64	3.48	8.38	16.21	2.70	4.65	8.60
E2	11.88	32.57	44.76	5.30	17.90	21.17	3.41	10.26	14.76	2.95	8.09	11.60
E3	15.04	36.91	54.54	6.42	16.45	20.90	4.03	10.54	12.04	2.98	6.32	6.91

Table 51: Temperature drops at each position for a dosing unit pressure of 4 bar

Length(m)	0.3			0.7			1.1			1.5		
Urea dosing rate	5	12.5	20	5	12.5	20	5	12.5	20	5	12.5	20
Middle	40.43	72.74	107.21	15.29	19.78	26.20	4.68	10.10	15.24	5.11	9.41	14.81
A1	37.63	74.30	109.73	15.12	20.22	27.75	3.62	12.08	17.15	5.33	11.65	17.22
A2	35.45	72.70	107.14	15.46	23.70	35.33	4.63	17.68	23.37	5.35	13.58	18.17
A3	29.05	60.43	86.01	19.38	37.37	50.24	6.77	18.93	26.64	4.80	10.99	15.52
B1	19.46	41.69	73.27	9.85	18.12	20.87	3.33	9.89	15.98	5.02	9.04	14.97
B2	7.46	24.90	40.13	6.54	13.92	17.89	2.41	10.13	15.97	3.81	8.86	13.83
B3	4.59	16.48	22.98	6.74	15.64	19.43	3.82	12.95	18.27	3.05	8.76	12.02
C1	16.54	33.76	57.45	8.08	19.38	16.85	3.19	6.44	10.53	3.78	6.80	11.59
C2	6.21	13.22	19.35	5.47	14.83	9.90	1.69	4.46	7.97	2.35	5.23	8.06
C3	1.80	5.77	6.25	4.68	11.72	8.28	2.11	5.37	7.78	1.23	6.11	5.16

D1	21.72	48.49	72.47	8.85	17.72	19.91	2.39	6.88	10.77	4.03	9.82	12.90
D2	12.20	35.26	48.27	7.25	15.17	18.54	1.83	5.67	9.54	3.27	7.18	12.83
D3	6.55	23.81	31.42	8.06	15.48	19.41	2.66	7.59	11.52	2.91	6.46	11.04
E1	36.81	76.33	112.16	11.78	20.06	27.18	3.10	9.82	15.75	2.76	7.09	11.11
E2	33.75	71.39	100.72	14.37	24.28	36.65	3.83	13.22	19.05	5.15	13.18	17.38
E3	20.54	43.42	65.61	18.41	34.47	51.15	5.68	16.64	24.56	4.37	9.72	13.67

Table 52: Temperature drops at each position for a spray angle of 35 degrees

Length(m)	0.3			0.7			1.1			1.5		
Urea dosing rate	5	12.5	20	5	12.5	20	5	12.5	20	5	12.5	20
Middle	29.62	64.79	96.31	8.90	20.05	25.09	5.28	11.86	14.95	4.03	8.85	15.82
A1	30.82	70.37	100.58	7.07	19.84	25.46	6.37	14.09	18.23	4.05	11.52	16.44
A2	32.09	70.01	102.10	8.74	22.34	31.24	6.85	18.06	23.19	4.57	12.89	16.01
A3	25.54	52.32	76.60	13.70	27.10	44.03	7.98	18.44	26.57	4.83	11.39	14.31
B1	20.82	45.61	68.11	4.54	12.02	19.95	4.18	11.50	15.18	3.24	7.47	13.87
B2	13.08	31.10	43.88	3.70	11.50	18.56	4.32	13.23	17.36	3.13	7.60	14.06
B3	6.29	15.00	20.64	5.30	14.35	19.51	5.06	14.62	18.75	3.71	8.64	12.62
C1	14.06	33.96	51.88	3.99	12.90	18.33	3.45	8.07	15.38	2.67	6.50	14.85
C2	4.61	13.88	17.46	1.88	6.76	11.62	3.06	6.25	13.39	2.33	5.13	10.92
C3	2.40	5.81	5.32	1.65	4.70	7.89	2.81	8.28	10.86	2.49	5.98	7.53
D1	21.63	47.71	72.93	5.24	15.35	20.93	3.55	7.26	11.78	2.88	7.96	12.58
D2	13.94	32.72	45.97	4.26	13.33	18.16	3.21	6.81	11.77	2.63	7.06	11.89
D3	6.91	18.28	25.24	5.47	13.01	17.70	3.21	8.40	13.52	2.82	6.83	10.65
E1	31.53	73.53	104.62	8.73	20.16	26.15	5.20	13.63	16.12	4.21	7.57	11.35
E2	32.21	72.33	97.54	11.41	23.36	33.48	5.54	16.35	18.20	4.24	12.06	15.90
E3	17.21	36.65	50.08	13.10	28.00	44.43	7.00	16.96	24.14	4.34	9.87	12.82

Table 53: Temperature drops at each position for a spray frequency of 4 Hz

Length(m)	0.3	0.7	1.1	1.5
Middle	69.14	33.64	18.63	12.77
A1	51.24	26.20	20.79	15.56
A2	56.17	22.12	17.27	12.31
A3	65.19	21.23	13.33	9.15
B1	49.39	22.16	14.96	11.59
B2	45.50	17.93	13.17	9.84
B3	38.14	15.57	11.44	7.88
C1	47.01	21.70	10.93	8.93
C2	33.78	16.24	9.39	7.64
C3	21.85	12.37	8.99	5.48
D1	47.96	21.07	13.87	10.21
D2	43.75	16.88	12.14	9.23
D3	39.13	15.05	11.01	6.68
E1	49.59	24.02	16.43	8.21
E2	61.90	21.20	14.17	10.96
E3	55.32	20.02	12.72	7.39

D. ANOVA-tables

Analysis of variance for pressure differences

Table 54: Analysis of variance for temperature drops at a gas temperature of 200 °C and a gas flow rate of 400 kg/h

Source	Sum of squares	DOF	Mean sum of squares	F	Prob>F
Position	18312.29	15	1220.82	22.44	0.00
Urea dosing rate	24974.47	2	12487.23	229.51	0.00
Dosing unit pressure	4783.78	1	4783.78	87.92	0.00
Position·Urea dosing rate	2702.58	30	90.09	1.66	0.09
Position·Dosing unit pressure	10580.03	15	705.34	12.96	0.00
Urea dosing rate · Dosing unit pressure	659.47	2	329.73	6.06	0.01
Error	1632.27	30	54.41		
Total	63644.89	95			

Table 55: Analysis of variance for temperature drops at a gas temperature of 200 °C and a gas flow rate of 1200 kg/h

Source	Sum of squares	DOF	Mean sum of squares	F	Prob>F
Position	6293.69	15	419.58	89.00	0.00
Urea dosing rate	6558.83	2	3279.41	695.61	0.00
Dosing unit pressure	39.62	1	39.62	8.40	0.01
Position·Urea dosing rate	1012.86	30	33.76	7.16	0.00
Position·Dosing unit pressure	985.34	15	65.69	13.93	0.00
Urea dosing rate · Dosing unit pressure	12.51	2	6.26	1.33	0.28
Error	141.43	30	4.71		
Total	15044.30	95			

Table 56: Analysis of variance for temperature drops at a gas temperature of 300 °C and a gas flow rate of 800 kg/h

Source	Sum of squares	DOF	Mean sum of squares	F	Prob>F
Position	9153.72	15	610.25	71.84	0.00
Urea dosing rate	1862.62	2	931.31	109.63	0.00
Dosing unit pressure	232.83	2	116.41	13.70	0.00
Position·Urea dosing rate	1674.22	30	55.81	6.57	0.00
Position·Dosing unit pressure	2028.82	30	67.63	7.96	0.00
Urea dosing rate · Dosing unit pressure	67.51	4	16.88	1.99	0.11
Error	509.69	60	8.49		
Total	15529.41	143			

Table 57:Analysis of variance for temperature drops at a gas temperature of 385 °C and a gas flow rate of 400 kg/h

Source	Sum of squares	DOF	Mean sum of squares	F	Prob>F
Position	2304.21	15	153.61	25.15	0.00
Urea dosing rate	1878.69	2	939.34	153.77	0.00
Dosing unit pressure	0.37	1	0.37	0.06	0.81
Position·Urea dosing rate	944.53	30	31.48	5.15	0.00
Position·Dosing unit pressure	201.44	15	13.43	2.20	0.03
Urea dosing rate · Dosing unit pressure	0.36	2	0.18	0.03	0.97
Error	183.27	30	6.11		
Total	5512.85	95			

Table 58: Analysis of variance for temperature drops at a gas temperature of 400 °C and a gas flow rate of 1200 kg/h

Source	Sum of squares	DOF	Mean sum of squares	F	Prob>F
Position	842.40	15	56.16	95.64	0.00
Urea dosing rate	483.04	2	241.52	411.29	0.00
Dosing unit pressure	2.73	1	2.73	4.64	0.04
Position·Urea dosing rate	220.85	30	7.36	12.54	0.00
Position·Dosing unit pressure	56.73	15	3.78	6.44	0.00
Urea dosing rate · Dosing unit pressure	4.98	2	2.49	4.24	0.02
Error	17.62	30	0.59		
Total	1628.35	95			

Analysis of variance for angle change

Table 59: Analysis of variance for temperature drops at a gas temperature of 200 °C and a gas flow rate of 400 kg/h

Source	Sum of squares	DOF	Mean sum of squares	F	Prob>F
Position	15510.44	15	1034.03	17.60	0.00
Urea dosing rate	23004.35	2	11502.17	195.83	0.00
Angle	3022.99	1	3022.99	51.47	0.00
Position·Urea dosing rate	2688.99	30	89.63	1.53	0.13
Position·Angle	9167.64	15	611.18	10.41	0.00
Urea dosing rate · Angle	340.18	2	170.09	2.90	0.07
Error	1762.07	30	58.74		
Total	55496.66	95			

Table 60: Analysis of variance for temperature drops at a gas temperature of 200 °C and a gas flow rate of 1200 kg/h

Source	Sum of squares	DOF	Mean sum of squares	F	Prob>F
Position	7171.68	15	478.11	72.10	0.00
Urea dosing rate	6956.41	2	3478.21	524.54	0.00
Angle	42.51	1	42.51	6.41	0.02
Position·Urea dosing rate	1117.25	30	37.24	5.62	0.00
Position·Angle	1374.83	15	91.66	13.82	0.00
Urea dosing rate · Angle	1.58	2	0.79	0.12	0.89
Error	198.93	30	6.63		
Total	16863.19	95			

Table 61: Analysis of variance for temperature drops at a gas temperature of 300 °C and a gas flow rate of 800 kg/h

Source	Sum of squares	DOF	Mean sum of squares	F	Prob>F
Position	11568.78	15	771.25	18.72	0.00
Urea dosing rate	5964.20	2	2982.10	72.36	0.00
Angle	990.89	1	990.89	24.04	0.00
Position·Urea dosing rate	4285.03	30	142.83	3.47	0.00
Position·Angle	3317.28	15	221.15	5.37	0.00
Urea dosing rate · Angle	335.16	2	167.58	4.07	0.03
Error	1236.31	30	41.21		
Total	27697.65	95			

Table 62: Analysis of variance for temperature drops at a gas temperature of 385 °C and a gas flow rate of 400 kg/h

Source	Sum of squares	DOF	Mean sum of squares	F	Prob>F
Position	1876.74	15	125.12	22.61	0.00
Urea dosing rate	1840.04	2	920.02	166.24	0.00
Angle	5.70	1	5.70	1.03	0.32
Position·Urea dosing rate	611.81	30	20.39	3.68	0.00
Position·Angle	377.98	15	25.20	4.55	0.00
Urea dosing rate · Angle	1.34	2	0.67	0.12	0.89
Error	166.03	30	5.53		
Total	4879.65	95			

Table 63: Analysis of variance for temperature drops at a gas temperature of 400 °C and a gas flow rate of 1200 kg/h

Source	Sum of squares	DOF	Mean sum of squares	F	Prob>F
Position	930.45	15	62.03	65.23	0.00
Urea dosing rate	514.40	2	257.20	270.48	0.00
Angle	13.35	1	13.35	14.03	0.00
Position·Urea dosing rate	259.02	30	8.63	9.08	0.00

Position·Angle	77.54	15	5.17	5.44	0.00
Urea dosing rate · Angle	2.45	2	1.23	1.29	0.29
Error	28.53	30	0.95		
Total	1825.74	95			

Analysis of variance for frequency change

Table 64: Analysis of variance for temperature drops at a gas temperature of 200 °C and a gas flow rate of 400 kg/h

Source	Sum of squares	DOF	Mean sum of squares	F	Prob>F
Position	3379.58	15	225.31	6.26	0.00
Frequency	90.17	1	90.17	2.50	0.13
Error	540.15	15	36.01		
Total	4009.90	31			

Table 65: Analysis of variance for temperature drops at a gas temperature of 200 °C and a gas flow rate of 1200 kg/h

Source	Sum of squares	DOF	Mean sum of squares	F	Prob>F
Position	3027.80	15	201.85	8.30	0.00
Frequency	95.34	1	95.34	3.92	0.07
Error	364.90	15	24.33		
Total	3488.04	31			

Table 66: Analysis of variance for temperature drops at a gas temperature of 300 °C and a gas flow rate of 800 kg/h

Source	Sum of squares	DOF	Mean sum of squares	F	Prob>F
Position	6831.79	15	455.45	22.79	0.00
Frequency	103.05	1	103.05	5.16	0.04
Error	299.81	15	19.99		
Total	7234.66	31			

Table 67: Analysis of variance for temperature drops at a gas temperature of 385 °C and a gas flow rate of 400 kg/h

Source	Sum of squares	DOF	Mean sum of squares	F	Prob>F
Position	1624.18	15	108.28	659.69	0.00
Frequency	3.41	1	3.41	20.76	0.00
Error	2.46	15	0.16		
Total	1630.05	31			

Table 68: Analysis of variance for temperature drops at a gas temperature of 400 °C and a gas flow rate of 1200 kg/h

Source	Sum of squares	DOF	Mean sum of squares	F	Prob>F
Position	639.84	15	42.66	49.57	0.00
Frequency	3.80	1	3.80	4.41	0.05
Error	12.91	15	0.86		
Total	656.54	31			